AD-A034 848

ATMOSPHERIC ELECTRICITY AND TETHERED AEROSTATS. VOLUME II

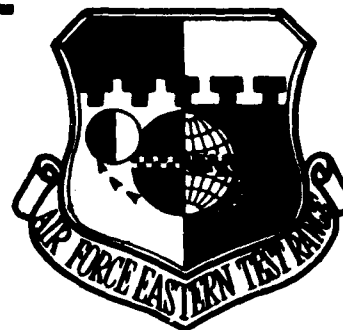AIR FORCE EASTERN TEST RANGE
PATRICK AIR FORCE BASE, FLORIDA

11 MAY 1976

028099

ADA034848

AFETR-TR-76-07

ATMOSPHERIC ELECTRICITY AND
TETHERED AEROSTATS, VOLUME II

Range Measurements Laboratory
Air Force Eastern Test Range (AFSC)
Patrick AFB, Florida

11 May 1976

Approved for Public Release;
distribution unlimited

Prepared for

DEFENSE ADVANCED RESEARCH PROJECTS AGENCY
1400 WILSON BLVD
ARLINGTON, VIRGINIA

LEGAL NOTICE

OTHER NOTICES

This technical report has been reviewed and is approved for publication.

TOXEY A. HALL, Project Engineer
Metric Engineering
Pan American World Airways, Inc.

ELMER E. SHEPPARD, Program Manager
Sensor Platforms Branch
Range Measurements Laboratory
Directorate of Range Engineering

WALTER H. MANNING, JR., Chief
Range Measurements Laboratory
Directorate of Range Engineering

FOR THE COMMANDER

ROBERT C. KORMONDY, Colonel, USAF
Director of Range Engineering

REPORT DOCUMENTATION PAGE		READ INSTRUCTIONS BEFORE COMPLETING FORM
1 REPORT NUMBER AFETR-TR 76-07	2. GOVT ACCESSION NO. N/A	3. RECIPIENT'S CATALOG NUMBER N/A
4. TITLE (and Subtitle) ATMOSPHERIC ELECTRICITY AND TETHERED AEROSTATS, VOL II		5. TYPE OF REPORT & PERIOD COVERED Final, 1 Apr 73 thru 30 Jun 74
		6. PERFORMING ORG. REPORT NUMBER Part B-3058, Part D-582
7. AUTHOR(s) Part A — Dr. Donald J. Latham Part B — Dr. Edward T. Pierce and Mr. Gary H. Price Parts C & D — Mr. James R. Staham		8. CONTRACT OR GRANT NUMBER(s) • A — F08606-73-C-0039 B — F08606-74-C-0034 C — F08606-73-C-0037 D — F08606-74-C-0031
9. PERFORMING ORGANIZATION NAME AND ADDRESS A — University of Miami, Miami, Fla. 33125 B — Stanford Research Institute, Menlo Park, Cal. 94025 C & D — Lightning & Transients Research Institute, Miami Beach, Florida, 33139		10. PROGRAM ELEMENT, PROJECT, TASK AREA & WORK UNIT NUMBERS N/A
11. CONTROLLING OFFICE NAME AND ADDRESS Defense Advanced Research Projects Agency 1400 Wilson Blvd		12. REPORT DATE 11 May 1976
		13. NUMBER OF PAGES 210
14. MONITORING AGENCY NAME & ADDRESS(if different from Controlling Office) Range Measurements Laboratory (ENL) Air Force Eastern Test Range Patrick Air Force Base, Florida 32925		15. SECURITY CLASS. (of this report) Unclassified
		15a. DECLASSIFICATION/DOWNGRADING SCHEDULE N/A

16. DISTRIBUTION STATEMENT (of this Report)

A

17. DISTRIBUTION STATEMENT (of the abstract entered in Block 20, if different from Report)

A

18. SUPPLEMENTARY NOTES

Volume II provides the Final Reports of four studies by outside contractors. (Volume I is a summary of in-house efforts and contracted studies.)

Item 8 — All contracts were issued under ARPA Order number 2176.

19. KEY WORDS (Continue on reverse side if necessary and identify by block number)

Atmospheric Electricity
Balloons
Conducting & Nonconducting Tethers
Corona Discharge
Electric-Field Perturbations
Faraday Cages

Lightning-Effects, Protection, Warning
Systems
Potential Gradient Anomalies
Space Charge Plumes
Tethered Balloons, Tether Currents

20. ABSTRACT (Continue on reverse side if necessary and identify by block number)

Part A, "Atmospheric Electrical Effects of and on Tethered Balloon Systems," by Latham includes airborne and ground measurements on three types of balloons, at altitudes from 1,400 to 7,500 feet, with various conducting and non-conducting tethers, plus theoretical calculations. The extent of agreement of measured results with theoretical calculations, space charge plume effects, corona dischargers, charging time constants and rates, lightning strike probability, and lightning warning device effectiveness radius are discussed.

Part B, "Natural Electrical Effect, on the Operation of Tethered Balloon Systems," by Pierce and Price discusses the interaction between tethered balloon systems and the natural electrical environment, comparative effects of conductive and non-conductive tethers, and it provides a methodical approach to predicting the probability of lightning strikes to tethered balloons

Part C, "Lightning Protection for a RML Tethered Balloon System, Phase I — Personnel Protection," by Stahman discusses the vulnerability of personnel to lightning strikes, protection for personnel (primarily Faraday cages plus bonding and grounding), and lightning warning devices.

Part D, "Lightning Protection for a RML Tethered Balloon System, Phases II and III - Winch, Cable and Balloon Protection" by Stahman discusses survivability of various tethers, lightning diverters and the protection they offer balloons, and the protection of on-board electronics and electro-explosive devices. Extensive testing of tether materials by artificial lightning was conducted.

VOLUME II

CONTENTS

ADVANCED RESEARCH PROJECTS AGENCY

1400 WILSON BOULEVARD
ARLINGTON, VIRGINIA 22209

PART A

FINAL REPORT

UNIVERSITY OF MIAMI

CONTRACT F08606-73-C-0039

14 Mar. 1974
(Date)

ARPA ORDER NO. 2176

RANGE MEASUREMENTS LABORATORY
PATRICK AIR FORCE BASE, FLORIDA 32925

FINAL REPORT

UNIVERSITY OF MIAMI

CONTRACT F08606-73-C-0039

Atmospheric Electrical Effects of and on

Tethered Ballon Systems

ARPA Order 2176   Dr. Don J. Latham (305) 284-2335
Contractor Code: 9B962

Effective Date of Contract: 14 Mar. 73
Contract Expiration Date: 14 Mar. 74
Amount of Contract: $21,750.00

ABSTRACT

This University of Miami study covers effects of lightning on large balloons with conducting and nonconducting tethers. It included overflights by instrumented aircraft measuring 3-axis E-field perturbations, ground stations with E-field and air-earth current sensors, measuring dc and induced tether currents, and isolating a conducting tether from ground and then regrounding it. Most measurements were made on the 5,300 ft^3 balloon system, with others on 84,000 and 205,000 ft^3 ones; at balloon altitudes from 1,400 to 7,500 feet. Various sizes and types of steel and nylon tethers were evaluated.

All flights confirmed that the ambient field was perturbed by conducting and nonconducting tethers in combination with the balloon. To estimate perturbations in the potential gradient over the balloon/tether, calculations were made to simulate a tether and a conducting balloon and were then tested against the measured data. Simple models based on ellipsoidal conductors failed to predict the perturbation of conductive tether systems due to a corona-produced space charge plume extending downwind. This plume decreases the strike probability of the tether but probably increases it for the balloon. Conducting systems should have corona dischargers topside.

E-field potential gradient measurements at the foot of balloon tethers seem to indicate that nonconducting tethers do not perturb the potential gradient structure there. Conducting tether perturbations at ground level can be calculated adequately from theory. Charging time constant of conducting tether systems are about 6 to 20 seconds and are governed by corona discharge, which depends on differences in potential between the atmosphere and tether. Nonconducting tethers seem to have a time constant from 1 to several hours due to the tether-to-ground capacitance; rain shortens this time constant considerably but does not create space charge plume. When the balloon is above the atmospheric mixing layer, the charging rate (which depends on tether cleanliness and altitude) is decreased.

Lightning can be expected to strike balloon systems with either conducting or nonconducting tethers. The latter, are probably less attractive to lightning, however. When the tether is wet, the strike probability increases.

Potential gradient anomalies were observed up to 1/2 the balloon's altitude over and around the balloon. Therefore, with conducting tethers, lightning warning devices should be more than one balloon altitude from the control site.

Additional data is needed on system behavior in high negative potential gradients - the types associated with lightning.

Toxey A. Hall, RML

CONTENTS

ILLUSTRATIONS

ILLUSTRATIONS (cont,

TABLES

SECTION 1 - <u>INTRODUCTION</u>

The primary purpose of this exercise was twofold - first, to assess the perturbation of an ambient atmospheric electric regime by a tethered balloon with both conducting and non-conducting tethers and, second, to establish some criteria for placement of warning devices for lightning activity.

Observational techniques used in this study were: (1) overflights of the balloons with a NASA aircraft equipped to measure three-axis electric field perturbations, (2) the placement of ground stations containing electric field and air-earth current sensors, (3) the measurement of tether currents, both DC and induced, and (4) the isolation from ground and subsequent regrounding of a conducting tether.

Operations performed

Several flights, mainly of the "Baldy" balloon system were conducted over a period spanning 14 Sept. - 7 Dec. A brief summary of these flights is given in Table 1.1.

TABLE 1.1

SUMMARY OF FLIGHTS

DATE	BALLOON	TETHER	ALT.	NASA 6	EQUIPMENT
14 Sept.	BJ + 3	.625		yes	current (tether)
25 Sept.	BJ + 3	.625/steel	3700	no	2 AEC, tether I
1 Oct.	Baldy	steel	3000	no	1E, 2I's, tether I
2 Oct.	Baldy	steel	1400	yes	tether current
2 Oct.	Baldy	nylon	2500	yes	tether current
15 Oct.	Baldy	steel	2400	no	3 mills, 4I, tether I NG
17 Oct.	Baldy	steel	2770	no	all
26 Oct.	Baldy	nylon	4000	yes	all
31 Oct.	Baldy	steel	3000	no	all
2 Nov.	Baldy	steel	2500	yes	all
8 Nov.	Baldy	steel	2730	yes	all (NASA data not usable
26 Nov.	Baldy	nylon	3500	no	all
28 Nov.	204	.775	7500	no	all
30 Nov.	204	.775	5000	no	all
6 Dec.	204	.775	?	yes	none
7 Dec.	204	.775	?	yes	none

2

SECTION 2 - NASA OVERFLIGHT DATA REDUCTION

The NASA flights producing reliable data by day appear in the first column, Table 2.1. Data was in the form of strip-chart recordings showing three components of the potential gradient (the <u>negative</u> of the field). All flights, whether for conducting or non-conducting tethers, confirmed the existence of a perturbation in the ambient field due to the presence of the balloon/tether combination.

Theoretical calculations based on prolate conducting ellipsoids (Appendixes A and B) were made to simulate a "free-standing" tether (long thin vertical ellipsoid in an ambient field) and a conducting balloon (horizontal prolate ellipsoid at zero potential, neglecting the tether) at altitude. Computer programs were written to evaluate the theoretical calculations. The object of these relatively simple calculations was to estimate the perturbation in the vertical component of the potential gradient immediately above the balloon/tether combination.

A more ambitious program to calculate the effects at points in space other than directly over the tether used a finite difference approximation to Poisson's equation ($\Delta^2\phi = \frac{\rho}{\epsilon_o}$, where ϕ is the electrical potential and ρ is space charge density); some results are shown in appendix D. (As of this writing, a balloon has not been put into this program, but a tether has).

Theoretical calculations of perturbations in potential gradient were tested against the data for three hypotheses:

1) the balloon was ignored and the potential gradient perturbation tested against the tether as an ellipsoid; this would be the case if the balloon, being a non-conductor, were not charged but merely acted as a

TABLE 2.1

NASA OVERFLIGHT DATA

Date of flight	Balloon/ Tether	Altitude (m)	Inversion height (m)	Ambient Pot. Grad. V/M	Capacitance (pf) of balloon	Charge on Balloon (coul)* Theoretical	Calculated
14 Sept '73	BJ + 3/ NOLARO	1067	N/A	80	900	-7.7×10^{-5}	-10^{-4}
2 Oct '73	BALDY/ STEEL	396	N/A	80	300	-9.5×10^{-6}	-2×10^{-4}
26 Oct '73	BALDY/ NYLON	1219	1500	35	300	-1.3×10^{-5}	-6×10^{-6}
2 Nov '73	BALDY/ STEEL	762	1200	150	300	-3.4×10^{-5}	-6×10^{-5}
6 Dec '73	FII (204)/ NOLARO	1524	1400	5 (at balloon)	8000	-1.2×10^{-3}	-3.5×10^{-5}

* Theoretical charge is calculated from Q = CV

Calculated charge is from measured electric field anomalies

4

low permittivity dielectric. Tables for this test are given on p A-11, appendix A.

2) the balloon was treated as a charged prolate ellipsoid in free space, neglecting the tether and the ground. For testing this hypothesis, a mean charge for the balloon was calculated from the NASA data using equation (15) p B-6 (appendix B). This mean charge was then re-inserted into equation (15) and the results were plotted on the original data plots (Figs. 2.1-2.5). The mean charge was also compared (Table 2.1) to a charge calculated from the assumption that if the ambient potential at the balloon height is "V", then for the balloon to be at zero potential, it must possess a charge $Q = -CV$. (We note that the assumption of neglecting the tether is quite reasonable over the top of the balloon if the balloon is treated as a conductor. It will certainly not hold underneath the balloon because of confluence lines, tether, etc.)

3) the tether was ignored and the balloon treated as a horizontal conducting prolate ellipsoid at zero electric potential (with respect to the earth) at an altitude above the ground such that the potential at the same horizontal distance from the balloon but far away had a value "V". (See appendix B). For this calculation, the effect of the ground, (i.e. an image balloon) was not included in the calculations; this is reasonable because the altitude of the balloon is much greater than its size (even for FII). The results of this test are presented in Table 2.2.

Results of Examination of Hypotheses

It is immediately apparent from the contrast of measured E_z/E_0 ratios with the calculated ones that the calculated ratios are simply too small
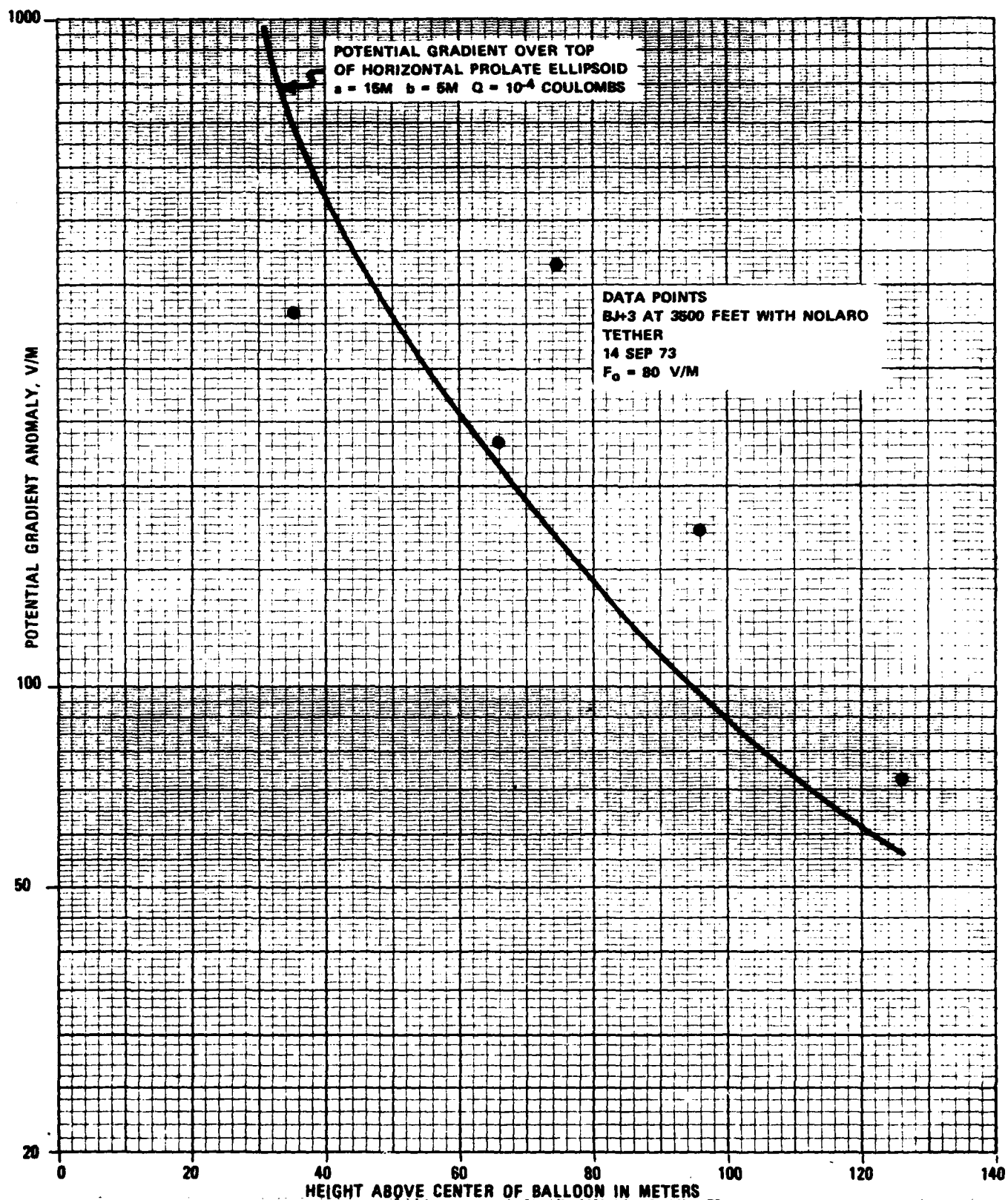
Figure 2.1 — Potential Gradient Anomaly Above Balloon, Nolaro Tether — 14 Sep 73

6
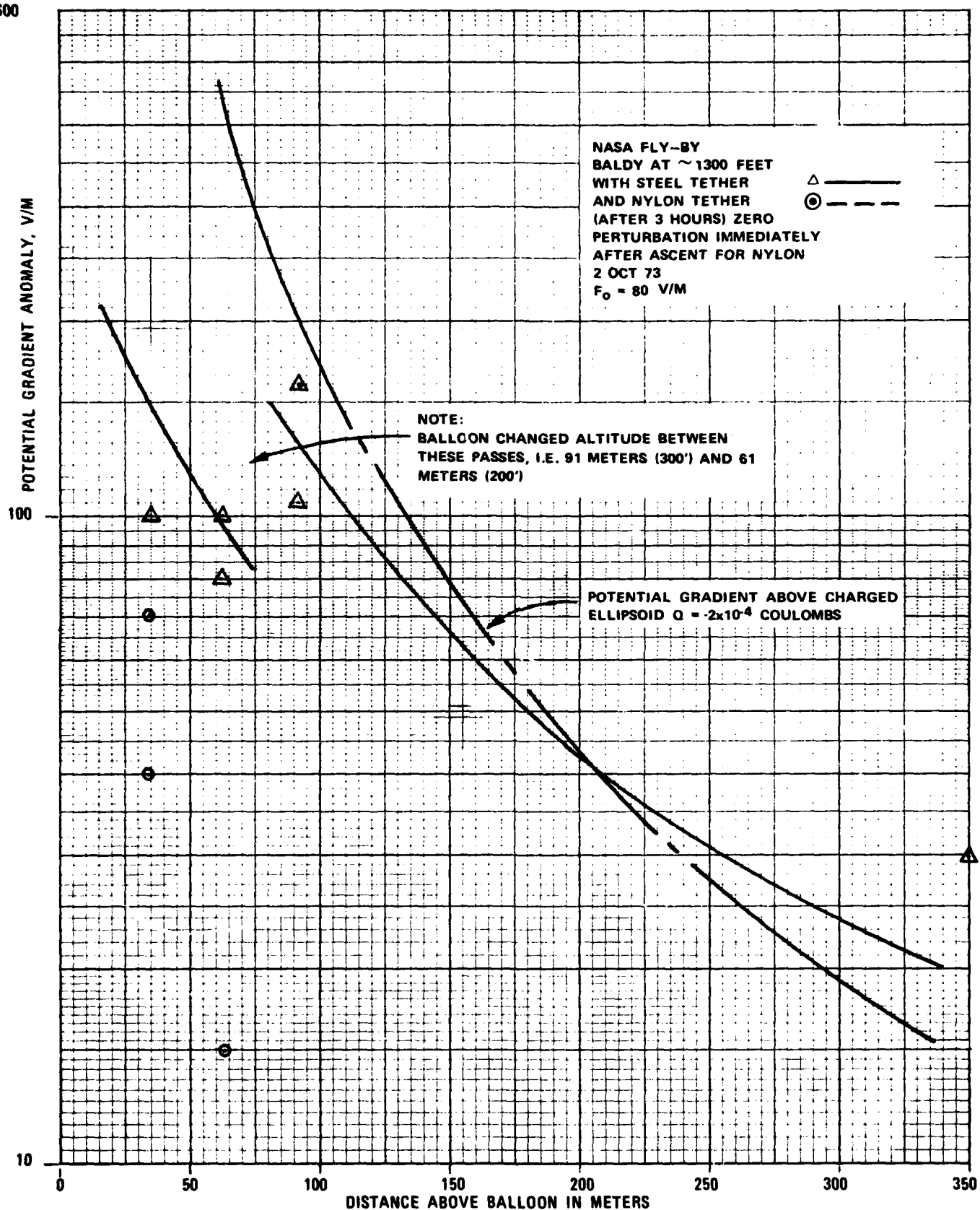
Figure 2.2 — Potential Gradient Anomaly Above Balloon, Steel & Nylon Tether — 2 Oct 73
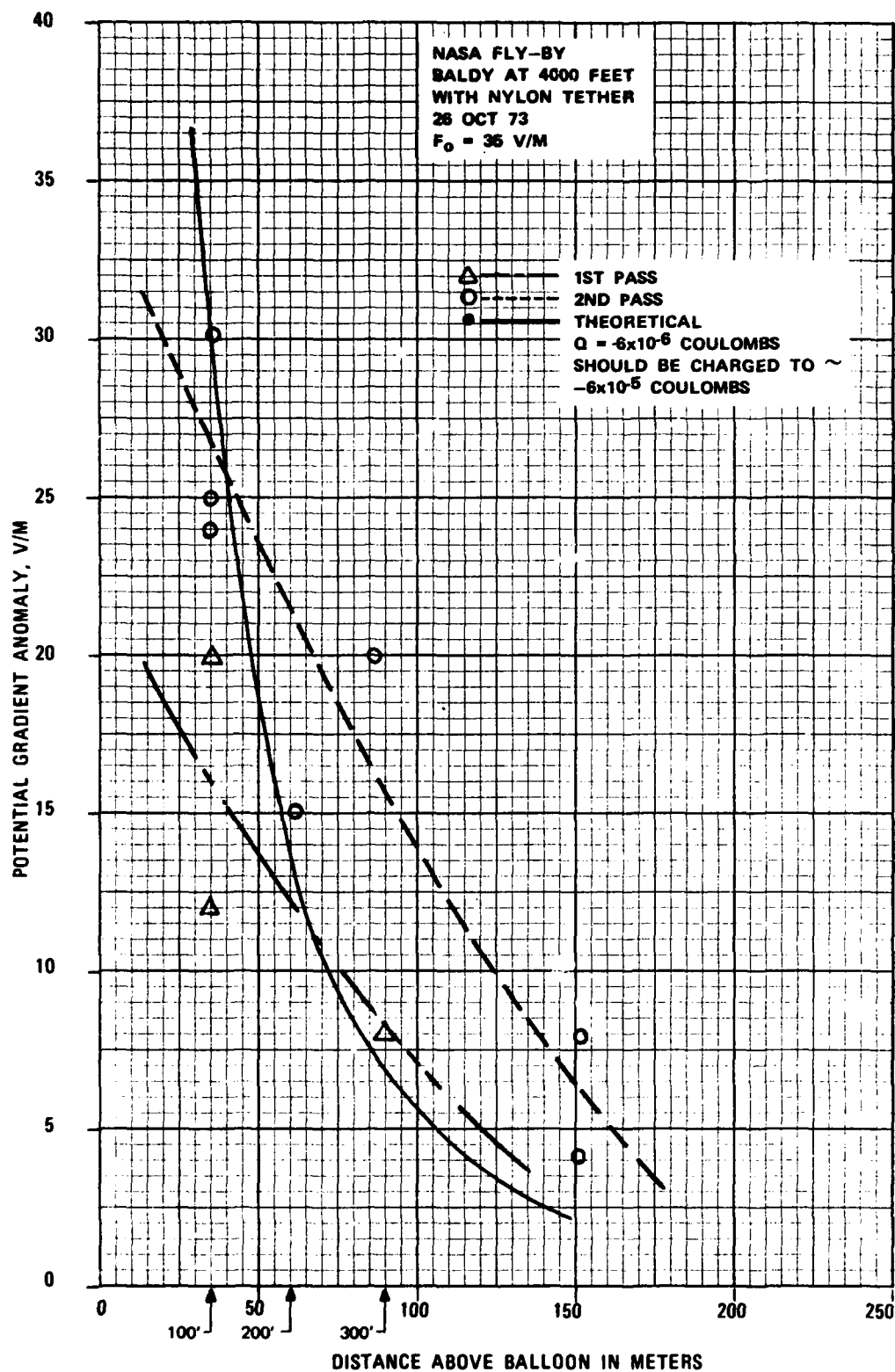
Figure 2.3 — Potential Gradient Anomaly Above Balloon, Nylon Tether — 26 Oct 73

NASA FLY-BY
BALDY AT 2500 FEET
WITH STEEL TETHER
2 NOV 73
$F_o = 150$ V/M
CALCULATED CHARGE $\cong 6 \times 10^{-5}$ **COULOMBS**

THEORETICAL
(CHARGED ELLIPSOID
MODEL)

POTENTIAL GRADIENT ANOMALY, V/M

HEIGHT ABOVE BALLOON IN METERS
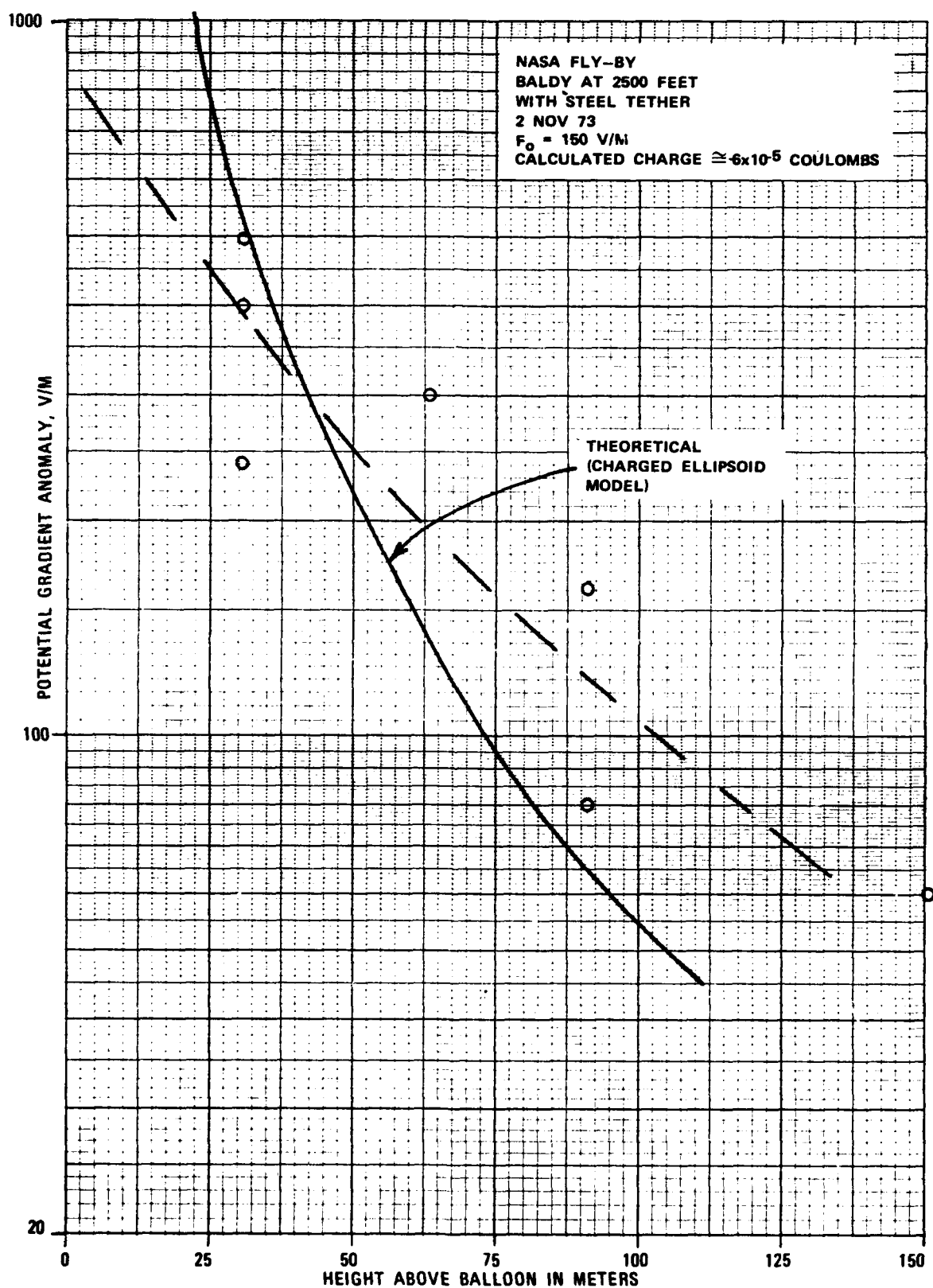
Figure 2.4 — Potential Gradient Anomaly Above Balloon, Steel Tether — 2 Nov 73

1-9
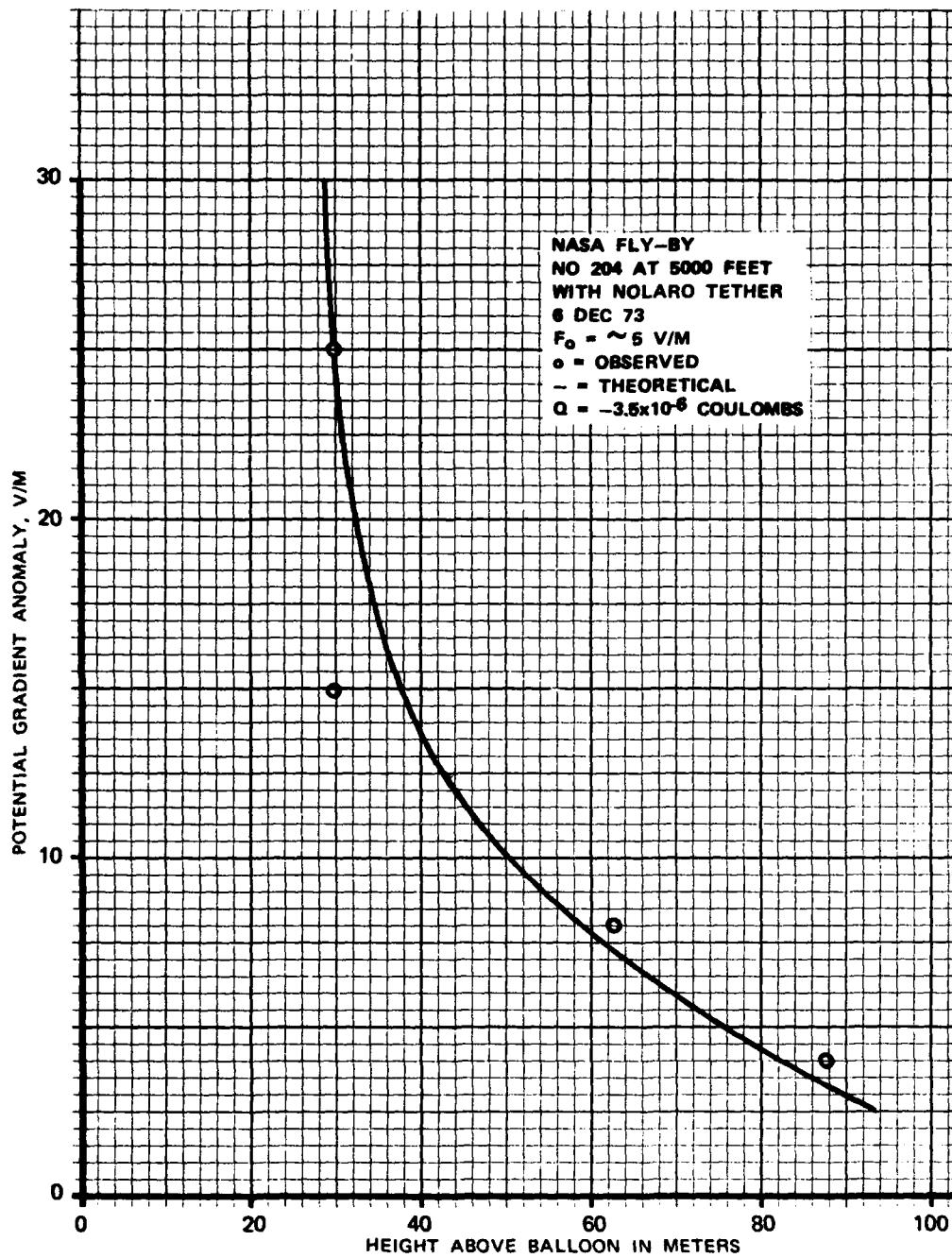
Figure 2.5 — Potential Gradient Anomaly Above Balloon, Nolaro Tether — 6 Dec 73

TABLE 2.2

COMPARISON OF ACTUAL MEASURED FIELD INTENSIFICATIONS
VS THEORETICAL FOR TWO GROUNDED BALLOON MODELS

14 Sept 73   BJ+3   a = 15m   (NOLARO)
                      b = 5m

ht (m) 1066.8

z	E_z/E_0	Appendix B* Calc E_z/E_0	Appendix A** Calc E_z/E_0
126	1.656	1	1.116
96	2.3625	1.01	1.167
66	3.625	1.05	1.271
35.5	5.125	1.55	1.571

2 Oct 73 Baldy (steel) a = 5m   1st fly-by (steel)
                         b = 1.5m

h = 396.24

z	E_z/E_0	Appendix B* Calc E_z/E_0	Appendix A** Calc E_z/E_0
253.5	1.19/1.375	1	1.007
154.5	1.625	1	1.017
*** 93.5	3/2.31	1	1.039
63.5	2.25	1	1.070
3.3	3.5	1	3.433

2 Nov 73 Baldy (steel) a = 5m $E_0 \sim$ 150 V/M
                         b = 1.5m

h = 731.5

z	E_z/E_0	Appendix B* Calc E_z/E_0	Appendix A** Calc E_z/E_0
154.5	1.4	1	1.044
93.5	2./1.53	1	1.091
63.5	3	1	1.154
33	4/33	1	1.350

NOTES

* Balloon only neglecting tether (modelled as a horizontal conducting prolate ellipsoid at zero potential).

** Tether only neglecting balloon (modelled as a vertical grounded prolate ellipsoid at zero potential).

*** The balloon changed altitude between these passes. The last two entries are in doubt as to height of pass. See Fig. 2.2.

When balloon and tether floating, E_z/E_0 cut to $\sim$ 1.5 at z = 33m, i.e. about in half. Could not see plume in airplane data.

to validate either of the two conductor-in-a-field hypotheses (#1 and #3). The E_z/E_0 ratios are somewhat larger for the "bare tether" hypothesis than they are for the "horizontal ellipsoid" model. This is not surprising, as the bare tether has a much smaller radius of curvature at its tip than the balloon over its top.

It is obvious that the charged ellipsoid model can be forced to fit the data (at least at one point on the P.G. anomaly vs. height curve) since the charge is calculated from the data. A look at Table 2.1 shows that the "observed" charge, i.e. that calculated from the NASA potential gradient data is in some cases close to the "theoretical" value and in some cases not. In addition, the curves (marked "theoretical") seem to consistently underestimate the potential gradient anomaly at large distances above the balloon and overestimate it at close distances. In short, no matter how carefully the charge is matched to the data (least-squares, average, etc.) the model does not seem to fit well.

The reason for this lack of good fit for all the proposed models for conducting tethers was found to be the presence of a plume of space charge extending down wind from the balloon. Fig. 2.8 shows the only really clear cut case in the NASA data for the existence of such a plume. For this aircraft pass, the potential gradient meters were set on a more sensitive scale than for any others during this run. Note that the perturbation directly above the balloon is off-scale; this was later remedied by the operator, but the record of the anomaly due to the presence of the plume is reduced in magnitude so far that no reliable values for the potential gradient anomaly can be obtained. Evidence for the presence of such a charged plume can be seen on the data from all NASA-6 flights for conducting

12
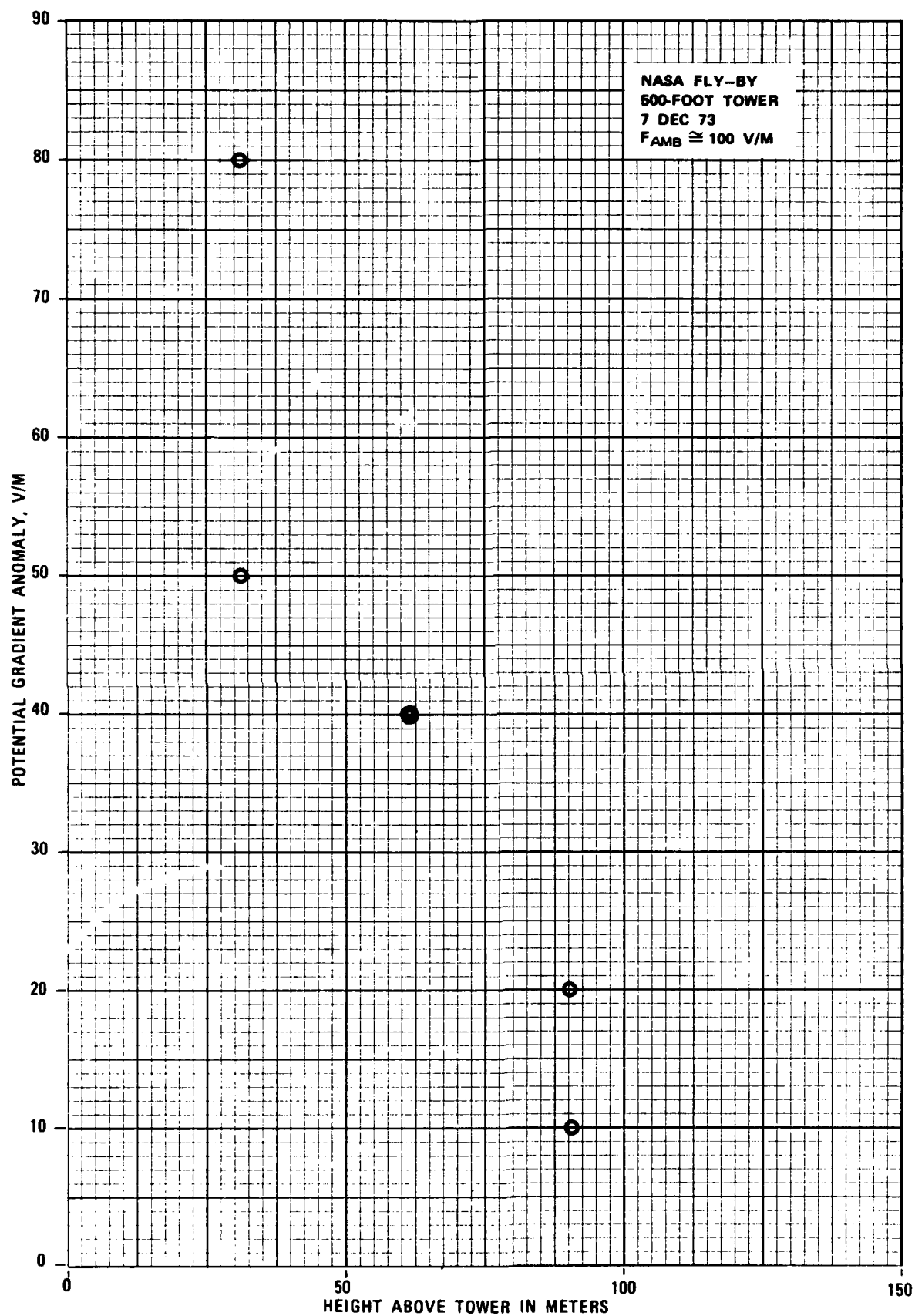
Figure 2.6 — Potential Gradient Anomaly Above 500-Foot Tower
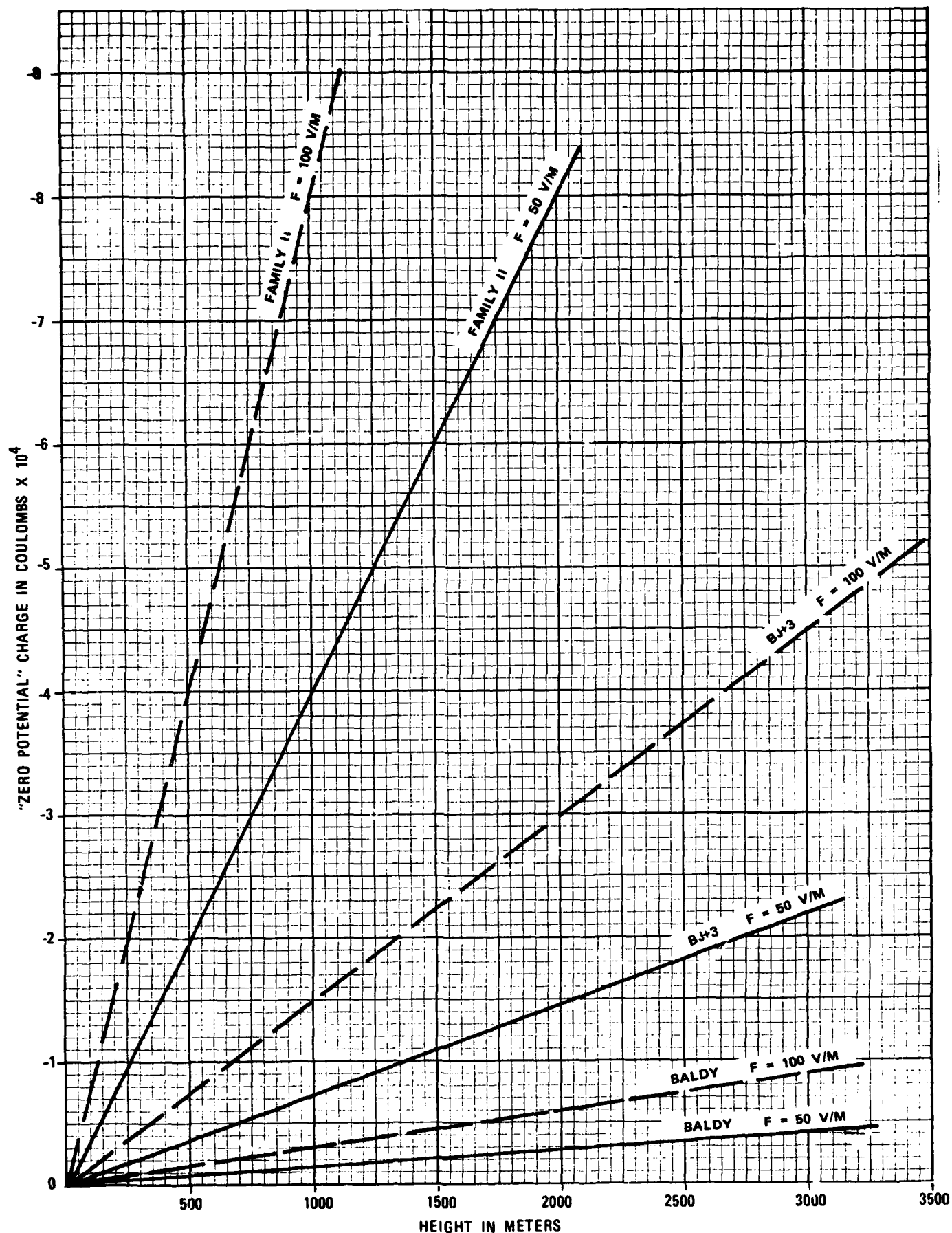
Figure 2.7 — Theoretical Charge on Balloons vs Altitude (Non-Conducting or Conducting Tethers) for Ambient Uniform Potential Gradients of 50 and 100 V/M

14
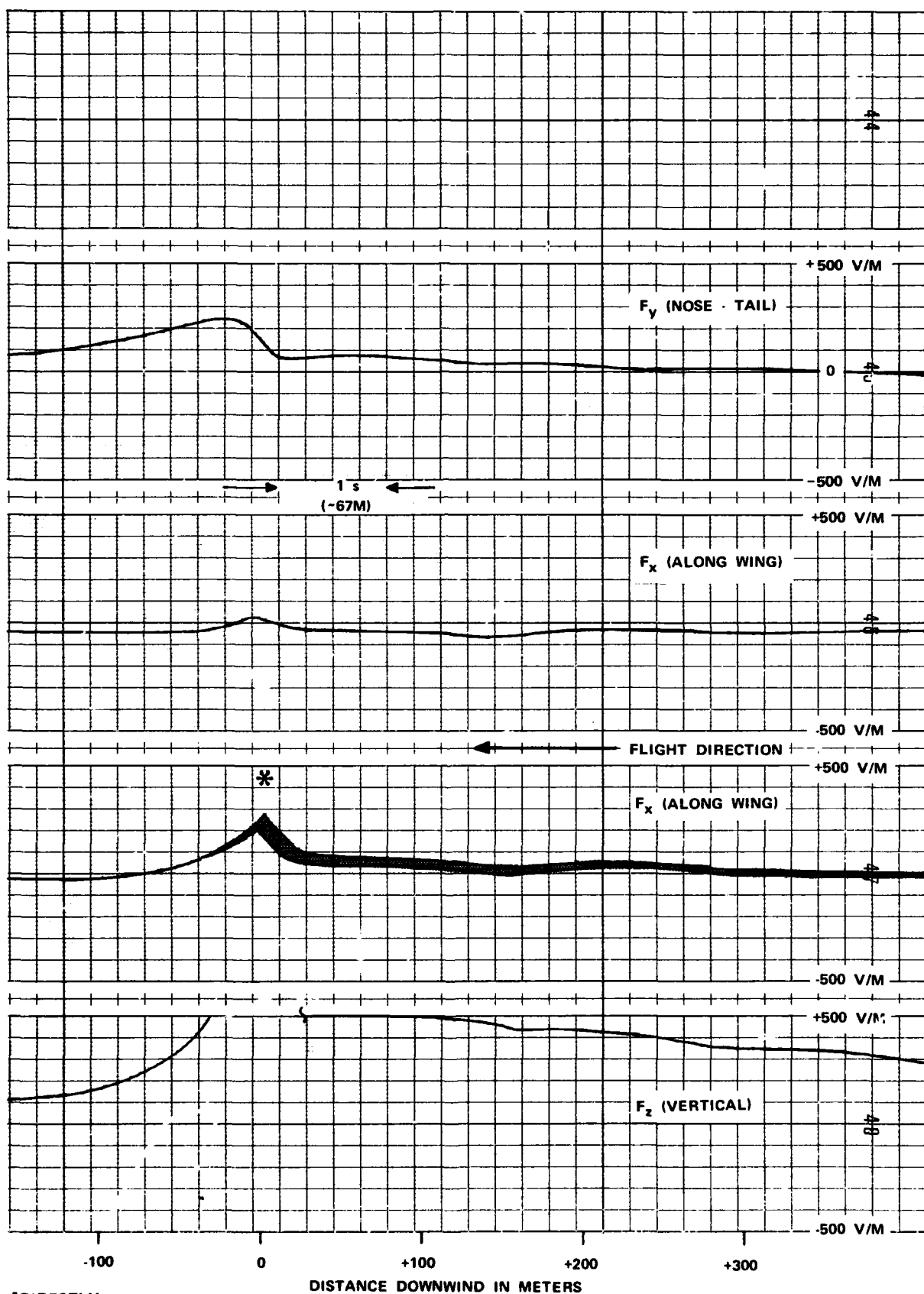
Figure 2-8. Potential Gradient 100 Feet Above a Steel Tethered Balloon at 2500 Feet Showing Effect of Corona Charge Plume

*DIRECTLY OVER BALLOON

1-15

tethers, but is absent from the non-conducting tether data.

The data shows that upwind passes have a gradual increase in F_z as the airplane approaches the balloon, indicating the presence of a plume of negative charge beneath the airplane (there being no reason for a positive space charge overhead). The cross-wind passes over the balloon do not show this increase in F_z but do indicate the presence of the plume by a change in F_x (along-wing) component of the potential gradient. This change in F_x is consistent in sign with a negative plume. A rough theoretical calculation was made in an attempt to model the charge plume (see appendix E for details). Briefly, since the current flow from the tether is measured at the ground, the value of the source for the plume, in coulombs/sec, can be assumed to be identical to the measured current. As indicated in appendix E, a planar wedge was assumed as the plume shape for purposes of calculation. At a wedge included angle of $10°$ ($\theta = 5°$ in appendix E), the charge/unit length*was relatively constant at a value of about 6.6×10^{-7} coul/meter. This implies a source current of 3.2×10^{-6} amps, whereas the measured current was 1.5×10^{-5} amps. The agreement is fairly good, considering that the altitude of the airplane relative to the plume is not well known. The charge "cone" angle calculated from this simple approach agrees quite well with the cone angles found under similar wind and stability conditions for turbulent diffusion from point sources of passive additives (as summarized in Pasquill). The value of the field at the ground due to this plume is of order 20 v/m.

A further glaring discrepancy with simple models can be seen in the NASA 6 data for a fly-by over a 500' tower (fig. 2.6). It is apparent from

* As calculated from the aircraft data

16

the table on p A-13 that the theory severely underestimates the experimental perturbation found for the tower. In addition, a real tower would have a larger "radius of curvature" at the tip than the assumed ellipsoid, leading to less intense potential gradients near the tip. It is clear that a space-charge plume is involved.

Two error sources with respect to the NASA-6 aircraft flights must be mentioned. It has been determined that the time constant of the NASA-6 field mill apparatus is on the order of 0.05 sec. This being the case, the true perturbations in the electric potential must be considered as being larger than the measurements as made by the aircraft passes. This is because the residence time of the aircraft in the vicinity of the balloon is of the same order as or less than (depending on which balloon is being used) the time constant of the mills.

One further source of error is the height estimate from the pilot of the aircraft. Even if 10% error is assumed, however, the hypotheses based on a conductor in an external field would fail.

It is possible that an extended model, based on the Poisson solver, and including the presence of corona discharge and other atmospheric ions and able to take into account such variables as the resistance of the tether and the field distribution around tether and balloon, might be able to successfully predict the field distribution around balloon and tether.

One important result of the NASA-6 flights arises from the measurements conducted over the 204 balloon. These are the only flights conducted for which the balloon was clearly above the atmospheric boundary layer either for conducting or non-conducting tethers. A preliminary conclusion can be

drawn as to the relatively small charge on this balloon as compared with the charge which should be present. If we accept that balloons with non-conducting tethers charge by means of current flow in the tether (which is a better conductor than the atmosphere in the boundary layer), then a balloon below the top of the boundary layer should become charged relatively quickly. If a portion of the tether and the balloon itself are above this layer, the surrounding air and the tether have resistances which are of the same order or at least much closer to each other than in the previous case. This condition implies that the current flow will be smaller, and the time the balloon takes to charge will be longer.

Summary - NASA-6 Overflights

1) Both conducting systems and non-conducting systems perturb the ambient electric potential gradient.

2) Both systems eventually reach an equilibrium condition, with equilibrium being reached by different processes.

3) Simple models based on ellipsoidal conductors fail to predict the perturbation for conducting systems.

4) This failure is due in the main to the presence of a plume of charge, extending downwind from a region near the top of the tether and generated by corona discharge.

5) Estimation of the charge on the balloon by setting $Q = -CF_o h$ where C is the capacitance of the balloon, F_o the ambient potential gradient and h is the height of the balloon fails to predict the charge adequately.

SECTION 3 - TETHER CURRENT MEASUREMENTS

The tether current measurements can be broken down into two categories
according to the type of tether; conducting or non-conducting.
Conducting tether measurements are given in Figures 3.1 - 3.5; non-conducting
measurements seemed to lie in the region 10^{-7} to 10^{-8} amps and be independent
of tether material and altitude.

Difficulties were encountered with both classes of measurement. Bad
grounding and currents from high-frequency induced noise in the tether were
present in almost all observations of conducting tether currents. Clouds of
space charge physically striking the insulated flying sheave produced noise
in the measurements on non-conducting tethers.

It is evident from the measurements summarized in Figs. 3.1 - 3.5 that
the current for conducting systems is much higher than can be supplied from
the normal air-earth current flow as perturbed by the presence of a conductor.
Although the air-earth current measurements made on the sites were complicated
by instrument mis-design (see appendix F), the air-earth current in the region
of the launch area was on the order of 1.5 - 2 x 10^{-12} Amps/m^2. This means
that for typical tether currents on the order of 5×10^{-6} amps, a capture area
of 2.5×10^{6} meters or an effective capture radius of approximately 900 meters
is necessary. If we take the "tip radius" of the tether as the tether
diameter, the effective capture radius is reasonably close to 1/2 the height
(C. B. Moore, private communication), a figure too small to account for the
magnitude of the tether current.

Obviously, in the light of the results of section 1, the current flow in
conducting tethers is due to corona discharge. Our values fall
close to those of Davis and Standring for tether currents, and are
somewhat larger than
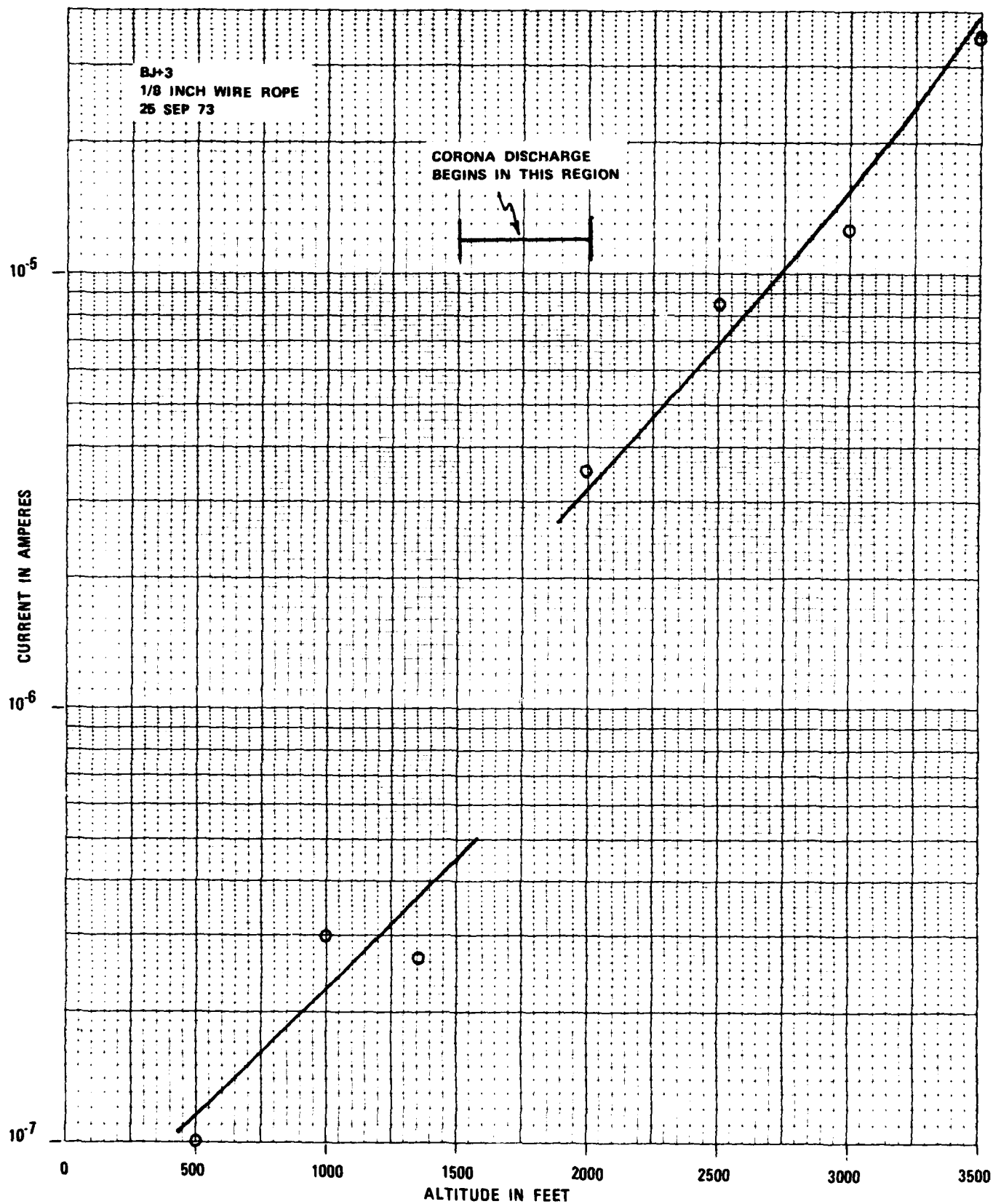
Figure 3.1 — Tether Current vs Balloon Altitude, BJ+3 — 25 Sep 73

20
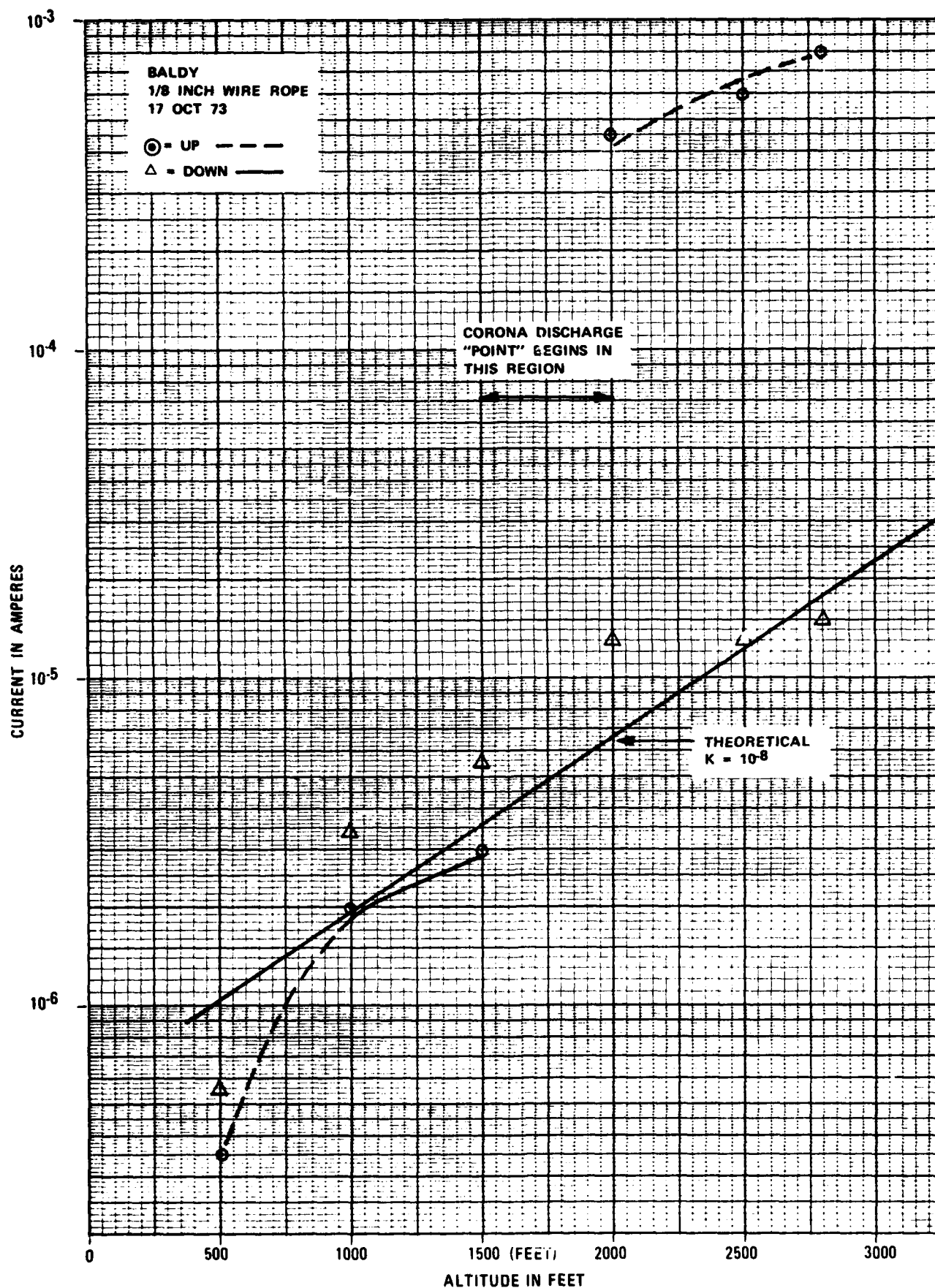
Figure 3.2 — Tether Current vs Balloon Altitude, Baldy — 17 Oct 73
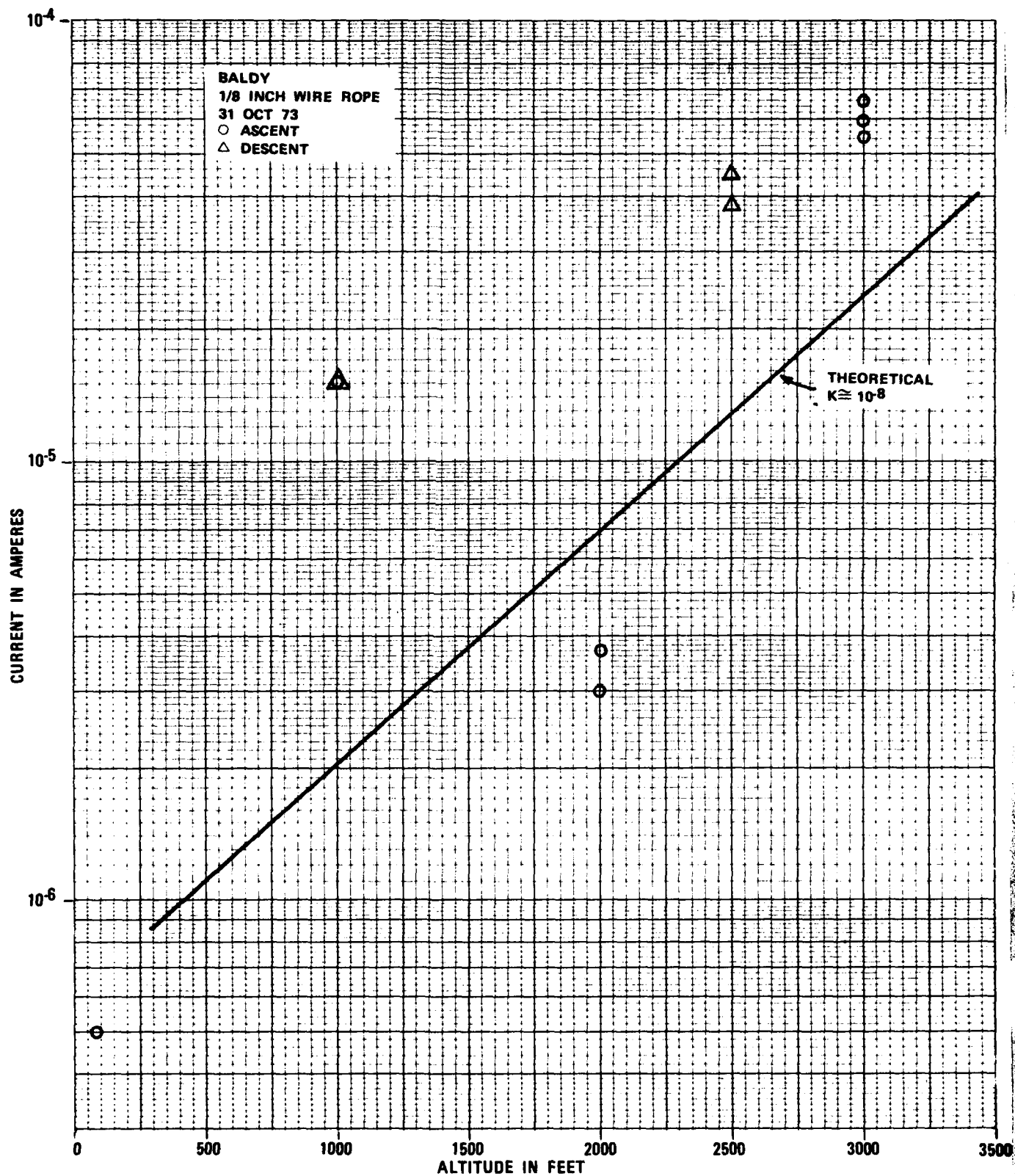
Figure 3.3 — Tether Current vs Balloon Altitude, Baldy — 31 Oct 73

22
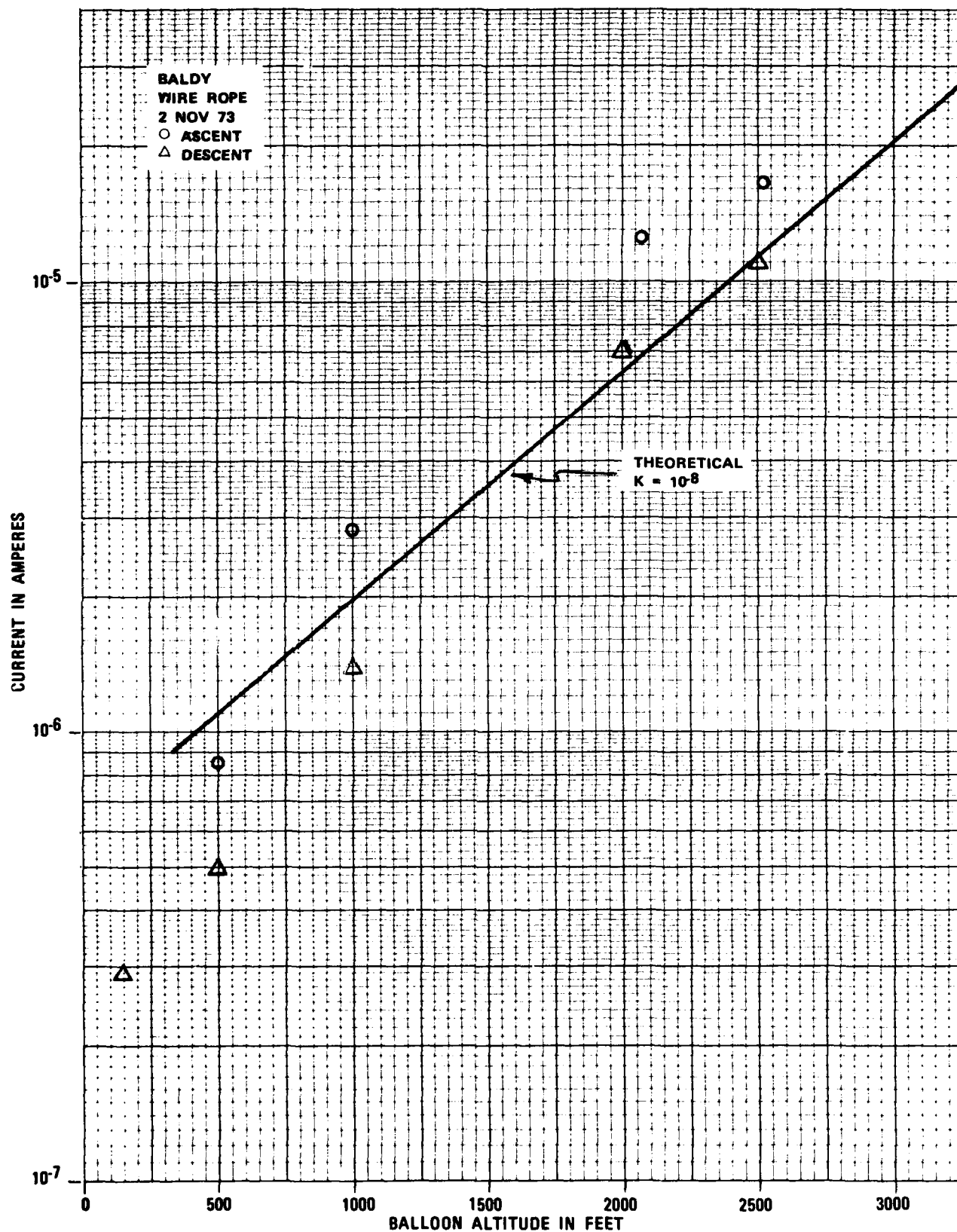
Figure 3.4 — Tether Current vs Balloon Altitude, Baldy — 2 Nov 73
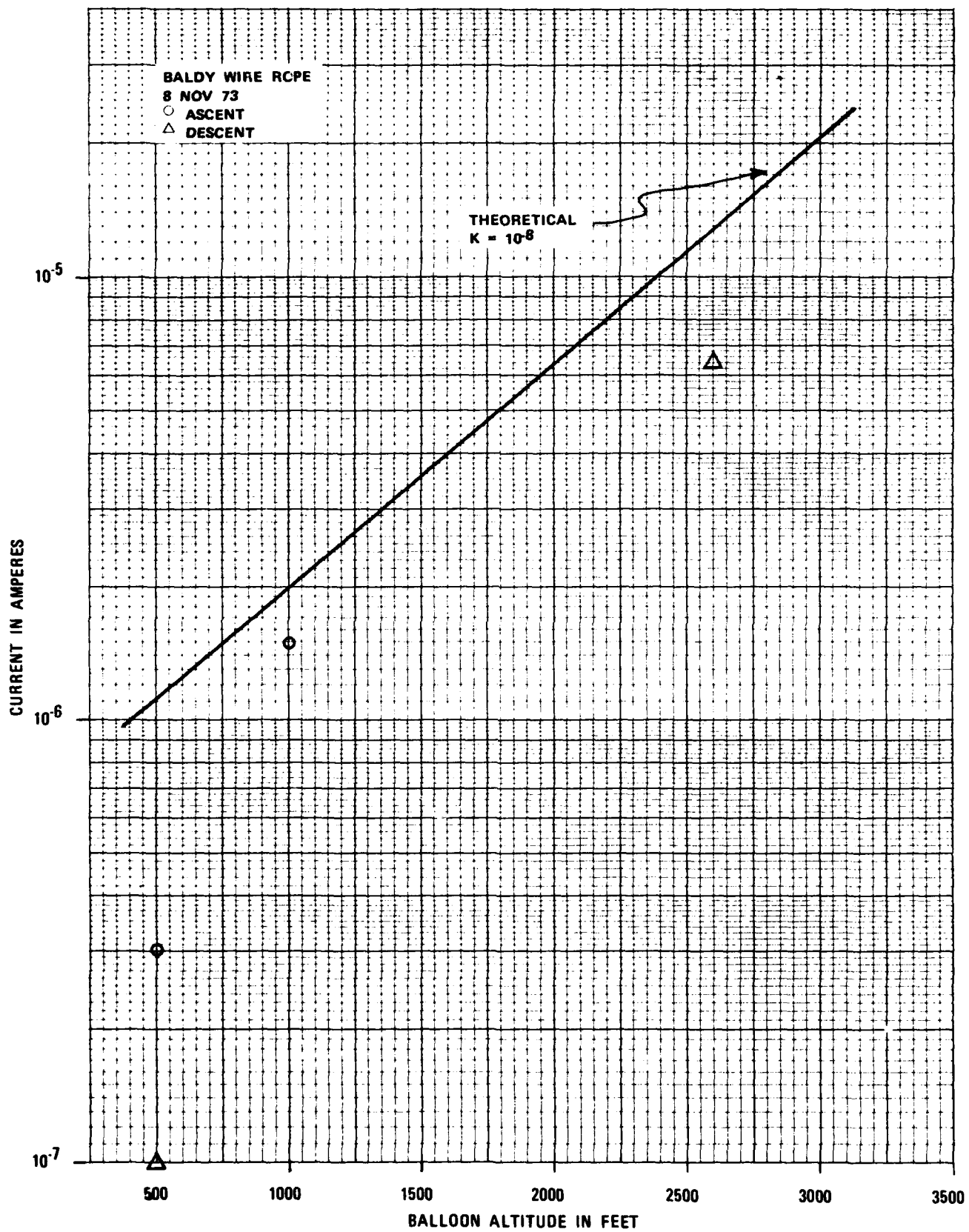
Figure 3.5 — Tether Current vs Balloon Altitude, Baldy — 8 Nov 73

24

those reported by Chalmers and Mapleson. The latter, however, had heights

significantly smaller than those of our tests. They also used a sharp

point discharger mounted on the top of the balloon as the corona current

source, whereas our corona currents arise from the tether.

Measurements seem to indicate that some sort of limiting value for

the tether current is being approached for the Baldy system. The one

experiment with the BJ+3 and a separate wire rope does not indicate such

an asymptote,even though the wire rope used in that test was identical

to the Baldy tether.

It is interesting to note that in the tests shown in Figs. 3.1 and 3.2

there is a jump in current at an altitude of 1500-2000 feet. This corresponds

to a potential in the ambient undisturbed air of approximately 3KV, and may

well represent the onset of corona discharge from the tether. It is

reasonably certain that the discharge does come from the main tether line -

the tip is effectively shielded from the ambient field by the balloon and

also has a spliced eye. We had hoped for a camera-observed night flight to

confirm this hypothesis but were unable to conduct one.

The onset and value of corona current can be crudely estimated. Over

most of the length of the wire, the field at the surface can be approximated

by that at $\xi = 0$ for the long thin ellipsoid of appendix A. If this is the

case, then we see on p A-14 that breakdown fields can exist even for a

1/8" cable at quite reasonable altitudes. This corona discharge in a

fair-weather field consists of negative charge leaving the tether,i.e.

a positive current into the measuring device, as is observed.

Chalmers and Mapleson, based on theory, have determined that corona

current from a balloon-borne point can be calculated from $I = K W^{1/4} (Fh)^{7/4}$ (where I is current in μA, W is wind speed in m/s, F is ambient potential gradient in v/m and h is balloon height in m) as a "rounded off" formula. This led to a value of K very close to 10^{-8} when applied to the Baldy data (see Figs. 3.2 - 3.5). Note that there is, of course, less current than predicted at low altitudes due to the threshold value of potential necessary to initiate corona from the relatively large tether. Otherwise, the data fits remarkably well. The value of K found here is about 6 orders of magnitude below that found by Chalmers and Mapleson; this is a direct reflection of the difference between a 1/8" dia. cable and a 0.25 mm diameter point. It is to be concluded that a larger cable, say 1/2" dia. may put out even less space charge and will, of course, require a higher potential for initiation.

Good records of tether currents for non-conducting tethers are available for two flights of the Baldy balloon with nylon tether line. The flight of 26 Nov. shows that the tether current started at about $.4 \times 10^{-7}$ amp, increased gradually to about 3×10^{-7} amp over a period of about 1 hour, then decreased to less than 10^{-7} amp and fluctuated about that value to the end of the run. Increases and decreases in this current correspond to increases and decreases at all four electric field stations (10', 100', 200' and 500' from tether point).

The data of 26 Oct. shows a similar gradual increase in tether current, accompanied by a gradual increase in potential gradient at the ground (the farthest ground station). In addition, variations in potential gradient are closely matched by variations in tether current, at least qualitatively.

The magnitude of these currents (i.e. 10^{-7} to 10^{-8} amps) seem characteristic of the currents into non-conducting tethers. This current range was also noted briefly in a BJ+3 flight and a FII (#204) flight and seems fairly typical of these also although the FII values are somewhat smaller. There seems to be a small increase of tether current with altitude, but certainly not two orders of magnitude.

These currents give rise to a "capture radius" on the order of 90 meters - a figure which is certainly very reasonable, and probably reflects current flow to the balloon dominating over that to the tether.

The slow charging of a balloon by this small current (slow attainment of ground potential by the balloon) is seen in the NASA-6 passes over a non-conducting tether/balloon combination, Fig. 2.3. It is readily apparent that the balloon is more negatively charged (closer to ground potential) on the second pass than on the first.

Data from AFETR experiments with tether resistance show resistances (Nolaro tether) ranging from 10^7 Ω/m to 10^{11} Ω/m. For a 1000 meter height, we have an effective charging resistance of 10^{10} - 10^{14} Ω. The ambient air has a resistance on the order of 10^{14} Ω/m, three orders of magnitude higher than even the best tether resistance. The charging current is thus not limited by the tether resistance but by the resistance of the surrounding air, and by the ambient electric potential gradient. From these considerations, we conclude that the method of estimating charging time for non-conducting systems based on a "time constant" cannot be considered accurate.

This viewpoint is strengthened by the behavior of the BJ+3 which apparently attained equilibrium after a period on the order of one hour,

whereas a simple R-C charging calculation predicts several hours. The measured current flow in the tether, $\sim 10^{-7}$ amp would theoretically charge the balloon in about 2 hours.

The fact that after a time period of about one hour the FII balloon during the flight of 6 Dec. was not significantly charged despite being in a high conductivity region (above the inversion) can be attributed to the very small ambient potential gradient (5 v/m) in the region near the balloon.

Summary

1) For both conducting and non-conducting systems, the ambient potential gradient plays the dominant role in determining current flow.

2) Tether current in conducting systems is due to corona discharge from the tether; the tether itself, rather than the odd point, seems to be in discharge over a small region near the upper end.

3) Tether current in non-conducting systems is a result of current flowing to the balloon/tether through the relatively poorly conducting atmosphere and is thus limited to 10-100 nA depending on ambient potential gradient and atmospheric conductivity, but not on the state of the system with respect to equilibrium.

4) As long as a non-conducting tether is more conductive than the atmosphere, but not sufficiently conductive to enable the generation of corona discharge, the time to equilibrium will be determined as outlined in (3).

SECTION 4 - ELECTRIC POTENTIAL GRADIENT PERTURBATION AT THE FOOT OF TETHERS

One of the reasons for this study was to determine the extent of perturbations of the local electric potential gradient at the ground near the tether point. Figures 4.1 and 4.2 show this effect as extracted from the data during the ascent and descent of Baldy with a steel tether for the flight of Nov. 2. We have presented this data in the form of two dimensionless ratios, distance from tether point along the ground divided by tether height vs. measured field at each station divided by the fields just before launch (Fig. 4.1) and after the balloon was down and winch truck driven away (Fig. 4.2). The fields have been corrected for site differences by considering that the ambient field was the same at all stations in the unperturbed case. This latter procedure probably accounts for much of the spread in the data. It is almost a certainty that the presence of the winch trailer accounts for the consistent departure of the data taken at #1 station from the rest of the data. The agreement of the remainder of the data with the simple calculation of appendix A is in general good.

On the other hand, non-conducting tethers do not seem to perturb the field at the ground to any great extent, although small perturbations do occur during inhaul due to the "rapid" physical lowering of the bound negative charge on the balloon. This can be seen in the records of the Nov. 26 Baldy Flight.

We would like if possible in the future to analyze both conducting and non-conducting tethers with respect to perturbations of the field due to both a stationary tether and the "haul-down" perturbation. Note that as the distance of "haul down" is known and the field perturbations are known, the charge on the balloon could be calculated and compared to the
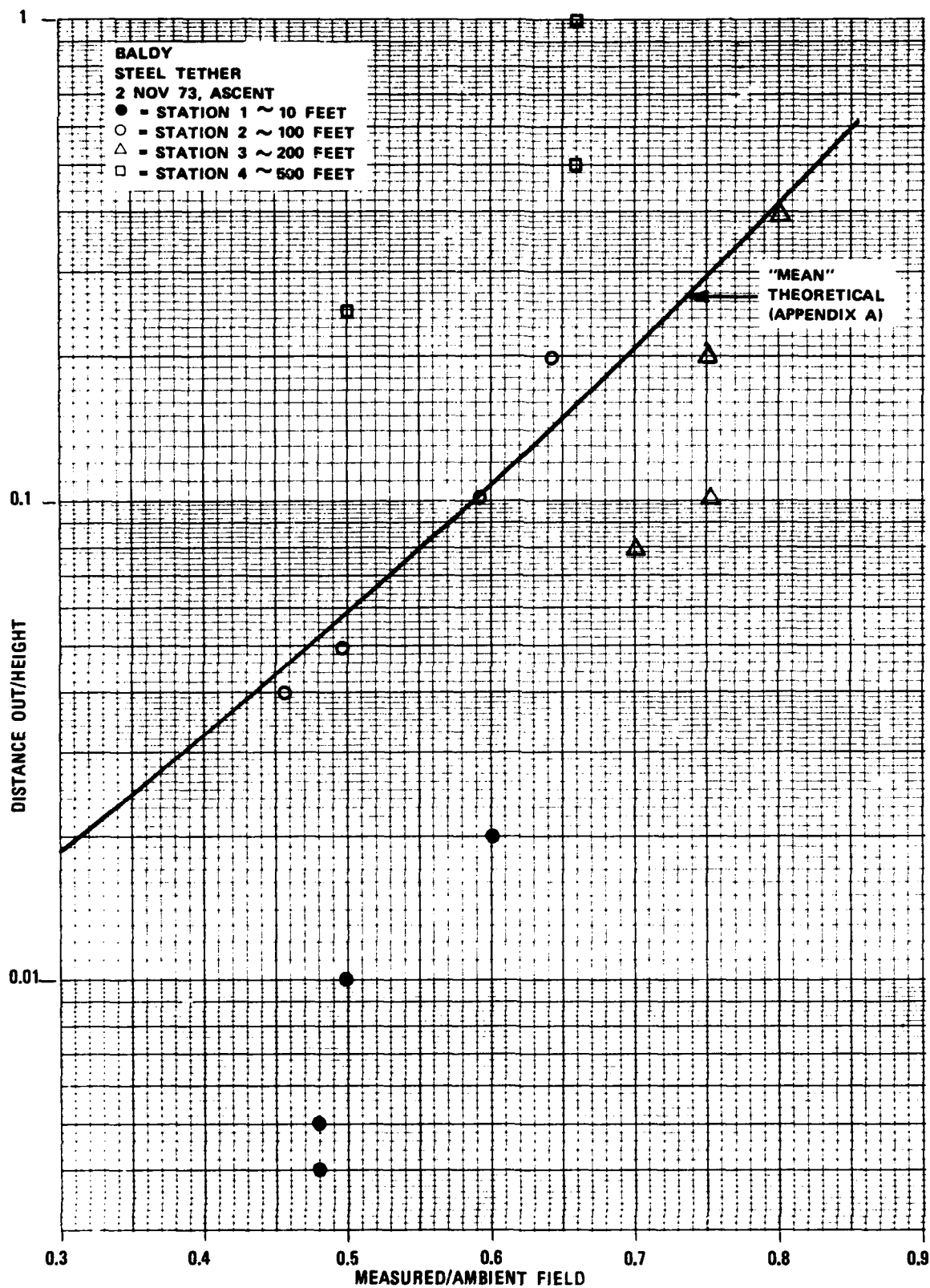
Figure 4.1 — Data Plot of Distance/Height vs Measured/Ambient Field, Ascent

30
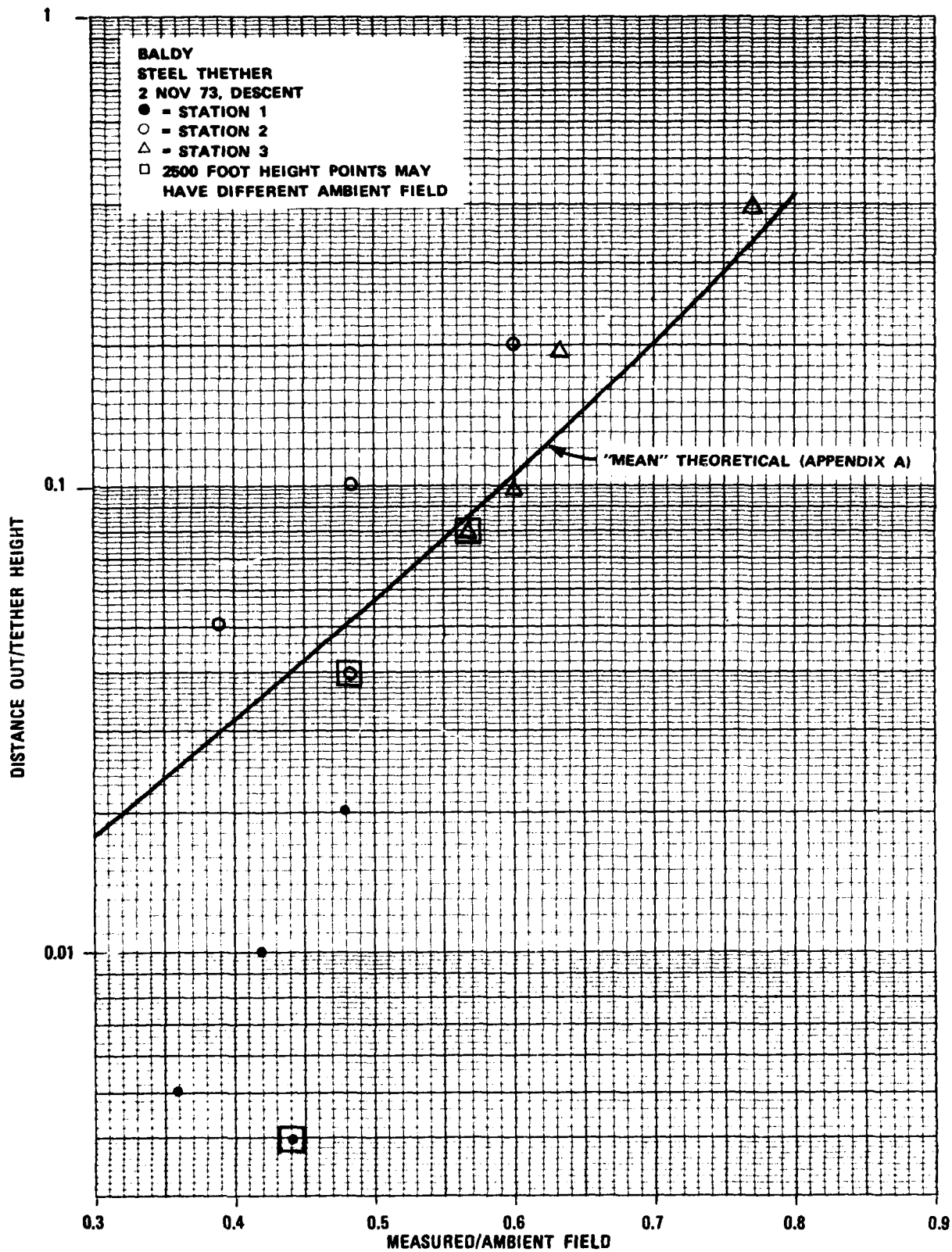
Figure 4.2 — Data Plot of Distance/Height vs Measured/Ambient Field, Descent

NASA-6 results as an independent check. Unfortunately, the air-earth current sensors were more sensitive to changes in electric field than to air-earth current. As field-change meters, they were very effective and may yield information based on this quirk. (This behavior is explained in appendix F).

Summary

1) Non-conducting tethers do not seem to perturb the potential gradient structure at the foot of the tether - we are not sure why.

2) Conducting tether perturbations at ground level can be adequately calculated for engineering purposes from simple theory.

SECTION 5 - RESULTS OF GROUNDING AND FLOATING A CONDUCTING TETHER

Figure 5.1 shows the data obtained from the Oct. 15 Baldy flight. Time intervals and voltages are summarized in Table 5.1.

If we assume that the balloon/tether is charging as an R-C system, and assuming that the final potential is 20 KV, we can find a time constant α from $V - V_0(1-e^{-t/}T)$ for each time and voltage. Table 5.1 shows that this time constant becomes larger as the balloon/tether reaches its equilibrium value. This is perfectly consistent with charging of the system by corona discharge. If the ambient potential at the top of the tether is roughly 50 V/m x 730 m or about 36.5 KV, the tether potential should reach approximately 18 KV, or 1/2 of the value spanned by the tether. This agrees quite well with the final value of $\sim$ 20 KV reached by the tether in this measurement.

The decrease of time constant with time is due to the decrease of the field at the tether surface. It is this field which causes the corona current which flows to the tether during rearrangement. Calculation indicates that the effective charging resistance is on the order of 10^{10} Ω, an appropriate value for corona current charging.

Fig. 5.2 shows data from another such measurement of the tether potential after the tether is released from ground. In this case, a calibrated field mill needing no connection to the tether was used to measure the tether potential. It is apparent that, even though the ambient electric potential gradient was approximately the same, the 31 Oct. measurement of Fig. 5.2 gives a rise time approximately 5 times as fast as the earlier experiment. In this case we seem to have a corona current charging resistance much lower than in the previous case.
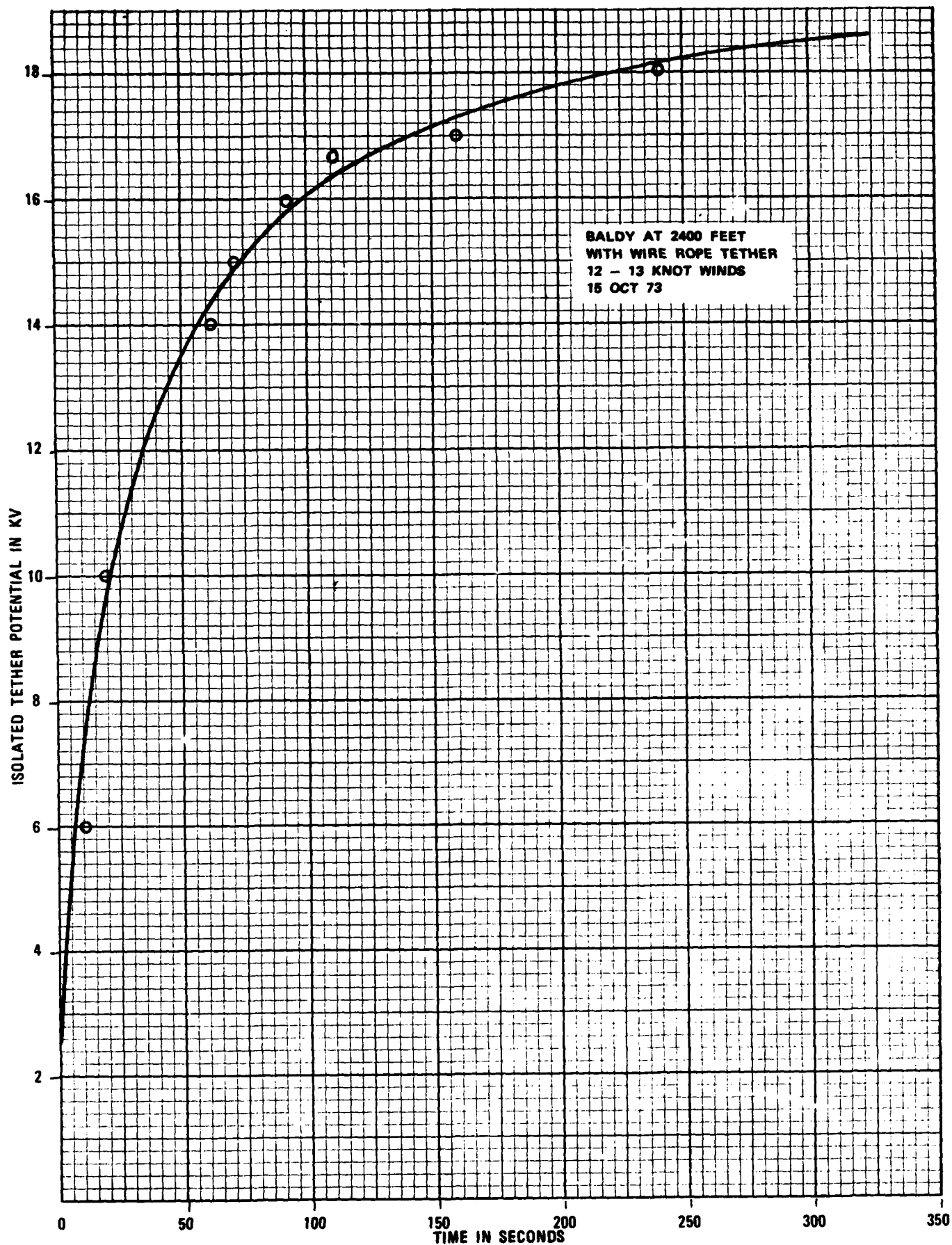
Figure 5.1 — Data Plot of Potential Gradient vs Time, Baldy — 15 Oct 73

The plot is labeled "BALDY AT 2400 FEET / WITH WIRE ROPE TETHER / 12 – 13 KNOT WINDS / 15 OCT 73". The vertical axis is "ISOLATED TETHER POTENTIAL IN KV" and the horizontal axis is "TIME IN SECONDS".

TABLE 5.1

MEASURED POTENTIAL FOR AN ISOLATED CONDUCTING TETHER
WELL ISOLATED FROM GROUND

time after tether lifted from ground (seconds)	potential of* tether (kV)	charging time** constant T (seconds)
10	6	27.7
20	10	28.6
60	14	50
70	15	50.5
90	16	55.6
120	16.6	66.7
160	17	83.3
240	18	104.2

*Measured with electrostatic voltmeter.

**Computed charging time constants based on isolated tether experiment.
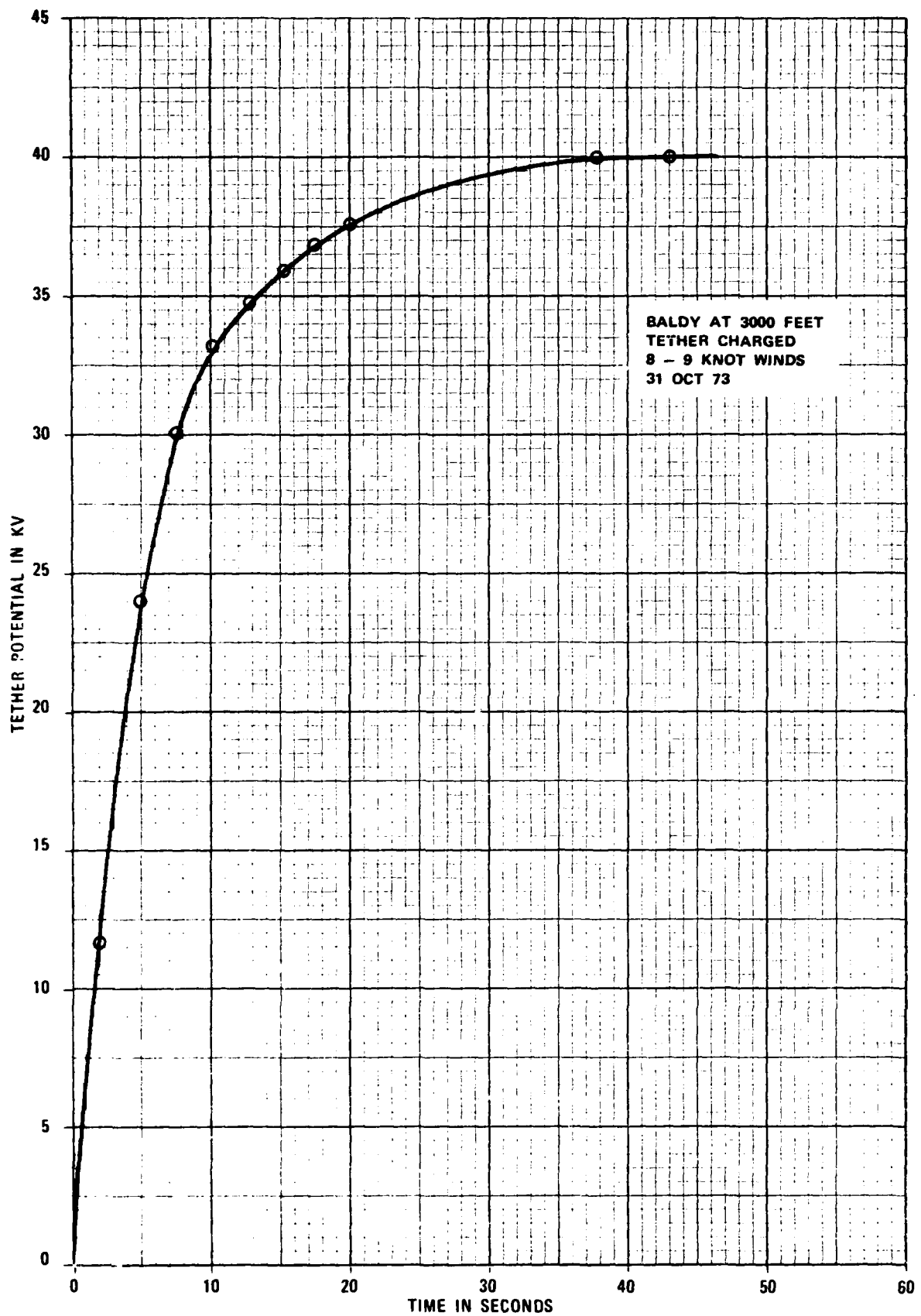
Figure 5.2 — Data Plot of Potential Gradient vs Time, Baldy — 31 Oct 73

The data of Oct. 17 and Nov. 8 show the same kind of pattern through potential gradient measurements made at distances of 10', 100', 200' and 500' from the tether point. Charging time on Nov. 8 was 80 sec, and on Oct. 17 40 sec. The heights were virtually identical on these days. The field at the ground on 8 Nov. was on the order of 100 V/m and on Oct. 17 was on that order also. Winds were 5-6 kt. on Oct. 17 and 2-4 kt. on Nov. 8; 12-13 kt. on 15 Oct. and 8-9 kt. on 31 Oct.

From the foregoing it appears that some anomaly existed during the Oct. 15 experiment. We have calculated T for the 31 Oct. experiment and find results as seen in Table 5.2. For the Baldy balloon, this yields an effective charging resistance of $\sim 1.5 \times 10^9$ Ω. Note that the charging resistance increases with time as is to be expected from corona charging if the potential gradient at the point of discharge is decreased due to increase in potential of the tether above the starting potential of OV. It would appear then, that the Oct. 15 data is spurious, perhaps due to the capacitance of the electrostatic voltmeter used for the potential measurement. From all measurements, it is clear that the tether is indeed assuming a potential reasonably close to 1/2 of the ambient near the top, which is theoretically expected.

Calculation of the charge involved is very simple: from Q = CV we find that for the Baldy at 2500 ft. with a resulting capacitance of 3550 pf (mostly in the tether) the charge transferred to the tether is 1.42×10^{-4} coul.

The time constants would of course be longer for a conducting tether/ balloon system such as the FII. In addition, the starting fields for corona current would be higher due to the larger tether diameter.

TABLE 5.2

MEASURED POTENTIAL FOR CONDUCTING
TETHER WELL ISOLATED FROM GROUND*

time (seconds)	potential (kV)	γ (seconds)
2.5	12	6.99
5	24	5.46
7.5	30	5.4
10	33.5	5.5
12.5	35	6.37
15	36.2	6.37
17.5	37	6.77
20	38	6.71
...		
37.5	40	——

*Measured with field mill which required no attachment to the tether.

Summary

1) By sequentially "floating" and grounding a conducting tether system, we have found the charging time constant to be on the order of 6-10 sec.

2) The charging of such a system is governed by a corona discharge process which is dependent on the difference between the ambient atmospheric potential and that of the tether where corona is taking place.

SECTION 6 - <u>INDUCED CURRENTS IN CONDUCTING TETHERS</u>

Unfortunately, the thunderstorm season was virtually over before any data concerning induced currents could be obtained. One visual determination was made for the BJ+3 flight with steel piggyback line. A current pulse in excess of 300 amperes peak-peak was seen from a storm which was at least 30 km away. One current pulse of order 25 amps peak-peak was recorded as a sferic from a storm which must have been (from the sferic characteristics) over 100 km away. Current pulses from close storms on the order of 2000 amperes have been recorded by Davis and Standring. Clearly, some measurements of this phenomenon are in order for summer '74, if possible.

SECTION 7 - CONCLUSIONS

We have found in this study that there is no simple model which can predict the potential gradient anomalies in the neighborhood of the balloon. Complications arise not only because the balloon is not a simple shape, but also, and of greater importance, because of the presence of space charge plumes generated by corona discharge from conducting tethers.

At the foot of the tether, and radially outward on the ground it appears that a conducting tether has a greater perturbation of the ambient field than a non-conducting one. The charging time constant for a conducting tether seems to be on the order of 10-20 sec, and charging is accomplished through corona discharge. This implies that the system is essentially in equilibrium as it is raised/lowered. Non-conducting tether systems seem to have a much longer time constant (see for example, the Baldy data in Fig. 2.3). Here, two passes some 2 hours apart demonstrated this slow charging toward the equilibrium state as determined by system capacitance, height, and ambient potential gradient. Certainly charging of a non-conducting tether and balloon is more complex than simply the resistance of the tether charging the capacitance of the balloon, because the capacitance of the tether to ground is on the same order as or larger than that of the balloon, leading to a distributed R-C system.

Passes over #204 indicate that if the balloon and part of the tether are in a high-conductivity region, i.e., above the atmospheric mixing layer, charging is inhibited because of the smaller difference in conductivities between the atmosphere and the tether and possible differences in triboelectric charging. Note, however, that this set of circumstances can only tend to slow down the charging, not inhibit it, depending on the state

of cleanliness of the tether and altitude with respect to the inversion.

Charging of non-conductive systems is also a function of tether cleanliness, both inside and out. It appears from data supplied by RML that, although highly variable, Nolaro tether resistances ran between $10^7 \Omega/m$ and $10^{11} \Omega/m$. Some samples improved when washed, others did not. It seems that capillary action in the interior of the tether plays a large part here.

In short, charging times for non-conducting tether systems will range from 1 to several hours, depending on circumstances, but the balloon/tether will finally acquire enough negative charge to be at effectively zero potential (ground). The question now remains as to the behavior of the two types of systems near an approaching or building thunderstorm.

It has been experimentally verified that lightning indeed strikes both types of systems. The data of Davis and Standring, coupled with that of known strikes to the TELTA systems at Cudjoe Key and strikes to lumber balloon-crane systems provides ample evidence. It might seem that the response time of the non-conductive system would tend to make such a system relatively immune to lightning. Even though this is so, the tether is still more conductive than the surrounding air, hence potential gradient distortion is still present, and even if the system is not in equilibrium from a charging standpoint, it still has a higher probability of sustaining a discharge than the air in the same place would have if the balloon were absent. It is interesting to note that the Cudjoe Key strikes occurred to the tether below the balloon, as might be expected if the upper part of the balloon/tether were in a relatively higher conductivity region than the lower part.

It appears from our work that the field perturbation due to either tether system is the same at least after the non-conductive tether system has come

42

to equilibrium - which will certainly be the case during flights of long duration. An additional factor which must be taken into account is wetting of balloon - tether by rain; the time constant to equilibrium (balloon essentially at zero potential) will be shortened considerably and may approach that of a conducting system. In this case, the system will look more like a conducting one - i.e., may have a shorter time constant than before wetting, and if any portion of the tether is kept dry near the ground, a "floating tether" can result with possible flashover on the dry portion to ground. There will not, however, be any corona discharge in the wet-tether case, and space-charge plumes will not exist. It is thus probable that the wet non-conducting tether has the highest strike probability of any combination.

A conducting tether system, with its relatively rapid response time, is almost certainly in equilibrium with the changing fields due to storm development or movement. There is, however, a plume of space charge, produced by corona discharge, associated with the tether. This plume will almost certainly lower the probability of a strike to the tether but may raise the probability of a strike to the balloon. Conducting systems should, according to this view, have corona dischargers on the topside of the balloon.

A primary question regarding direct strikes to balloons or tethers is the type of discharge. Are these typical of strikes to tall towers and buildings, i.e. a direct breakdown with downward travel of current pulse, or simply a stepped leader which has found a home and produces a regular multiple discharge with the current pulse traveling upward? Davis and Standring indicate that both types happen, with the former in preponderance

by about 2/3. They do not, however, note any particular conditions under which each type takes place, if any - this would be a desirable study.

The NASA-6 results point out that the anomalies in potential gradient over the top of the balloon can be observed at distances of 1/2 to 1/3 the height of the balloon. Since typical cloud bases for Cape Kennedy storms are ~1 km, the balloon will be close to or in the negative charge region of a storm, and the effective height of the balloon will be extended well above the balloon. In addition, calculations indicate that the horizontal extent of the balloon's influence on potential gradient at the balloon altitude are also on the order of 1/2 to 1/3 of the height.

This in turn implies that even if part of the lower charge in the storm were to be drained by the tether, there is a possibility of a "cloud-stroke" type of discharge directly to the balloon, and a "ground-stroke" type to the tether below the cloud.

Regardless of these speculations, we draw the conclusion that for equal height, the probability of a stroke to the balloon/tether system is roughly the same for both conducting and non-conducting tethers and probably higher for wet non-conducting tethers. A further, but weaker, assertion is made that the stroke will probably for either system occur to the tether rather than the balloon, although the latter is not excluded. We have found that each system perturbs the environment to about the same extent, but that a non-conducting tether has a far longer response time to changes in the ambient potential gradient, even if wet, since no corona is likely to be present. Clearly we need some data in high field conditions.

It would be somewhat presumptuous at this state to say - a balloon at

44

height h will sustain a stroke from a storm x miles away with a probability p - this probability might go down if the balloon is in cloud; it might go down for charge centers so close that copious corona discharge from a conducting tether or from balloon "dischargers" results - this study cannot determine this; a body of data is needed which is not available, specifically system behavior in high negative potential gradients.

We can state that the influence of the balloon surely is small at a distance from the balloon equal to twice its height - provided the balloon is not in cloud. It appears that a "strike zone" might be established consisting of a cylinder of radius = height of balloon and height = 2x height of balloon. Hence with safety factors, a storm more than 5 miles away will have a relatively low probability of striking the balloon, with the probability increasing with decreasing distance to the storm.

We have definitely determined that warning devices based on electric field amplitudes will not be affected if the warning system detectors are more than 1 balloon altitude away, and, if closer, effects can be crudely predicted from theory as on pp A-8 thru A-10, appendix A. Confirming data was good for this finding, and the result of Davis and Standring that the potential gradient is unaffected by a tether must be held questionable. It is quite clear that a conductive tether can be used as part of its own warning system through monitoring of the tether current.

Clearly, if at all possible, more information is desirable as to behavior during high negative fields, and especially for conducting tethers, behavior with regard to induced pulses. We feel that this information could be gotten in conjunction with routine flights.

APPENDIX A

THEORETICAL CALCULATION OF POTENTIAL AND FIELD
FOR VERTICAL GROUNDED ELLIPSOID

Uniform external field
$\vec{E}_0$ in - z direction

$\vec{E}_0$

z

r

a = ellipsoid height

b = base radius

$c = \sqrt{a^2 - b^2}$
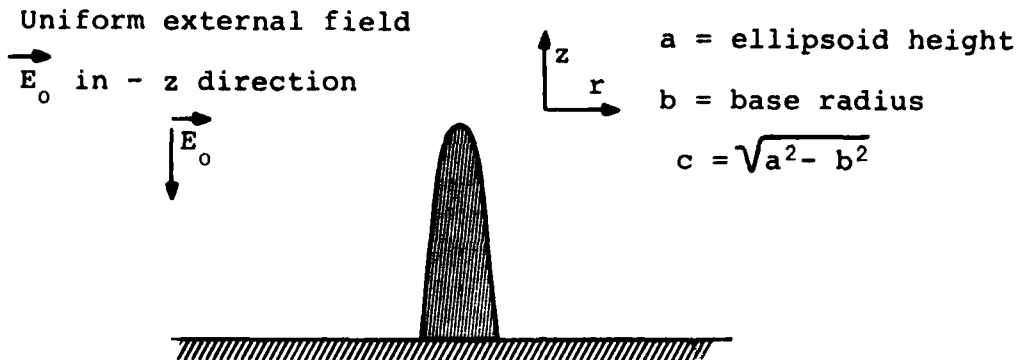
Define a set of confocal ellipsoids such that

$$\frac{z^2}{\xi + a^2} + \frac{r^2}{\xi + b^2} = 1 \tag{1}$$

The potential distribution has been given (e.g. Stratton,

"Electromagnetic Theory") as:

$$\phi = -E_0 z \left(1 - \frac{\int_{\xi}^{\infty} \dfrac{ds}{(s + a^2)^{3/2}(s + b^2)}}{\int_{0}^{\infty} \dfrac{ds}{(s + a^2)^{3/2}(s + b^2)}} \right) \tag{2}$$

The field components can be easily found from (2) by

differentiation:

$$E_z = -\frac{\partial \phi}{\partial z} \quad ; \quad E_r = -\frac{\partial \phi}{\partial r} \tag{3}$$

and if we symbolize the integrals in (2) by $\int_\xi^\infty$ and $\int_0^\infty$

$$E_z = E_0 \left(1 - \frac{\int_\xi^\infty}{\int_0^\infty}\right) + E_0 z \frac{\partial}{\partial z}\left(1 - \frac{\int_\xi^\infty}{\int_0^\infty}\right) \tag{4}$$

$$= -\frac{\phi}{z} + E_0 z \frac{\partial \xi}{\partial z}\cdot \frac{\partial}{\partial \xi}\left(1 - \frac{\int_\xi^\infty}{\int_0^\infty}\right) \tag{5}$$

$$= -\frac{\phi}{z} - E_0 z \frac{\partial \xi}{\partial z}\cdot \frac{1}{\int_0^\infty}\cdot \frac{\partial}{\partial \xi}\left(\int_\xi^\infty\right) \tag{6}$$

Now Liebniz' rule states:

$$\frac{d}{dq}\int_{g(q)}^{h(q)} f(x,q)dx = \int_g^h \frac{\partial}{\partial q} f(\gamma,q)\ dx + f(h,q)\frac{dh}{dq} - f(g,q)\frac{\partial g}{\partial q} \tag{7}$$

Hence, since $\frac{\partial}{\partial \xi}$ of the $f(s,a,b)$ of (1) = 0:

$$\frac{\partial}{\partial \xi}\left(\int_\xi^\infty\right) = -\frac{1}{\left(\xi + a^2\right)^{3/2}\left(\xi + b^2\right)} \tag{8}$$

Now from (1) we obtain:

$$\xi^2 + \xi(a^2 + b^2 - r^2 - z^2) + a^2 b^2 - z^2 b^2 - r^2 a^2 = 0 \tag{9}$$

A-2

then

$$\frac{\partial \xi}{\partial z} = \frac{2z(\xi + b^2)}{2\xi + a^2 + b^2 - r^2 - z^2} \tag{10}$$

and from (6) and (10)

$$E_z = -\frac{\phi}{z} + \frac{E_o z}{\int_0^\infty} \left(\frac{2\,z}{(\xi + a^2)^{3/2}(2\xi + a^2 + b^2 - r^2 - z^2)} \right) \tag{11}$$

Now to find E_r, we use (3) and (2):

$$-\frac{\partial \phi}{\partial r} = -\frac{E_o z}{\int_0^\infty} \frac{\partial \xi}{\partial r} \cdot \frac{\partial}{\partial r} \int_\xi^\infty \tag{12}$$

Similar to (10), we find

$$\frac{\partial \xi}{\partial r} = \frac{2r(\xi + a^2)}{2\xi + a^2 + b^2 - r^2 - z^2} \tag{13}$$

and

$$\frac{\partial \phi}{\partial r} = +\frac{E_o z}{\int_0^\infty} \left(\frac{2\,r}{(\xi + a^2)^{3/2}(\xi + b^2)(2\xi + a^2 + b^2 - z^2 - r^2)} \right) \tag{14}$$

Evaluating the integral of (2):

$$\int \frac{ds}{(s + a^2)^{3/2}(s + b^2)} = \frac{2}{c^2\sqrt{s + a^2}} + \frac{1}{c^3} \ln \frac{\sqrt{s + a^2} - c}{\sqrt{s + a^2} + c} \tag{15}$$

at s = ∞, the integral vanishes, and using the lower limit s = 0:

$$\int_0^\infty = -\frac{2}{ac^2} - \frac{1}{c^3} \ln \frac{a-c}{a+c} \qquad (16)$$

Substituting the values of (15) and (16) into (2):

$$\phi = -E_0 z \left(1 - \frac{\frac{2}{\sqrt{\xi+a^2}} + \frac{1}{c} \ln \frac{\sqrt{\xi+a^2}-c}{\sqrt{\xi+a^2}+c}}{\frac{2}{a} + \frac{1}{c} \ln \frac{a-c}{a+c}} \right) \qquad (17)$$

The complete expression for E_z is then

$$E_z = E_0 \left(1 - \frac{\frac{2}{\sqrt{\xi+a^2}} + \frac{1}{c} \ln \frac{\sqrt{\xi+a^2}-c}{\sqrt{\xi+a^2}+c}}{\frac{2}{a} + \frac{1}{c} \ln \frac{a-c}{a+c}} \right)$$

$$-2E_0 z^2 \left[\left[\frac{2}{ac^2} + \frac{1}{c^3} \ln \frac{a-c}{a+c} \right] \left[(\xi+a^2)^{3/2} (2\xi+a^2+b^2-z^2-r^2) \right] \right] \qquad (18)$$

and, for E_r:

$$E_r = -2E_0 rz \left/ \left(\left[\frac{2}{ac^2} + \frac{1}{c^3} \ln \frac{a-c}{a+c} \right] \left[(\xi+a^2)^{1/2} (\xi+b^2)(2\xi+a^2+b^2-z^2-r^2 \right. \right. \right.$$

$$(19)$$

A computer program (p A-6 and A-7) was written to evaluate (17), (18), and (19). Two cases were run using this program, but it was quickly seen that a separate run for each case of the field data was not feasible from a monetary and analysis time stand-point.

We are primarily interested in two specific cases: the z - component of the electric field at the ground (E_z for $Z = 0$, $r > b$) and the Z - component above the tether center (E_z for $r = 0, Z > a$). These correspond to the ground station data and the NASA flights. For these cases and for tethers which are of small diameter, the condition $a \gg b$ (or alternatively $a \approx c$) in order to simplify the equations.

At the ground, $Z = 0$ and

$$\xi = r^2 - b^2 \tag{20}$$

The second term in (18) vanishes, and

$$\frac{E_z}{E_o} = 1 - \frac{\dfrac{2}{\sqrt{r^2 + c^2}} + \dfrac{1}{c} \ln \dfrac{\sqrt{r^2 + c^2} - c}{\sqrt{r^2 + c^2} + c}}{\dfrac{2}{a} + \dfrac{1}{c} \ln \dfrac{a - c}{a + c}} \tag{21}$$

TABLE A.1

COMPUTER PROGRAM FOR CALCULATING POTENTIALS AND FIELD NEAR A
VERTICAL CONDUCTING GROUNDED PROLATE ELLIPSOID

```
FURPUR 25.1-06/28-16:03
DJL*DJLLIB.ELLIPSE
    1              DOUBLE PRECISION EO,A,B,C,F,D,X,R,S,RR,T,XI,DD,
    2             1XIX,XIR,E,XIA,AA,AB,AC,PHI,EX,ER
    3              DIMENSION X(100),R(100),PHI(4),EX(4),ER(4)
    4       C        ENTER A,B,EO
    5              EO=1.DO
    6              A=1000.DO
    7              B=.01DO
    8              C=DSQRT(A**2-B**2)
    9              F=DLOG(B**2/(4.DO*A**2))
   10              D=-2.DO/(A*C**2)
   11              D=D-F/C**3
   12       C        CALCULATE X'S&R'S
   13              N=40
   14              M=20
   15              X(1)=50.
   16              DO 10 1=2,N
   17       10    X(I)=X(I-1)+X(1)
   18              R(1)+2.DO
   19              DO 20 J=2,M
   20       20    R(J)=R(J-1)+R(1)
   21       C         CALCULATE XI AND FIELD VALUES FOR X,R GOING OUT
   22              K=0
   23              DO 30 I=1,N
   24              WRITE(6,1000)X(I)
   25     1000    FORMAT(10X,'XEQUALS',F10.5/)
   26              DO 35 J=1,M
   27              K=K+1
   28       C        CALC. XI
   29              S=A**2+B**2-X(I)**2-R(J)**2
   30              RR=-X(I)**2*B**2-R(J)**2*A**2+A**2*B**2
   31              T=S**2-4.DO*RR
   32              XI=-S+DSQRT(T)
   33              XI=XI/2.DO
   34       C        CALC DXI/DX,DXI/DR
   35              DD=2.DO*XI+S
   36              XIX=2.DO*X(I)*(XI +B**2)/DD
   37              XIR=2.DO*R(J)*(XI+A**2)/DD
   38       C        CALC PHI
   39              XIA=DSQRT(XI+A**2)
   40              AA=DLOG((XIA-C)/(XIA+C))
   41              AB=-(2.DO/XIA)/C**2
   42              AC=-AA/C**3
   43              AB=1.DO-(AB+AC)/D
   44              PHI(K)=EO*X(I)*AB
```

```
45      C           CALC EX
46                  E=(EO*X(I)/D)*(1.DO/XIA**3/(XI+B**2))
47                  EX(K)=E*XIX+PHI(K)/X(I)
48                  ER(K)=E*XIR
49                  IF(K.NE.4)GO TO 35
50                  L=J-4
51                  WRITE(6,1001)(R(L+N),PHI(N),EX(N),ER(N),N=1,4)
52            1001  FORMAT(1X,4(4F8.3)/)
53                  K=0
54        35        CONTINUE
55        30        CONTINUE
56                  CALL EXIT
57                  END
```

NOTES:

1. EO is undisturbed ambient field (Eo)

2. A is (a) ⎤
    B is (b) ⎬   Parameters defined on p A-1
    C is (c) ⎦
    R is Radial distance (r)
    X is height (z)

3. PHI is potential at the point z,r
    (ϕ given by equation 17)

4. EX is vertical field component
    (E_z given by equation 18)

5. ER is radial component
    (E_r given by equation 19)

Applying a ≈ c >> b:

$$\frac{E_z}{E_0} = 1 - \frac{\sqrt{\dfrac{2}{\sqrt{r^2 + a^2}} + \dfrac{1}{a} \ln \dfrac{\sqrt{r^2 + a^2} - a}{\sqrt{r^2 + a^2} + a}}}{\dfrac{2}{a} + \dfrac{1}{a} \ln \left(\dfrac{b^2}{4a^2}\right)}$$ (22)

and, in terms of the parameter $x = \sqrt{1 - r^2/a^2}$:

$$\frac{E_z}{E_0} = 1 - \frac{\dfrac{2}{x} + \ln \dfrac{x - 1}{x + 1}}{2 + \ln \dfrac{b^2}{4a^2}}$$ (23)

We can develop the following table for r/a (distance from tether/ tether height) vs. E_z/E_0 (Field at distance r/undisturbed field), keeping in mind that in reality, sensor location and the nonuniformity of E_0 with height and, to a lesser extent, spatial location make deviation from this ideal case likely.

We calculate first the denominator, taking

$$D = \frac{1}{2 \left(1 + \ln \dfrac{b}{2a}\right)}$$ (24)

For b = 1/8"

a(ft)	D
500	-.0477
1000	-.0448
1500	-.0432
2000	-.0422
2900	-.0414
3000	-.0408
4000	-.0398
5000	-.0391

For b = 3/4"

a(ft)	D
1000	-.0533
2000	-.0497
4000	-.0465
8000	-.0437
10,000	-.0428

A-8

and the numerator, covering most cases of interest;

$$N = \frac{2}{\sqrt{1 + \dfrac{r^2}{a^2}}} + \ln \frac{\sqrt{1 + \dfrac{r^2}{a^2}} - 1}{\sqrt{1 + \dfrac{r^2}{a^2}} + 1} \tag{25}$$

r/a	N
1	- .3485
.1	-4.0064
.01	-8.5968
.001	-13.2018

Some of this family of curves is shown on p A-10.

$$E_z/E_0 = \left(1 - DN\right) \tag{26}$$

Now over the top of the tether (or tower); $r = 0$ and from (1)

$$z^2 = \xi + a^2 \tag{27}$$

Substituting into (18) we find:

$$E_z = E_0 \left(1 - \frac{\dfrac{2}{z} + \dfrac{1}{c} \ln \dfrac{z - c}{z + c}}{\dfrac{2}{a} + \dfrac{1}{c} \ln \dfrac{a - c}{a + c}} \right)$$

$$- \frac{E_0 z^2}{\left(\dfrac{2}{ac^2} + \dfrac{1}{c^3} \ln \dfrac{a - c}{a + c} \right) (z^3)(z^2 - c^2)} \tag{28}$$

Again, appealing to $a \simeq c \gg b$; $Z > a$:

$$E_z \simeq E_0 \left(1 - \frac{\dfrac{2}{z} + \dfrac{1}{a} \ln \dfrac{z - a}{z + a}}{\dfrac{2}{a} + \dfrac{1}{a} \ln \left(\dfrac{b}{2a}\right)^2} \right) - \frac{E_0}{\left(\dfrac{2}{a^3} + \dfrac{1}{a^3} \ln \left(\dfrac{b}{2a}\right)^2 \right)(z)(z^2 - a^2)} \tag{29}$$
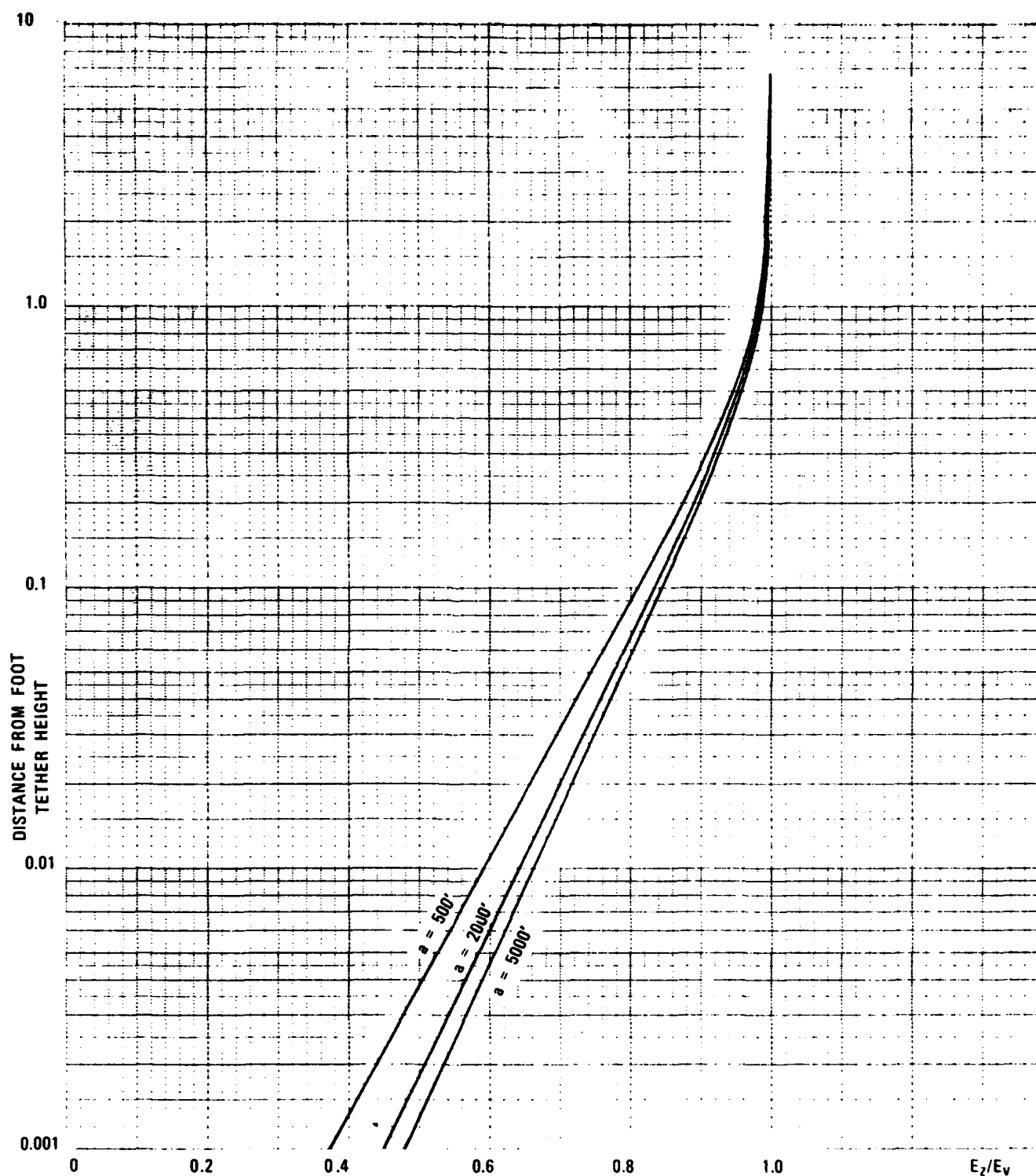
Figure A.1 — Suppression of Vertical Field (E_z) on the Ground at Some Distance (R) from the Tether Point With a Balloon at Altitude (a)

$$= E_o \left(1 - \frac{\frac{2}{z} + \ln \frac{z - a}{z + a}}{2 + \ln\left(\frac{b}{2a}\right)^2} - \frac{a^3}{2 + \ln\left(\frac{b}{2a}\right)^2 (z)(z^2 - a^2)} \right) \qquad (30)$$

Following are some values of a,b,Z. The program can be found on p A-12.

For b = 1/8" (tether diameter)

and a = 500'   a = 1000'   a = 2500'

Z-a	E_z/E_0		Z-a	E_z/E_0		Z-a	E_z/E_C
100'	1.06		100'	1.14		100'	1.40
200'	1.01		200'	1.05		200'	1.17
500'	1.00		500'	1.01		500'	1.05
						1000'	1.02

for b = 3/4"

and a = 1000'   a = 2000'   a = 3000'

Z-a	E_z/E_0		Z-a	E_z/E_0		Z-a	E_z/E_0
100	1.17		100	1.37		100	1.58
200	1.06		200	1.15		200	1.25
500	1.01		500	1.04		500	1.07
1000	1.00		1000	1.01		1000	1.02

a = 5000'   a = 10,000'

Z-a	E_z/E_0		Z-a	E_z/E_0
100	1.98		100	2.97
200	1.45		200	1.93
500	1.14		500	1.32
1000	1.05		1000	1.13

TABLE A.2

VERTICAL FIELD INTENSIFICATION ABOVE
BALLOON (EQUATION 30)

```
Oprt,s dlib.fieldex
FURPUR 25.1-0 1/28-12:12
HWP*DLIB.FIELDEX
     1              WRITE(6,10)
     2           10 FORMAT('1',3X,'X',4X,'A',4X,'B',8X,'EX'//)
     3        C
     4           20 READ(5,30,END=100)X,AA,BB
     5           30 FORMAT(4F5.0)
     6              IF(X,LE.0.0)GO TO 100
     7              IF(AA.NE.0.0)A=AA
     8              IF(BB.NE.0.0)B=BB
     9              IF(A.LT.Z)GO TO 50
    10              WRITE(6,40)X,A
    11              GO TO 20
    12           50 P1=2.*A/X+ALOG((X-A)/(X+A))
    13              P2=2.+ALOG((B/2.*A)**2)
    14              P3=2.+ALOG((B/2.*A)**2) * X *(X*X - A*A)
    15              EX=1.-P1/P2-A**3/P3
    16              WRITE(6,60)EX,P1,P2,P3
    17           60 FORMAT(21X,F10.2,10X,5E13.5)
    18           40 FORMAT(/',A GREATER THAN X !!!'/1X,2F5.1)
    19              GO TO 20
    20        C
    21          100 WRITE (6,110)
    22          110 FORMAT (//'PROCESSING ENDED')
    23              CALL EXIT
    24              END
```

for B = 1.5' and a = 500' (tower)

Z-a	E_z/E_O
100	1.14
200	1
300	1

at $\xi = 0$, the surface of the ellipsoid,

$$E_r = \frac{E_o z}{\int_0^\infty} \left(\frac{2r}{ab^2 (a^2 + b^2 - r^2 - z^2)} \right) \tag{31}$$

and if $a \gg b$

$$E_r = \frac{E_o z}{\int_0^\infty} \cdot \frac{2}{a^3 b \left[1 - \frac{z^2}{a^2} \right]^{1/2}} \tag{32}$$

$$\sim \frac{-E_o z}{2b \left[1 + \ln \frac{b}{2a} \right] \sqrt{1 - \frac{z^2}{a^2}}} \tag{33}$$

Using values from p A-8, we find that near the tip of a 1/8"
tether $(Z^2/a^2 = 0.99)$

a(ft)	E_r/E_O
500	2.29×10^4
1000	4.30×10^4
1500	6.22×10^4
2000	8.10×10^4
2500	9.94×10^4

This function, plotted for a = 2500' and b = 1/8 is shown
on p A-14.
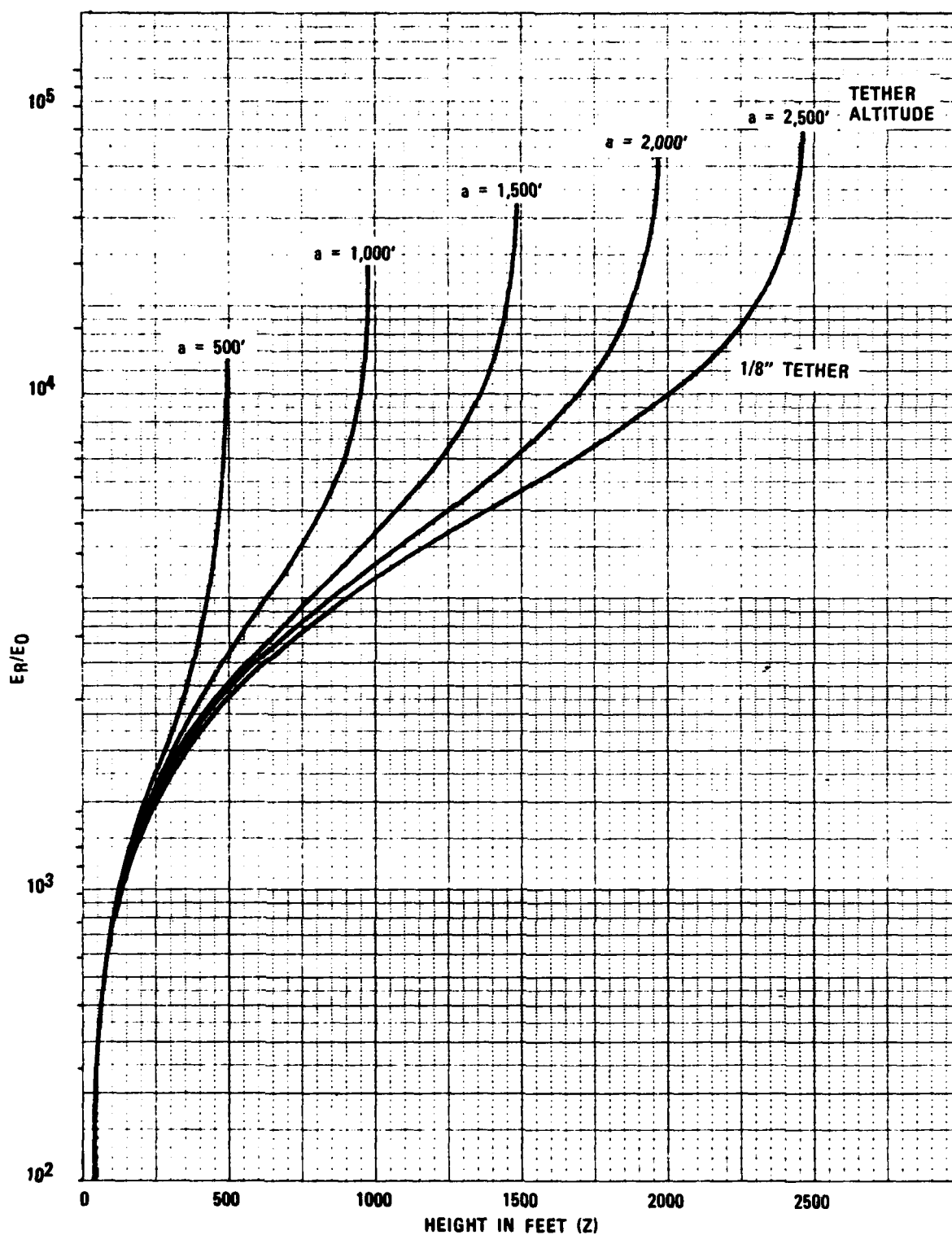
Figure A.2 — Intensification of Radial Component of Electrical Field (E$_R$) Near Tether at Altitude (a)

A-14

APPENDIX B

HORIZONTAL CONDUCTING PROLATE ELLIPSOID IN AN EXTERNAL FIELD

$$c^2 = \sqrt{a^2 - b^2}$$
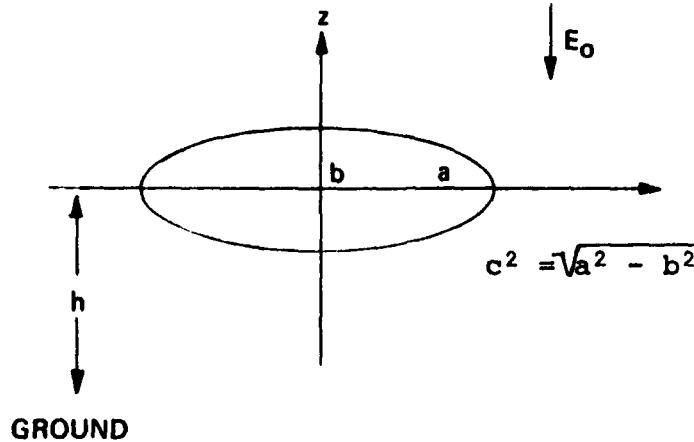
GROUND

We assume that a grounded body at altitude (h) (e.g. a tethered conducting balloon) has a capacitance to ground very little different from its capacitance to free space. That is, we can neglect effects due to the ground and the image balloon as well as the tether, the latter over the top of the body. The potential ϕ_0 can be expressed in this case as $\phi_0 = -E_0 (z + h)$, placing the potential on the axis of the body at a horizontal distance of $\phi_0 = -E_0 h$ (E_0 is the uniform external field). We thus have (again from Stratton)

$$\phi = -E_0 (z + h) + \frac{E_0 (z + h)}{\displaystyle\int_0^\infty \frac{ds}{(s + b^2)^2 \sqrt{s + a^2}}} \cdot \int_\xi^\infty \frac{ds}{(s + b^2)^2 (s + a^2)^{1/2}} \tag{1}$$

since the potential of the body is zero. If $c^2 = a^2 - b^2$ as before, the integral has the form:

$$\int \frac{ds}{(s + b^2)^2 \sqrt{s + a^2}} = -\frac{\sqrt{s + a^2}}{c^2 (s + b^2)} - \frac{1}{2c^3} \ln \frac{\sqrt{s + a^2} - c}{\sqrt{s + a^2} + c} \tag{2}$$

and

$$\phi = -E_0(z + h) + \frac{E_0\ (z + h)}{\dfrac{a}{c^2 b^2} + \dfrac{1}{2c^3}\ln\dfrac{a - c}{a + c}}$$

$$\left(\frac{\sqrt{\xi + a^2}}{c^2\ (\xi + b^2)} + \frac{1}{2c^3}\ \ln\ \frac{\sqrt{\xi + a^2} - c}{\sqrt{\xi + a^2} + c}\right) \tag{3}$$

Again, we wish only the solution for E_z above the center of the body (i.e. $x = 0$), starting from (1) again:

$$-\frac{\partial \phi}{\partial z} = E_z = E_0 - \frac{E_0\ \xi}{\int_0^\infty} \int^\infty - \frac{E_0\ (z + h)}{\int_0^\infty} \frac{\partial \xi}{\partial z} \cdot \frac{\partial}{\partial \xi} \int_\xi^\infty \tag{4}$$

And since $z^2 = \xi + b^2$ @ $x = 0$ $\frac{\partial \xi}{\partial z} = 2z$;

$$\frac{\partial}{\partial \xi} \int_\xi^\infty = -\frac{1}{z^4\ \sqrt{z^2 + c^2}} \tag{5}$$

B-2

and

$$\frac{E_z}{E_0} = 1 - \frac{\dfrac{\sqrt{z^2 - c^2}}{z^2} + \dfrac{1}{2c}\ln\dfrac{\sqrt{z^2 + c^2} - c}{\sqrt{z^2 + c^2} + c}}{\dfrac{a}{b^2} + \dfrac{1}{2c}\ln\dfrac{a - c}{a + c}}$$

$$+ \frac{2(z+h)c^2}{\left(\dfrac{a}{b^2} + \dfrac{1}{2c}\ln\dfrac{a - c}{a + c}\right) z^3 \sqrt{z^2 + c^2}} \tag{6}$$

A program to evaluate this function is given on p B-4.

Field Calculations for a Horizontal Charged Prolate Ellipsoidal Body

Again, as in the first part of Appendix B:

$$\frac{x^2}{\xi + a^2} + \frac{z^2}{\xi + b^2} = 1 \tag{7}$$

And, from Stratton:

$$\phi = \frac{Q}{8\pi\epsilon_0} \int_{\xi}^{\infty} \frac{ds}{(s + b)(s + a)^{1/2}} \tag{8}$$

TABLE B.1

INTENSIFICATION OF VERTICAL FIELD ABOVE
THE BALLOON

```
Oprt,s dlib.fieldex
FURPUR 25.1-02/98-10:18
HWP*DI.IB.FIELDEX
     1              WRITE(6,5)
     2           5  FORMAT('1',3X,'X',4X,'A',4X,'B',4X,'H',8X,'EX'//)
     3        C
     4          20  READ(5,30,END=100)Z,AA,BB,HH
     5          30  FORMAT(4F5.0)
     6              IF(Z.LE.0.0)GO TO 100
     7              IF(AA.NE.0.0)A=AA
     8              IF(NH.NE.0.0)H=HH
     9              IF(BB.NE.0.0)B=BB
    10              IF(A.LT.Z)GO TO 50
    11              WRITE(6,40)X,A
    12              GO TO 20
    13          50  C2=A*A-B*B
    14              C=SQRT(C2)
    15              Z2C2=SQRT(Z*Z*C*C)
    16        C
    17              P1=Z2C2/Z**2+ALOG((Z2C2-C)/(Z2C2+C))/(2.*C)
    18              P2=A/B**2+ALOG((A-C)/(A+C))/(2.*C)
    19              P3=2.*(Z+H)*C**2
    20              P4=P2*Z**3*Z2C2
    21              EX=1.+P1/P2+P3/P4
    22              WRITE(6,60)EX,P1,P2,P3,P4
    23          60  FORMAT(26X,F10.2,10X,5E13.5)
    24          40  FORMAT(/' A GREATER THAN Z'/1X,2F5.1)
    25              GO TO 20
    26        C
    27         100  WRITE(6,110)
    28         110  FORMAT(//I PROCESSING ENDED')
    29              CALL EXIT
    30              END
```

NOTES: X is height above balloon (Z)
            A is major-axis intercept (a) or 1/2 balloon length
            B is minor-axis intercept (b) or 1/2 radius
            H is balloon flight altitude (h)
            EX is vertical component of E-field (E_z)

where Q is the charge on the body, Then,

$$\phi = \frac{Q}{8\pi\varepsilon_0} \cdot \left[\frac{1}{c} \ln \frac{\sqrt{\xi + a^2} + c}{\sqrt{\xi + a^2} - c} \right] \tag{9}$$

* NOTE   z is now the height of measurement point above balloon;
         not the height above ground.

Again we find the fields from (8):

$$E_z = - \frac{\partial \phi}{\partial z}; \quad E_x = - \frac{\partial \phi}{\partial x} \tag{10}$$

$$- \frac{\partial \phi}{\partial z} = - \frac{Q}{8\pi\varepsilon_0} \cdot \frac{\partial \xi}{\partial z} \cdot \frac{\partial}{\partial \xi} \int_{\xi}^{\infty} \frac{ds}{(s + b^2)(s + a^2)^{1/2}} \tag{11}$$

$$= - \frac{Q}{8\pi\varepsilon_0} \cdot \frac{2z(\xi + a^2)}{2\xi + a^2 + b^2 - x^2 + z^2} \cdot \frac{-1}{(\xi + b^2)(\xi + a^2)^{1/2}} \tag{12}$$

$$= \frac{Q}{4\pi\varepsilon_0} \frac{z(\xi + a^2)^{1/2}}{(2\xi + a^2 + b^2 - x^2 - z^2)(\xi + b^2)} \tag{13}$$

and similarly

$$E_x = \frac{Q}{4\pi\varepsilon_0} \cdot \frac{x}{(2\xi + a^2 + b^2 - x^2 - z^2)(\xi + a^2)^{1/2}} \tag{14}$$

Above the top, $z^2 = \xi + b^2$, and:

$$E_z = \frac{Q}{4\pi\epsilon_0} \cdot \frac{1}{z(z^2 + c^2)^{1/2}} \qquad (15)$$

For a natural shape balloon, $c = 0$ and we recover the expected result for the sphere:

$$E_z = \frac{Q}{4\pi\epsilon_0} \cdot \frac{1}{z^2} \qquad (16)$$

APPENDIX C

SOME STATIC ELECTRICAL CHARACTERISTICS OF BALLOONS AND TETHERS

Capacitance of balloons:

The capacitance to free space of a prolate ellipsoid is given as:

$$C = \frac{8\pi \epsilon_0 c}{\ln \frac{a+c}{a-c}} \tag{1}$$

where a, b, and c are defined as in appendixes A and B. For the balloons in use during tests:

Baldy: $a = 5$ m $b = 1.5$ m $c = 4.77$ m $c^2 = 22.75$

$\quad\quad\quad$ C $\simeq$ 300 pF

BJ+3: $a = 15$ m $b = 5$ m $c = 14.14$ m $c^2 = 200$

$\quad\quad\quad$ C $\simeq$ 900 pF

Family II (204) $a = 24.8$ m $b = 8.07$ m $c = 23.45$ m $c^2 = 550$

$\quad\quad\quad$ C $\simeq$ 0.008 μF

Capacitance to ground of tethers:

(From Scientific Papers of the NBS #568: Methods, Formulas and Tables for Calculation of Antenna Capacity)

FOR SINGLE WIRE VERTICAL ANTENNAS:

if a = tether height (ft)

$\quad$ h = height off ground of tether bottom (ft)

$\quad$ d = diameter of tether (ft)

Then

$$C = \frac{7.36a}{\log_{10} \frac{2a}{d} - k} \quad \text{pF} \tag{1}$$

where k is determined from:

$$k = 0.4343 \log_{10} \frac{h}{a} + \frac{h}{a} \log_{10} \frac{4h}{a} + \left(1 + \frac{h}{a}\right) \log_{10}\left(1 + \frac{h}{a}\right)$$

$$- \left(1 + \frac{2h}{a}\right) \log_{10}\left(1 + \frac{2h}{a}\right) \qquad \frac{h}{a} \le 1 \tag{2}$$

with $h/a \ll 1$, and for reasonable values of a and d, we have the highly approximate but "good enough" relationship:

$$\underline{C(pF) \simeq 1.3a \ (ft)}$$

FIELD ENHANCEMENT AT TOP OF TETHERED BALLOONS

Assume that the balloon is essentially at ground potential. This means that if the balloon is at height h in a uniform field E_0, it can be treated as an isolated charged body with charge $Q = -CV = -E_0 hC$.

Then

$$\frac{F_{top}}{F_0} = \frac{2ch}{ab \ \ln\frac{a+c}{a-c}} \tag{3}$$

For Baldy:
$$F_{top}/F_0 = 0.5h(m)$$

For BJ+3:
$$F_{top}/F_0 = 0.1h$$

And for
FII(204):
$$F_{top}/F_0 = 0.66h$$

As an example, a FII balloon at 4 km altitude in an external potential gradient of 50 V/m will have a gradient at the top surface of 13.1 kV/m.

APPENDIX D

A CYLINDRICALLY SYMMETRICAL POISSON SOLVER

This program solves $\nabla^2 \phi = \dfrac{\rho}{\epsilon_o}$ where ϕ is potential and ρ is the space charge concentration at a gridpoint. The equation reduces to

$$\frac{1}{r} \frac{\partial^2 \phi}{\partial r^2} + \frac{\partial^2 \phi}{\partial z^2} = \frac{\rho (r,z)}{\epsilon_o} \tag{1}$$

and is solved by numerical approximation in an over-relaxation technique. The program automatically reads input potentials at gridpoints. Any of these that are zero are assumed to be conductors connected to a common zero potential point. The program, p D-2, has been annotated and is self-explanatory; some results are given on p D-4 and show that the theoretical approach (appendix A) is satisfactory.

FINITE DIFFERENCE SOLUTION COMPUTER PROGRAM
FOR POISSONS EQUATION

```
Oprt,s hwplib.pot
HWP*HWPLIB.POT
    1              COMPILER (DIAG=2)
    2              SUBROUTINE POT(PHI,R,Z,N,M,Q,K)
    3              DIMENSION PHI(N,M),R(N),Z(M),Q(N,M)
    4              E=1.
    5              A=1.1
    6              NN=N-1
    7              MM=M-1
    8              K=0
    9              F=1.8094E-8
   10      30      DO 50 I=2,NM
   11       6 FORMAT(1X,10E8.3)
   12              DO 50 J=2,MM
   13              IF (PHI(I,J).EQ.0.) GO TO 50
   14              IF(PHI(1.J).NE.0.)PHI(1,J)=PHI(2,J)
   15              DIFG=Z(J+1)-Z(J)
   16              DIFJ=Z(J+1)-Z(J-1)
   17              DIFH=DIFJ-DIFG
   18              DIFA=R(I+1)-R(I)
   19              DIFB=R(I+1)-R(I-1)
   20              DIFC=DIFB-DIFA
   21              DIFE=R(I+1)-2.*R(I)+R(I-1)
   22              AA=((DIFC/R(I))+2.)/(DIFA*DIFB)
   23              BB=(2.-(DIFA/R(I)))/(DIFC*DIFB)
   24              CC=((DIFE/R(I)-2.)/DIFA*DIFC))-2./(DIFG*DIFH))
   25              DD=2./(DIFG*DIFJ)
   26              EE=2./(DIFH*DIFJ)
   27              S=AA*PHI(I+1,J)+BB*PHI(I-1,J)+CC+PHI(I,J)+DD*PHI(I,J+1
   28             1+EE*PHI(I,J-1)-F*Q(I,J)
   29              PHI(I,J)=PHI(I,J)-S*A/CC
   30              RN=ABS(S*A/CC)
   31      50 IF(RN.GT.RO)RO=RN
   32              K=K+1
   33              IF(K.GT.50)GO TO 70
   34              IF(RO1.LT.RO.AND.RO2.LT.RO1)GO TO 80
   35              RO2=RO1
   36              RO1=RO
   37              RO=0.
   38              IF(RO1.GT.E)GO TO 30
   39              GO TO 90
   40      70 WRITE(6,71)
   41      71 FORMAT(1X,'STOP,EXCESSIVE STEPS')
   42              GO TO 90
   43      80 WRITE(6,81)
   44      81 FORMAT(1X,'STOP,DIVERGING REMAINDER')
   45      90      RETURN
   46              END
```

NOTES:

Card No	Note
4	Minimum error in ϕ
5	Relaxacion constant
8	Iteration counter
9	Charge in particles/M^3 multiplier
13	Check boundaries, etc. for conductors
14	$E_r = 0$ at $r = 0$ for nonconducting core
15-21	Calculate differences (non-equal grid spacing)
22-26	Calculate V^2 coefficient
27,28	Calculates $\nabla^2\phi - FQ$ = remainder(s)
29	Corrects ϕ (I,J) for next pass
30,31	Sets maximum error in pass
32	Test for maximum number of iterations
34-36	Tests for convergence
38,39	Tests for (maximum error) < (error bound)
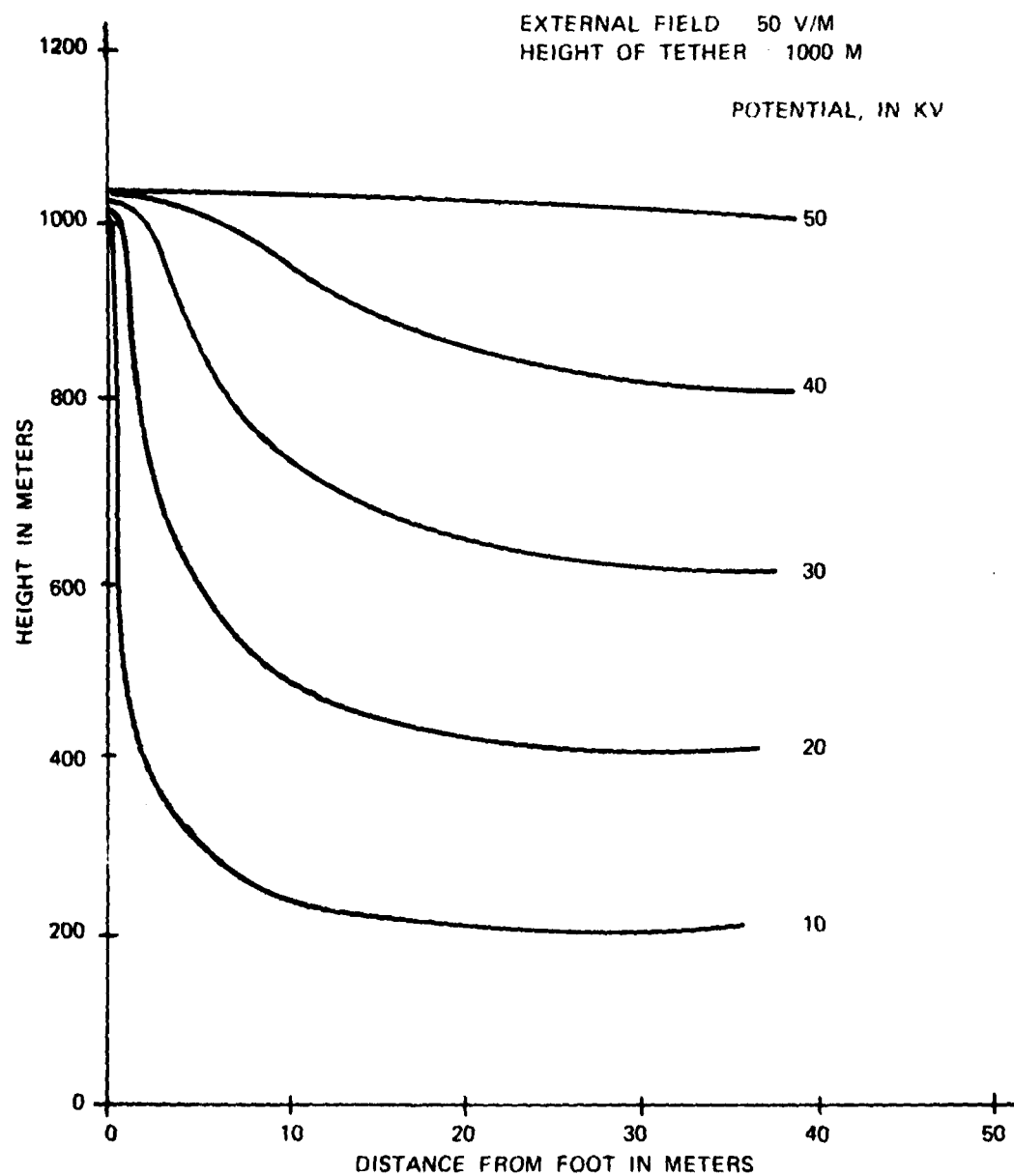
Figure D.1 — Poisson Solver Curves for Various Potentials

D-4

APPENDIX E

CHARGE TRANSFER TO AIR BY CORONA CURRENT FROM TETHER

We begin by calculating the length of tether from which current flows neglecting shielding, i.e., assuming wind strips off ions as they are formed by corona discharge (this will give max value). The field value for initiation of corona discharge is taken as 3×10^6 V/m. From p A-11, A-13, and A-14 it is evident that in an external field of 50 V/m, corona discharge occurs only near the tip of the tether, say in the last few feet. For practical purposes then, the corona discharge can be considered as a point source and will spread as a passive contaminant introduced into a turbulent field. Note that we have assumed that the field enhancement is occurring near the tip of a long, thin needle-shape whereas we have a constant diameter cylinder terminated in a "blob" (confluence point). It is possible that some point near the confluence point is actually in corona, i.e., a stray cable end or some similar point. Against this is the small value of K (Chalmers & Mapleson) found for our system (sect. 3). Even so, the geometry near the tip will control, and we still have a point source. For either case, the length over which the discharge takes place is small compared to other dimensions of the problem, and a point source can be assumed. For a 1/8 inch tether (00.1 ft) 1000 wire diameters is only 3 meters downstream, and the wake effects due to the tether have effectively vanished (Slichting, Boundary Layer Theory). Since the wake grows as $x^{1/2}$ (x downstream coordinate)

the width of the wake at this point is of the order 1.4 meters, which is on the order of the distance down from the tip of the ellipsoid over which corona production can be expected. We, therefore, expect a conical plume of space charge, extending downwind, which has a constant source of ions at its head. Experiment (Fig. 3.4, etc.) shows that at 2,300 ft altitude, we can expect a tether (corona) current on the order of 10^{-5} ampere (with no corona "point"). This is a source strength of 10^{-5} coul/s, or $\sim 6 \times 10^{13}$ e/s.

The following picture thus emerges so far: we have a point source of a passive additive to the airflow which leads to the formation of a cone of charge growing downstream from the point. We are also looking for a steady-state solution, as the time to establish the cone will be short compared to the time at altitude for the source. We also expect that far enough downstream the charges will be spread throughout the boundary layer.

We now need to find the spreading of this cone as a function of downstream distance and mean wind speed. Pasquill ("Atmospheric Diffusion," Van Nostrand, 1962) indicates that a Gaussian profile for the concentration holds, such that if x is the downwind distance from the point of origin (cone axis) z is vertical and y is horizontal,

$$X(x,y,z) = \frac{Q}{2\pi \bar{u} \sigma_y \sigma_z} \, e^{-\frac{1}{2} \left(\frac{y^2}{\sigma_y^2} + \frac{z^2}{\sigma_z^2} \right)} \tag{1}$$

where x,y,z measured from point of origin of the "contaminant."
Here, $\bar{u}$ is the mean wind, Q is the source strength, χ is con-
centration, and σ_y and σ_z are the variances of χ in the u and
z directions. We now need to relate σ_y and σ_z to the cross-
wind and vertical velocity variances in turbulent flow, σ_v and
σ_w.

Lumley and Panofsky (The Structure of Atmospheric Turbulence,
Wiley, 1964), p. 145 gives some data from Brookhaven which in-
dicates σ_v does not vary much w/height and thus for our wind
speeds ($\sim$ 5 m/s to 10 m/s) we have a $\sigma_v \sim 1.0$ to 2.0 m/s.

The vertical variance depends strongly on the stability of the
atmosphere, increasing upwards (in the boundary layer) in un-
stable air and decreasing upwards in stable air. Since during
our experiments there were nearly always small cu present, we
can assum moderately unstable air and thus assume σ_w to be on
the order of σ_v, and the form of the space charge anomaly will
be conical. We now need to convert σ_v, σ_w, into σ_θ, σ_ϕ, the

variances in wind angle, application to the formulations in
Pasquill. We find σ_θ (deg) $= \dfrac{\sigma_w}{\bar{u}} \cdot \dfrac{180°}{\pi}$ and for our assumed value
of $\sigma_w \sim 1.5$ m/s, and a mean wind ~ 7.5 m/s, $\sigma_\theta \sim \sigma_\phi \sim 10°$ hence
from Pasquill,

$$\sigma_y \sim 0.18x \sim \sigma_z.$$

Note this is an overestimate if anything and, since we assume
equal spreading in y and z, Eq.(1) can be rewritten as

$$X = \frac{Q}{2\pi\bar{u}\,(0.03)\,x^2}\; e^{-\frac{y^2}{0.03x^2}} \tag{2}$$

If $\sigma_y \sim \sigma_z \sim 0.18x$, this means 30% of distribution is within
radius of $0.18x$ downstream of the point of initiation of the
discharge; this in turn means that the vertical field component
as seen at the aircraft will be that of a line source whose
charge/unit length decreases steadily downwind of the balloon
(since for all except the closest passes the aircraft will be
above most of the distribution).

Since the potential gradient components due to the cone model
as discussed above are relatively intractable, we will discuss
a much simpler one which, as we shall see, will give a quite
reasonable picture of the potential gradient behavior. We
assume (as would be the case under stable atmospheric conditions)
that the plume of charge is essentially two-dimensional, as in
the following plan view:

E-4
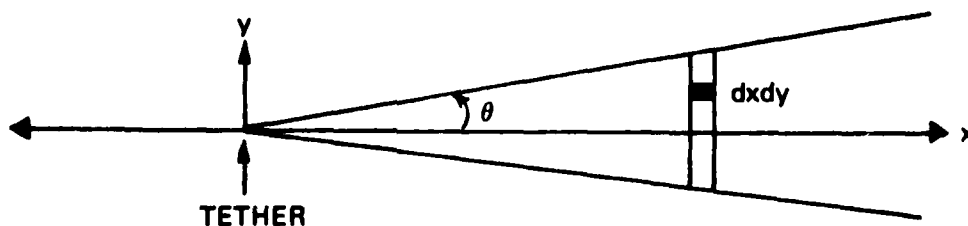
Let the "unspread" line charge density be λ; it is given by $\lambda = i/\bar{u}$ where i is the corona current and $\bar{u}$ is the mean wind velocity. Assume further a "top hat" distribution for the charge rather than a Gaussian.

The charge, dq, at element dxdy is:

$$dq = \frac{dxdy}{2x\ \tan\theta} \tag{3}$$

and, if the aircraft is instantaneously located at x_0, y_0 (=0), z_0, the potential is given by:

$$\phi = \frac{\lambda}{4\pi\varepsilon_0} \int_0^\infty dx \int_{-x\tan\theta}^{x\tan\theta} dy \cdot \frac{1}{2x\ \tan\theta} \cdot \frac{1}{\sqrt{(x-x_0)^2 + y^2 + z_0^2}} \tag{4}$$

which, with a lot of fuss, is approximately

$$\phi \approx \frac{\lambda}{4\pi\varepsilon_0} \left\{ \left(\frac{1}{\sqrt{1+\tan^2\phi}} - \frac{\tan^2\theta}{3(1+\tan^2\phi)^{3/2}} \right) \right.$$

$$\left[\ln\left(2\sqrt{(1+\tan^2\theta)(x_0^2+z_0^2)} - 2x_0\right) \right]$$

$$\left. + \frac{\left(\sqrt{z_0^2+x_0^2}\right)x_0\ \tan^2\theta}{3(1+\tan^2\theta)\left[(1+\tan^2\theta)(x_0^2+z_0^2)-x_0^2\right]} \right\} \tag{5}$$

and the vertical potential gradient is

$$F = \frac{\lambda}{4\pi\epsilon_0} \left\{ \left[\frac{1}{\sqrt{1+\tan^2\theta}} - \frac{\tan^2\theta}{3(1+\tan^2\theta)^{3/2}} \right] \right.$$

$$\left[\frac{z_0}{\left(\sqrt{(1+\tan^2\theta)(x_0^2+z_0^2)} \right)\left(\sqrt{(1+\tan^2\theta)(z_0^2+x_0^2)} \right) - x_0} \right]$$

$$+\frac{x_0 \tan^2\theta}{3(1-\tan^2\theta)} \left[\frac{z_0}{\left[(1+\tan^2\theta)(x_0^2+z_0^2)-x_0 \right]\sqrt{z_0 + x_0^2}} \right.$$

$$\left. \left. - \frac{2(1+\tan^2\theta)z_0}{\left[(1+\tan^2\theta)(x_0^2+z_0^2)-x_0^2 \right]^2} \right] \right\} \qquad (6)$$

The horizontal potential gradient in the direction of flight
(along x) can be expressed as:

$$F_x = \frac{\lambda}{4\pi\epsilon_0} \left[\left(\frac{1}{\sqrt{1+\tan^2\theta}} - \frac{\tan^2\theta}{3(1+\tan^2\theta)^{3/2}} \right) \right.$$

$$\left(\frac{\partial}{\partial x_0} \ln\left(2\sqrt{(1+\tan^2\theta)(x_0^2+z_0^2)} - 2x_0 \right) \right)$$

$$\left. +\frac{\partial}{\partial x} \frac{x_0 \tan^2\theta}{3(1+\tan^2\theta)\left[(1+\tan^2_0)(x_0^2+z_0^2)-x_0^2 \right]^2} \right] \qquad (7)$$

Programs for evaluating

$$G_z = \frac{F_z (4\pi \epsilon_o)}{\lambda} \quad \text{and} \quad G_x = \frac{F_x (4\pi \epsilon_o)}{\lambda}$$

are found on pages E-8 and E-9 respectively, followed by some representative plots.

TABLE E.1

COMPUTER PROGRAM FOR DETERMINING VERTICAL COMPONENT OF POTENTIAL GRADIENT ABOVE A WEDGE-SHAPED SPACE CHARGE DISTRIBUTION

```
Oprt,s dlib.gz
FURPUR 25.1-03/06-09:32
HWP*DLIB.GZ
     1    C
     2    C.....MORE FIELD ENHANCEMENT CALCULATIONS FOR DON...GX
     3    C
     4       10  READ(5,20,END=100)TH,ZZ,XX
     5       20  FORMAT(3F5.0)
     6           IF(ZZ.NE.0.)Z=ZZ
     7           IF(XX.NE.0.)X=XX
     8           IF(TH.NE.0.)TT=TH
     9           T=TAN(TT)**2
    10           T1=T+1
    11           TM1=1.-T
    12           XZ=X*X+Z*Z
    13           RT1=SQRT(T1)
    14           RXZ=SQRT(XZ)
    15    C
    16           A=1./RT1-T/(3.*T1**1.5)
    17    C
    18           B=Z/((RT1*RXZ-X)*SQRT(TM1)*RXZ)
    19    C
    20           C=X*Z*T/(3.*TM1)
    21    C
    22           D=(T1*XZ-X*X)*RXZ
    23    C
    24           E=2.*T1/(T1*XZ-X*X)**2
    25    C
    26           GZ=A*B+C*(1./D-E)
    27    C
    28           WRITE(6,30)GZ,A,B,C,D,E
    29       30  FORMAT(15X,F10.3,10X,5E13.5)
    30           GO TO 10
    31    C
    32      100  WRITE(6,110)
    33      110  FORMAT(/' PROCESSING ENDED. ')
    34           CALL EXIT
    35           END
```

TABLE E.2

COMPUTER PROGRAM FOR DETERMINING HORIZONTAL COMPONENT OF POTENTIAL GRADIENT ABOVE A WEDGE-SHAPED SPACE CHARGE DISTRIBUTION

```
Oprt,s dlib.gx
FURPUR 25.1-03/12-14:55
HWP*DLIB.GX
      1     C
      2     C.....MORE FIELD ENHANCEMENT CALCULATIONS FOR DON...GX
      3     C
      4        10 READ(5,20,END=100)X,ZZ,TT
      5        20 FORMAT(3F5.0)
      6           IF(ZZ.GT.0.)Z=ZZ
      7           IF(TT.GT.0.0)T=TT
      8           T2=TAN(T)**2
      9           TP1=T2+1
     10           TM1=1.+T2
     11           ZX=X*X+Z*Z
     12           RTM1=SQRT(TM1)
     13           Z2=Z*Z
     14     C
     15           A=1./RTM1-T2/(3.*TRM1**3)
     16     C
     17           B=X*TP1-SQRT(TP1*ZX)
     18     C
     19           C=(TP1*ZX-X*SQRT(TP1*ZX))
     20     C
     21           D=T2/(3.*TP1)
     22     C
     23           E=T2*ZX+Z2
     24     C
     25           F=SQRT(ZX)/E
     26     C
     27           G=X*X/(E*SQRT(ZX))
     28     C
     29           H=2.*X*X*SQRT(ZX)*T2/(T2*ZX+Z2)**2
     30     C
     31           GX=A*B/C+D*(F+G-H)
     32     C
     33           WRITE(6,30)GX,A,B,C,D,E,F,G,
     34        30 FORMAT(20X,F10.4,10X,8E10.5)
     35           GO TO 10
     36     C
     37       100 WRITE(6,110)
     38       110 FORMAT(///' PROCESSING ENDED')
     39           CALL EXIT
     40           END
```
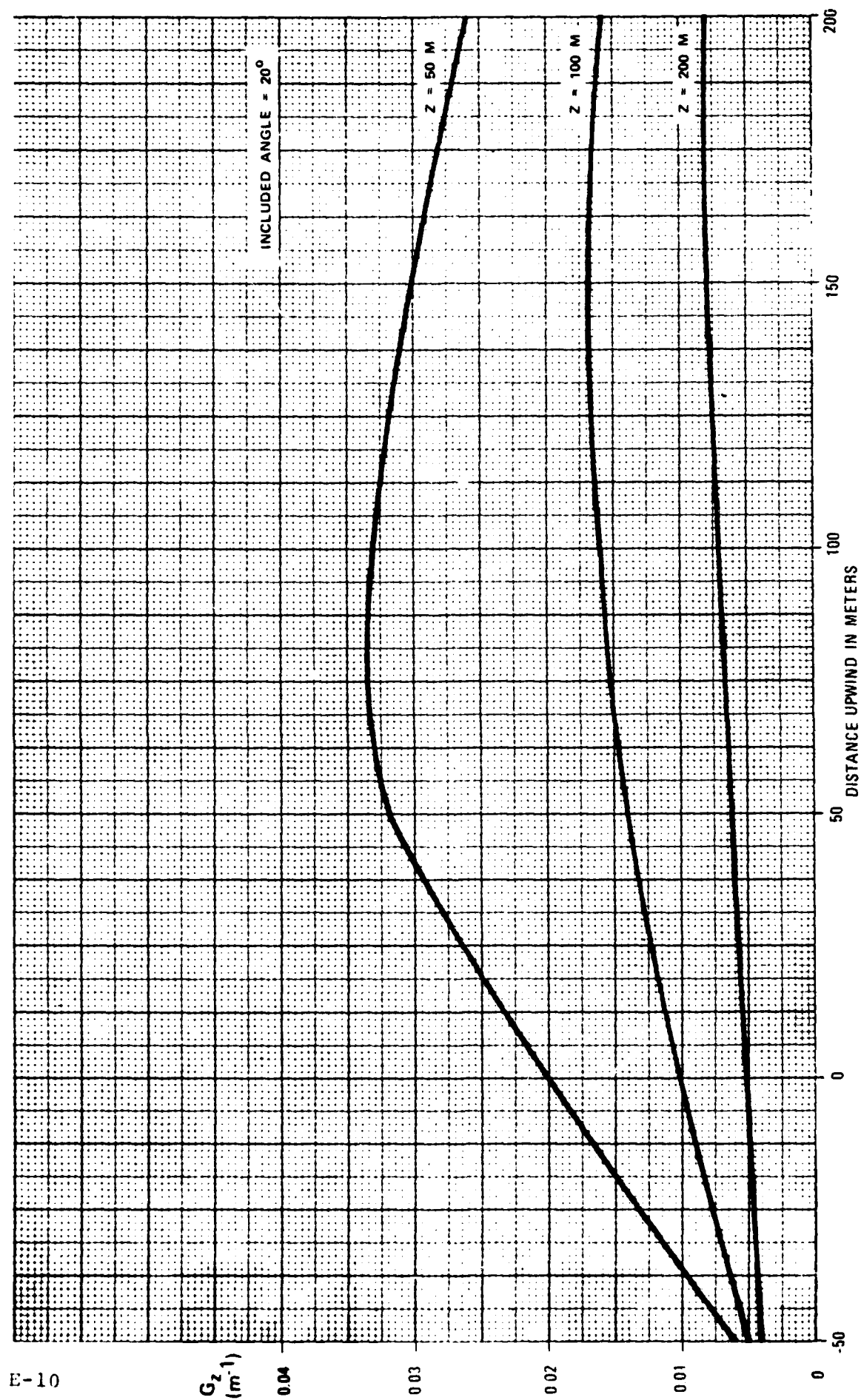
Figure E.1 -- Theoretical Curves for Traverse Over Flat Wedge-Shaped Ion
Concentration -- Vertical Potential Gradient Component
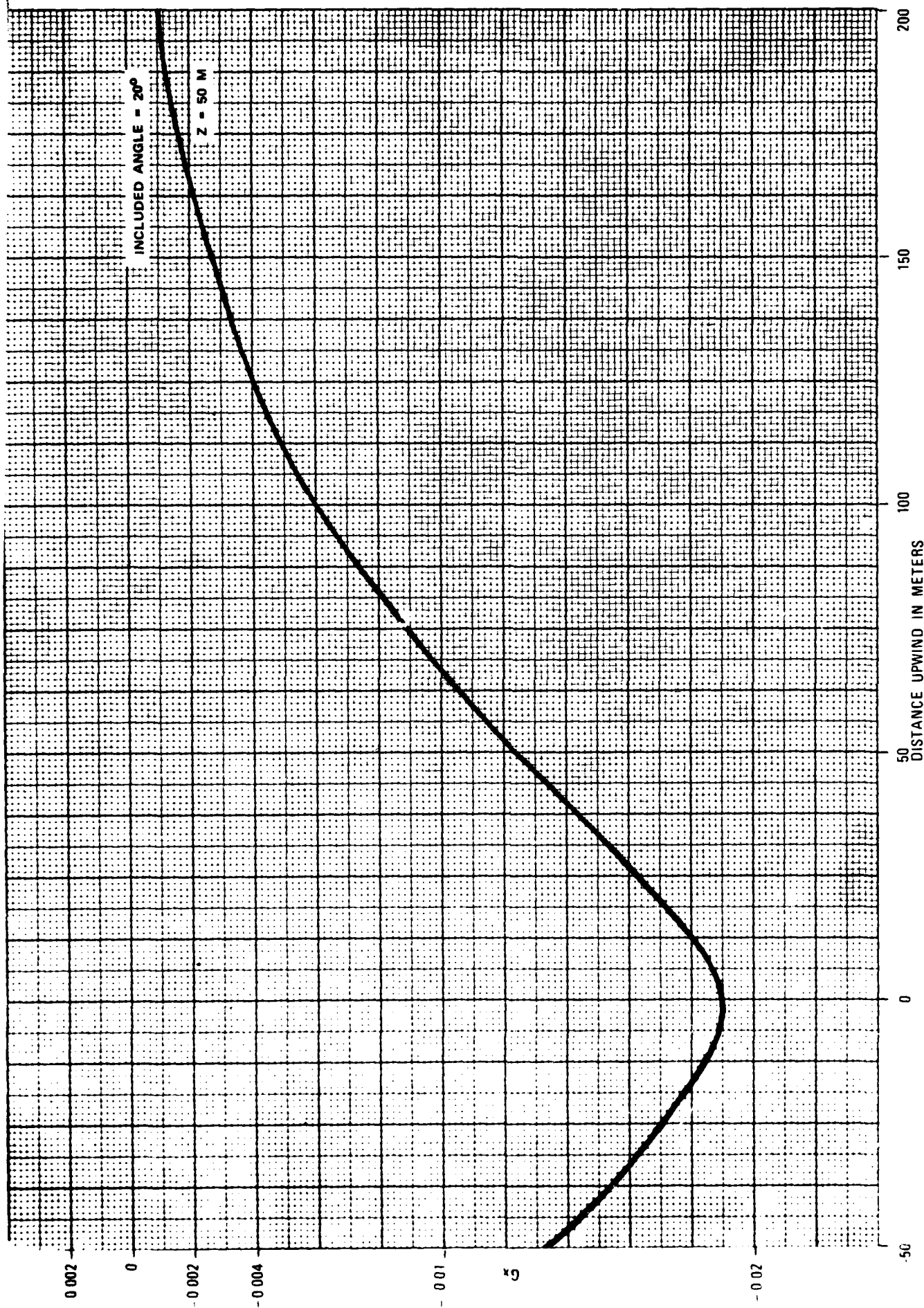
Figure E.2 — Theoretical Curve for Traverse Over Flat Wedge-Shaped Ion
Concentration — Flight-Axis Potential Gradient Component

E-11

APPENDIX F

CONSIDERATION OF AIR-EARTH CURRENT MEASURING EQUIPMENT

A simplified schematic of the air-earth current amplifier can be drawn as follows:
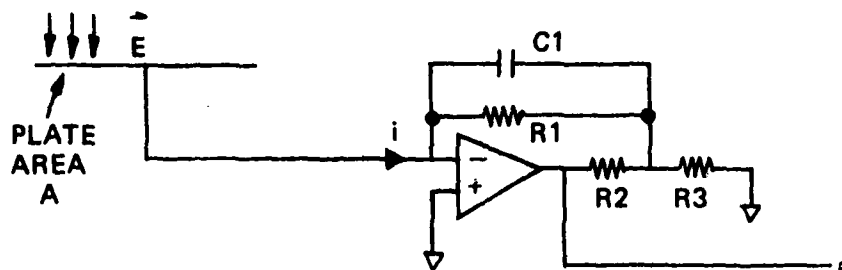
Originally, the purpose of C_1 was to act as a low-pass filter for the air-earth current measurement. It became apparent, on examination of the data that the circuit was also acting as a charge amplifier, hence as a "slow antenna" with the response time limited essentially by the slow rate of the amplifier. For the circuit actually used in practice, the following relationship was obtained:

$$\Delta e = -\frac{\Delta Q}{C} = -\frac{\varepsilon_0 \Delta E A}{C_1} \tag{1}$$

where ΔE is a change in the external electric field, and Δe is the corresponding change in amplifier output voltage. If ΔF is the potential gradient change, our instruments give

$$\Delta F = 22.6 \Delta e \tag{2}$$

for the "5 pA" scale,

$$\Delta F = 2.26 \Delta e \tag{3}$$

and

$$\Delta F = 0.226 \Delta e \tag{4}$$

on the "500 pA" scale.

Note that if the external potential gradient changes by a fixed amount ΔF, the resulting Δe will gradually decay to zero with a time constant of about 200 sec. for the component values used in our instruments.

APPENDIX G
BIBLIOGRAPHY

1. Stratton, J. A. "Electromagnetic Theory," McGraw Hill, N.Y. 1941.

2. Chalmers, J. A., and Mapleson, W. W. "Point Discharge Currents from a Captive Balloon," J.A.T.P. $\underline{6}$ 149, 1955.

3. Davis, R. & Standring, M. A. "Discharge Currents Associated with Kite Balloons," Proc. Roy. Soc. $\underline{191}$, 304, 1947.

4. Moore, C. B. "Lightning Around Elevated Structures" (private communication).

5. Schlichting, H. "Boundary Layer Theory," McGraw Hill, N.Y. 1960.

6. Lumley, J. L. and Panofsky, H. A. "The Structure of Atmospheric Turbulence," John Wiley & Sons, N.Y. 1964.

ADVANCED RESEARCH PROJECTS AGENCY

1400 WILSON BOULEVARD
ARLINGTON, VIRGINIA 22209

PART B

NATURAL ELECTRICAL EFFECTS ON THE
OPERATION OF TETHERED BALLOON SYSTEMS

E. T. PIERCE   G. H. PRICE

STANFORD RESEARCH INSTITUTE
MENLO PARK, CALIFORNIA 94025

ARPA ORDER NO. ___2176___

RANGE MEASUREMENTS LABORATORY
PATRICK AIR FORCE BASE, FLORIDA 32925

Final Technical Report

March 1974

NATURAL ELECTRICAL EFFECTS ON THE OPERATION OF TETHERED BALLOON SYSTEMS

By: E. T. PIERCE   G. H. PRICE

Approved by:

DAVID A. JOHNSON, *Director*
Radio Physics Laboratory

RAY L. LEADABRAND, *Executive Director*
Electronics and Radio Sciences Division

ABSTRACT

The interactions between a tethered-balloon system and the natural electrical environment under both fair and disturbed conditions are discussed. The tethered-balloon system perturbs the ambient electrical environment significantly. The incidence of lightning strikes to a balloon flown in the Patrick AFB area on a conducting tether of about 1 km length is determined to be on the order of 100 times per annum. Strike incidence with a nonconducting tether may be somewhat less, but not significantly less. Lightning to the tethered-balloon system will include more positive strokes than lightning to open ground; the distribution of currents for these positive strokes includes a higher fraction of both very high and very low currents than does the distribution for conventional negative lightning. A balanced consideration of practical factors suggests that conducting tethers are to be preferred over nonconducting ones.

CONTENTS

ILLUSTRATIONS

TABLES

* I   INTRODUCTION

Tethered balloons offer many possible advantages as platforms for the development of military and other equipment. Unfortunately, some natural electrical phenomena—notably lightning—represent hazards to the operation of tethered balloons. The purpose of this report is to discuss briefly the interactions between a balloon system and the natural electrical environment, under both fair and disturbed conditions, and to indicate some interpretations of pilot measurements made at the Eastern Test Range (ETR).

A valuable and extensive review of the general areas of concern has already been published by Battelle.[1] * Accordingly, to avoid duplication, this report will concentrate on presenting information not covered in Ref. 1, on modifying some of the data and interpretations given there, and on discussing some of the new experimental results.

---

* References are listed at the end of this report.

II THE NATURAL ELECTRICAL ENVIRONMENT

In fair weather and quiet unpolluted conditions the atmospheric electric field E_z is directed vertically, and decreases fairly steadily with increasing height, perhaps from +100 V/m at z = 0 to 10 V/m at z = 4 km.* Atmospheric convection and pollution modify this simple picture especially in the lower atmospheric layers. If the atmospheric conductivity at height z is λ_z, we have the relation

$$J_z = E_z \lambda_z$$

where J_z is the air-earth current. Measurements[2] show that J_z is relatively constant with height, as compared with E_z and λ_z. Typically, $J_z = 2 \times 10^{-12}$ A/m^2. At ground level λ_z might be 2×10^{-14} mho/m in an unpolluted locality with a corresponding value of $E_o = 100$ V/m.

When clouds are present, the fair-weather environment is changed in two respects. The cloud particles modify the profile of λ_z with height, while charge-generating mechanisms become active within the clouds. The electric fields increase in magnitude over fair-weather conditions and--because of the charge generation--may be of either sign.

The greatest electrification is associated with thunderclouds. The field at the ground below a thundercloud rarely exceeds 10 kV/m and does not change greatly between ground level and the cloud base.[3] Within the cloud, the general peak fields are typically 40 to 50 kV/m, but there is

---

*
We use the normal sign convention of atmospheric electricity by which a positive charge in the upper atmosphere produces a positive field at the earth's surface below.

some evidence that localized very intense fields approaching 400 kV/m also exist.[4] The electrical structure of a thundercloud is very complicated in detail, but can often be represented macroscopically by a net positive charge in the upper part of the cloud, an excess of negative charge in the main body of the cloud, and a small net positive charge toward the cloud base.

Lightning characteristics have recently been thoroughly reviewed by Cianos and Pierce;[6] some of the salient points in this review are also reproduced in Ref. 1.

4

III INTERACTIONS OF A TETHERED BALLOON WITH THE ELECTRICAL ENVIRONMENT

A. Fair-Weather Conditions

The classic--and indeed almost the only--paper on the electrical effects accompanying balloon operation is that by Davis and Standring.[6] This research is the yardstick against which other work must be compared, and it is accordingly surprising to find Davis and Standring's paper not even discussed in Ref. 1.

We consider the case of a conducting tether in a fair-weather environment. The lines of force (air-earth current flow) of the electric field will tend to concentrate on the tether and its tip, while distortion of the equipotentials by the conducting tether will lead to reductions in field at ground level adjacent to the balloon site. As the tether extends, the potential difference between the tether and the ambient atmosphere will become sufficiently large for corona to occur from the tether. The current in the tether will consist of contributions both from corona and from interception of the natural air-earth current. Space charge liberated at the tether by corona will be carried downwind, and will there act to distort the natural field distribution.

We can give some simple mathematical expressions for the tether current, T. The contribution J_L, from interception of the air-earth current, may be written as

$$J_L \approx J \, A(L) \tag{1}$$

where $A(L)$, the interception area of the tether, is a function primarily of tether length L.

The intercepting area, $A(L)$, can be estimated in Eq. (1) from the idealized model of a prolate spheroid, at zero potential, immersed in an initially uniform field. The resultant potential function is well known for this model.[7] The attendant field perturbation at the earth's surface (represented in the model by the symmetry plane that bisects the spheroid axis) can be integrated analytically, as described in the Appendix, to determine the charge residing on the half spheroid. The ratio of this charge to the unperturbed surface-charge density is exactly the intercepting area, which is given approximately by

$$A(L) \sim \frac{L^2}{\ln\left(\frac{2L}{b}\right) - 1} \qquad (2)$$

for $b/L \ll 1$, where b is the base radius of the half spheroid. It is noteworthy that Eq. (2) also results from Davis and Standring's superficially rather different model for the tether charge distribution.[8]

It is well known in atmospheric electricity[9] that corona currents depend on the potential difference between the corona emitter and the adjacent atmosphere, and on the efficacy of the removal of the space charge created; this removal may be by wind, by ionic motion under electrical forces, or by any combination of these two factors. We may write, for the corona current $i(d\ell)$ from an element $d\ell$ of the tether,

$$i(d\ell) = C(V_\ell - V_o) f(w, kV_\ell) d\ell \qquad (3)$$

where V_o is the onset potential difference for corona, V_ℓ is the potential difference from the element to the surrounding atmosphere, w is the windspeed, and C and k are dimensional constants. The function $f(w, kV_\ell)$ has different forms according to the vector relationships involved between w and kV_ℓ: normally, however, over most of the tether both will be

6

dominantly horizontally directed. In the absence of wind, Eq. (3) re-
duces to the simple form

$$i(d\ell) = C(V_\ell - V_o)kV_\ell \ d\ell$$

$$\approx kCV_\ell^2 \ d\ell \qquad . \tag{3a}$$

When wind is present it usually dominates the space-charge removal for
even quite small wind speeds; Eq. (3) then reduces to

$$i(d\ell) = wC(V_\ell - V_o)d\ell \approx wCV_\ell \ d\ell \qquad . \tag{3b}$$

Note that

$$V_\ell = \int_o^\ell E_z \cdot dz \qquad . \tag{4}$$

Thus, for the complete tether current, T_L, we have

$$T_L = J_L + I_L \tag{5}$$

where J_L is defined by Eq. (1) while I_L is obtained from the integration
of Eqs. (3) and (4) over the entire length L of the tether. Usually,
except at the lower heights I_L will be much greater than J_L.

The field perturbation about the tether can also be considered to
consist of two distinct elements. One of these is the perturbation of
the field caused by the surface-charge redistribution from the ground
surface to the tether; this perturbation is described approximately by
the prolate-spheroid model. This model gives,[9] for the field at the
earth's surface, $E_{z=o}$,

$$\frac{E_{z=0}}{E_\infty} = 1 - \frac{\coth^{-1}\eta - \frac{1}{\eta}}{\coth^{-1}\eta_0 - \frac{1}{\eta_0}} \tag{6}$$

relative to the unperturbed field E_∞. The surfaces η constant constitute confocal spheroids, of which $\eta = \eta_0$ models the tether surface. On the earth's surface, η is related to r, the distance from the spheroid axis, by

$$\eta = \left[1 + \frac{(r/L)^2}{1 - (b/L)^2} \right]^{1/2} \tag{7}$$

with $r = b$ giving $\eta = \eta_0$. This component of the field perturbation decreases rapidly with increasing distance from the spheroid axis for a highly elongated spheroid ($b/L \ll 1$), as is the case when a balloon tether is modeled.

Additionally, the space charge injected into the surrounding air by corona current from the tether also perturbs the field. The net injected space charge terminates lines of force that otherwise would terminate on surface charge. As the space charge drifts away from the tether, the surface-charge distribution responds accordingly. The net effect at the earth's surface can be viewed as a combination of the initial (perturbed by the presence of the tether) surface charge plus that induced by the space charge and its image. The space charge produced by the corona current $i(\ell)$ from an element $d\ell$ of the tether can be modeled (ignoring diffusion, recombination, and other dissipative processes) as a semi-infinite horizontal line charge extending downwind from the tether. At a distance r from the tether base, the potential-gradient perturbation at the earth's surface due to the line charge at height ℓ is[8],[10]

$$dE_z = \frac{i(\ell)d\ell}{2\pi\epsilon_o w\ell}\left[1 + \frac{r}{(r^2 + \ell^2)^{1/2}}\right] \quad . \qquad (8)$$

Integration over the length L of the tether then gives the total change in E_z.

The field perturbation in the space above the tether/balloon system can be expected to be less well modeled by a thin prolate spheroid than is the perturbation near the ground. At distances above the balloon the order of its characteristic length or less, the field perturbation will be essentially that of the balloon alone, at ground potential, so long as the balloon conductivity is appreciable. Thus, the perturbation of the field in this region can be modeled by an isolated prolate spheroid, with axis horizontal, at ground potential. At greater distances from the balloon, the dominance of this perturbation component will diminish, with the field perturbation becoming more nearly that given by the prolate-spheroid tether model, but with an increased base-to-height ratio to account for the effect of the balloon size upon the field structure at the top of the tether/balloon system.

B. Fair-Weather Observations

In discussing the extensive data obtained at ETR, we will necessarily be confined to examination of several highlights, since the opportunity to study the data in detail was somewhat limited relative to the quantity available. The data examined by us were generally obtained from flights during fair weather in which winds were light, with balloon altitudes (actually, length of tether played out) up to about 1000 m. Tethers used included 1/8-inch (3.2 mm) diameter steel, 1/4-inch (6.4 mm) diameter nylon, and 0.775-inch (19.7 mm) diameter Nolaro.

Comparison of the data with those obtained by Davis and Standring[6] forms a natural starting point. The most direct comparison is provided by measurements of the current to ground flowing through conducting tethers. Fluctuations in the tether current unrelated to changes in the balloon altitude are also common; two data samples relatively free from such effects were chosen for comparison. These are shown in Figure 1, together with comparable data from Figure 1 of Davis and Standring.[6]

The two sets of data shown in Figure 1 are generally compatible, although the rate of current increase with increasing balloon altitude is markedly greater at the higher altitudes for Curve A than would be expected on the basis of the Davis and Standring[6] data. Any difference in currents, due to differences in tether diameter, between the two sets of data is masked by the range of variation within each set.

The currents in all instances appear to be too large to result primarily from diversion to the tether of the normal air-earth current as a result of field distortion. For an altitude of 600 m, Eq. (2) gives an intercepting area of 9×10^4 m^2 for an 1/8-inch-diameter tether. If a nominal fair-weather air-earth current density of 2×10^{-12} $A \cdot m^{-2}$ is assumed, the resultant tether current due to field distortion is 0.18 μA. The result is not much changed (to 0.19 μA) for the slightly larger tether employed by Davis and Standring.[6]

These values are quite compatible with those derived by Davis and Standring[6] through direct consideration of the currents flowing to the tether in the perturbed field. They calculated a current of 0.3 μA for a balloon altitude of 900 m in a nominal unperturbed field of 100 $V \cdot m^{-1}$; the use of Eq. (2) yields a value of 0.4 μA under the same conditions. The difference in these two values is just that to be expected from the difference in air conductivity implicit in the two calculations. The values assumed by Davis and Standring[6] for ionic mobility, production
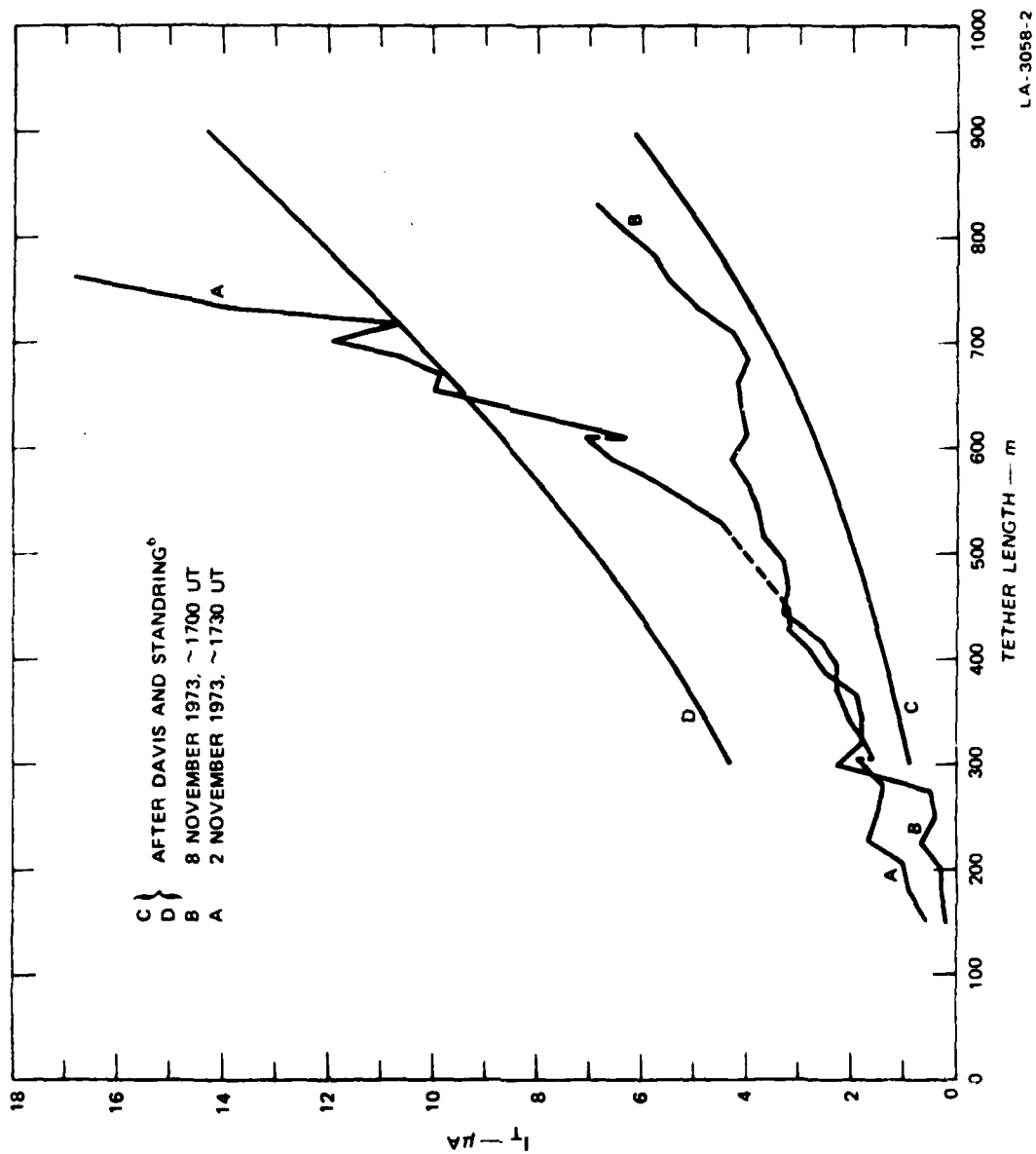
FIGURE 1   CURRENT IN CONDUCTING TETHER AS A FUNCTION OF BALLOON ALTITUDE

11

rate, and lifetime yield a conductivity of 1.4×10^{-14} mho $\cdot$ m^{-1}, while a conductivity of 2×10^{-14} mho $\cdot$ m^{-1} is necessary to make the 100 V $\cdot$ m^{-1} unperturbed field assumed by them consistent with the 2×10^{-12} A $\cdot$ m^{-2} unperturbed air-earth current assumed by us.

If we assume that both the field and the wind are independent of height, Eqs. (3b) and (4) can be readily integrated to yield $I_L \propto L^2$ for a tether current due to corona controlled by wind dispersal of the resultant space charge. The fact that this relation is roughly satisfied by the curves shown in Figure 1 should not be overlooked, although it would be a mistake to infer proof therefrom that such a model is accurate in detail. We note in support of this caution, for example, that the somewhat greater wind speed for 2 November 1973 than for 8 November 1973 suggested by Curves A and B of Figure 1 is not borne out by direct surface measurements of the wind speed at the times of interest.

The various potential-gradient and air-earth current measurements on the ground and the potential-gradient measurements above the balloon invite comparison with models of the distortion of the field produced by the balloon and tether. Comparison requires, however, that the field distortion be isolated from other sources of field and current perturbations, some of which are experimentally significant (such as space charge injected into the air by corona discharge from the tether), and some of which are not (such as variations in the field-mill calibration factors due to site anomalies, or drifting space charge from other sources).

This separation of effects is not easily made. The data obtained from the 2 November 1973 flight are representative. The potential-gradient and air-earth current measurements obtained during the initial ascent of the balloon are shown in Figure 2. Data were taken 10 f+ (E_1, I_1), 100 ft (E_2, I_2), 200 ft (E_3, I_3), and 500 ft (E_4, I_4) from the tether base. The ascent was made in a series of steps, with relatively
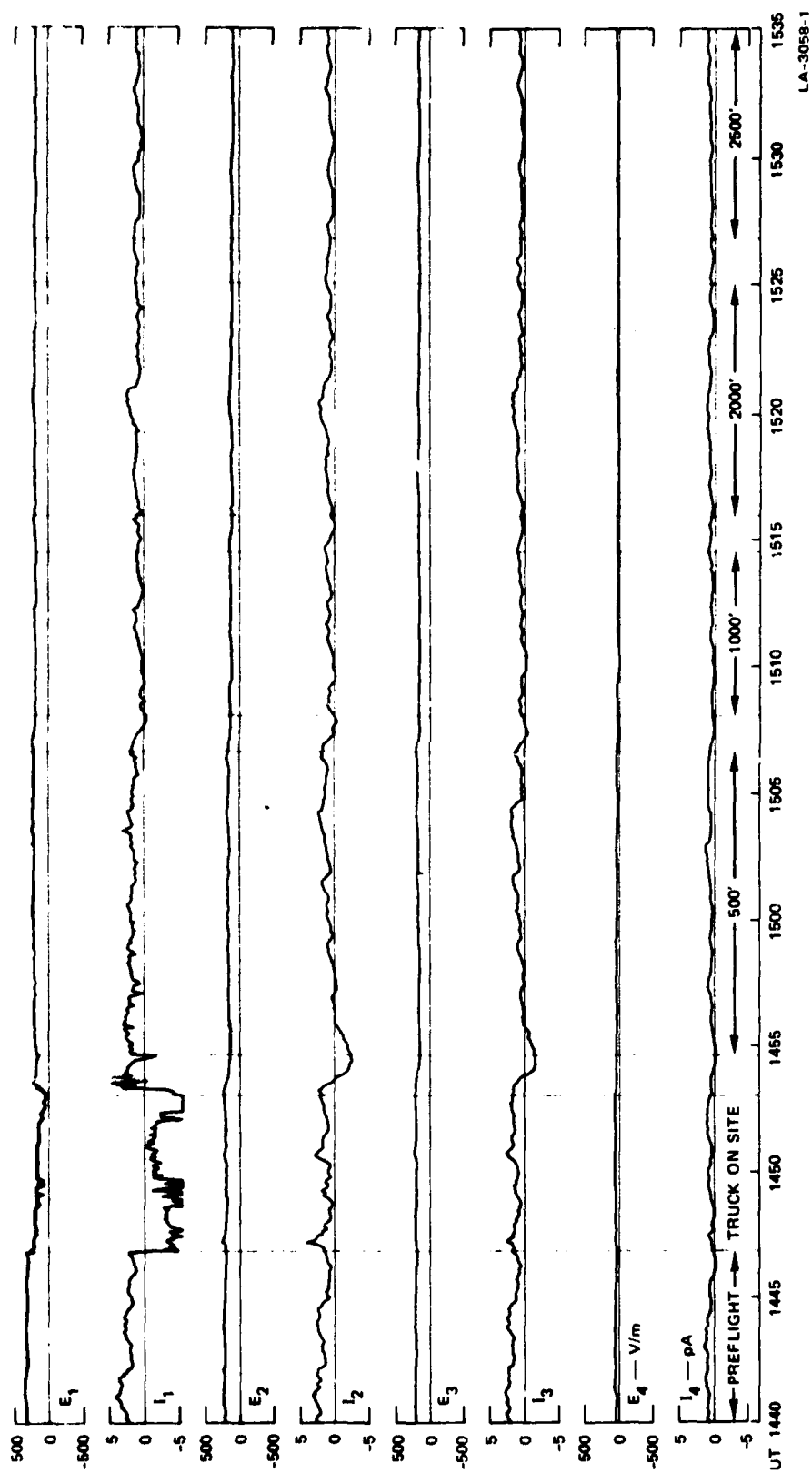
FIGURE 2   POTENTIAL GRADIENT AND AIR-EARTH CURRENT DURING ASCENT OF 2 NOVEMBER 1973

LA-3058-1

13

long intervals between them; the balloon altitude is indicated in the figure for each of the constant-altitude intervals. The potential gradient is reasonably stable during these intervals, and it usually changes discernibly during the ascending periods. The air-earth current, although usually varying consistently with the potential gradient during the ascending periods, fluctuates rather severely throughout, making interpretation difficult. Therefore in the following analysis attention was restricted to the potential-gradient variations.

The potential gradient at each recording site was sampled once a minute and averaged to determine a value for each of the constant-altitude intervals. These values are given in Table 1. The first line of the

Table 1

POTENTIAL GRADIENT AT GROUND LEVEL
DURING BALLOON ASCENT OF 2 NOVEMBER 1973

Balloon Altitude (ft)	Potential Gradient ($V \cdot m^{-1}$)			
	10 ft from Tether Base	100 ft from Tether Base	200 ft from Tether Base	500 ft from Tether Base
--*	329	231	215	55
~20†	178	214	210	54
500	203	159	167	29
1000	100	122	15:	27
2000	176	113	154	22
2500	170	101	143	20

*Measurements prior to arrival of winch truck.

†Measurements with winch truck on site, prior to ascent.

table contains the values measured prior to the arrival of the winch truck. It is evident, from the differences in the potential gradient measured at the different locations, that local site anomalies significantly affect the instrument calibrations or otherwise cause the potential gradient to vary substantially over the area sampled by the measurements. Comparison of this initial set of measurements with those made after the arrival on site of the winch truck indicate that the presence of the truck strongly perturbs the potential-gradient measurement 10 ft from the tether base, as is only to be expected. Measurements at greater distances are not much affected by the arrival of the truck. With the exception of the measurements at 10 ft, the qualitative dependence of potential gradient upon balloon altitude shown by Table 1 is reasonable.

We next consider the field perturbation in the context of the prolate spheroid tether model. This model suggests, as indicated by Eq. (A-15) of the Appendix, that the fractional perturbation of the potential gradient at the ground surface is primarily a function of r/L, the ratio of the distance from the tether base to the tether height. The data given in Table 1 are plotted in this form in Figure 3, along with the corresponding values calculated with this model. The potential gradient measured at each distance prior to the arrival of the winch truck was used to determine the fractional change at that distance as the balloon was elevated; this normalization minimizes the effects upon the data of local site anomalies and calibration errors.

The departure of the data in Figure 3 from the values calculated with the model remains substantial even with this precaution; this discrepancy is probably real. It is significant that the observed perturbations of the potential gradient all are greater than those calculated. Such a discrepancy is consistent with the presence of space charge above

15
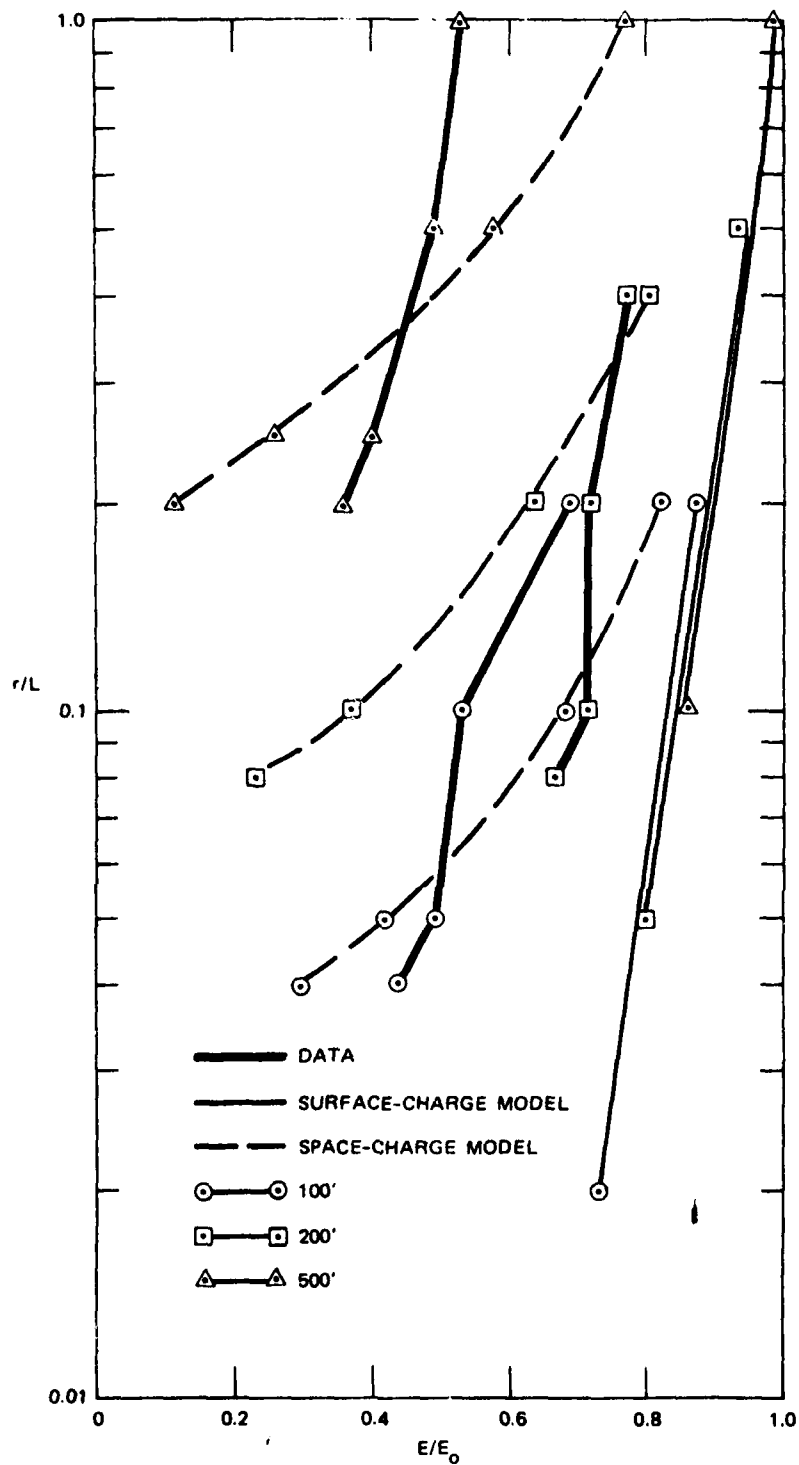
FIGURE 3   POTENTIAL-GRADIENT PERTURBATION ON THE GROUND
AT VARIOUS DISTANCES FROM BASE OF CONDUCTING
TETHER

16

the measurement points, as would be expected downwind from the tether.[*]
The tilt of the tether from vertical would also increase the potential-
gradient perturbation downwind relative to that produced by the vertical
tether assumed in the model.

In order to estimate the influence of space charge upon the potential
gradient at the ground, Eq. (8) was integrated using the wind-controlled
expression, Eq. (3b), for $i(\ell)$. The result is

$$\frac{\Delta E}{E_o} = - \frac{C}{2\pi\epsilon_o} L \left\{ 1 + \frac{r}{L} \ell n \left(\frac{1 + [1 + (r/L)^2]^{1/2}}{r/L} \right) \right\} \quad . \tag{9}$$

Equation (9) was then evaluated using a value of 8×10^{-4} m^{-1} for $C/2\pi\epsilon_o$,
as determined (very roughly) by a fit of the I_L obtained by integration
of Eq. (3b), to the tether-current curves A and B of Figure 1. In this
fit, the wind speed was taken to be 6 knots (3.1 m/s) and the unperturbed
potential gradient 250 V $\cdot$ m^{-1}, as measured near the tether base. The
results of this calculation are indicated in Figure 3. Although this
crude model cannot be said to describe the observed potential-gradient
perturbation accurately, these results certainly suggest that space
charge is a major factor in the determination of this perturbation.

The conducting tether was also isolated from ground and its potential
measured on several occasions. The field perturbation produced by this
"floating" tether differs greatly from that produced by the grounded
tether. First, we note that the potential of the floating tether will
ultimately stabilize, as the net surface charge leaks off, at a value
intermediate between that of the ground (conventionally zero) and that
of the unperturbed field at the height of its top.

---

[*]The measurement points were nominally laid out on a line extending down-
wind from the tether base.

17

The stabilization potential is determined by the requirement that the resultant current across the air gap at the tether base equal that into the air over the upper portion of the tether. This potential is often assumed to be just half the potential difference between the ground and the height of the tether tip, but qualitative consideration of the perturbed field configuration suggests a slightly lower value. It is perhaps worth noting, in passing, that were the air a perfect insulator, no change in the field configuration would occur upon isolation and re-grounding of the tether. Thus, the dynamics of the adjustment of the tether potential are of interest as further indicators of the nature of the currents flowing to and from the tether.

We shall examine here the measurements of the potential gradient and air-earth current perturbations at the ground in response to isolation and regrounding of the conducting tether. Two examples of these pertur-bations, both obtained during the 8 November 1973 flight, are shown in Figure 4. The data plotted in Figure 4 were obtained at distances of 10 ft (E_1, I_1), 100 ft (E_2, I_2), and 200 ft (E_3, I_3) from the tether base. Although these sites were initially set up along a line downwind from the tether base, a subsequent shift in wind direction placed the line at approximately right angles to this direction.

The time of isolation of the tether is denoted $t = 0$ in each instance; regrounding occurs subsequently at $t = 164$ s in one instance and at $t = 254$ s in the other. The results are generally consistent for the two cases, showing an approximately exponential adjustment of the potential gradient to a new static value following isolation of the tether and a very rapid return to approximately the pre-isolation value upon its regrounding. The magnitude of the adjustment decreases with increasing distance from the tether base. The time constant [t at which $\Delta E = (1 - e^{-1})\Delta E_{max}$] of the adjustment of the potential gradient following isolation of the tether was calculated for the 1520 UT data to be

18
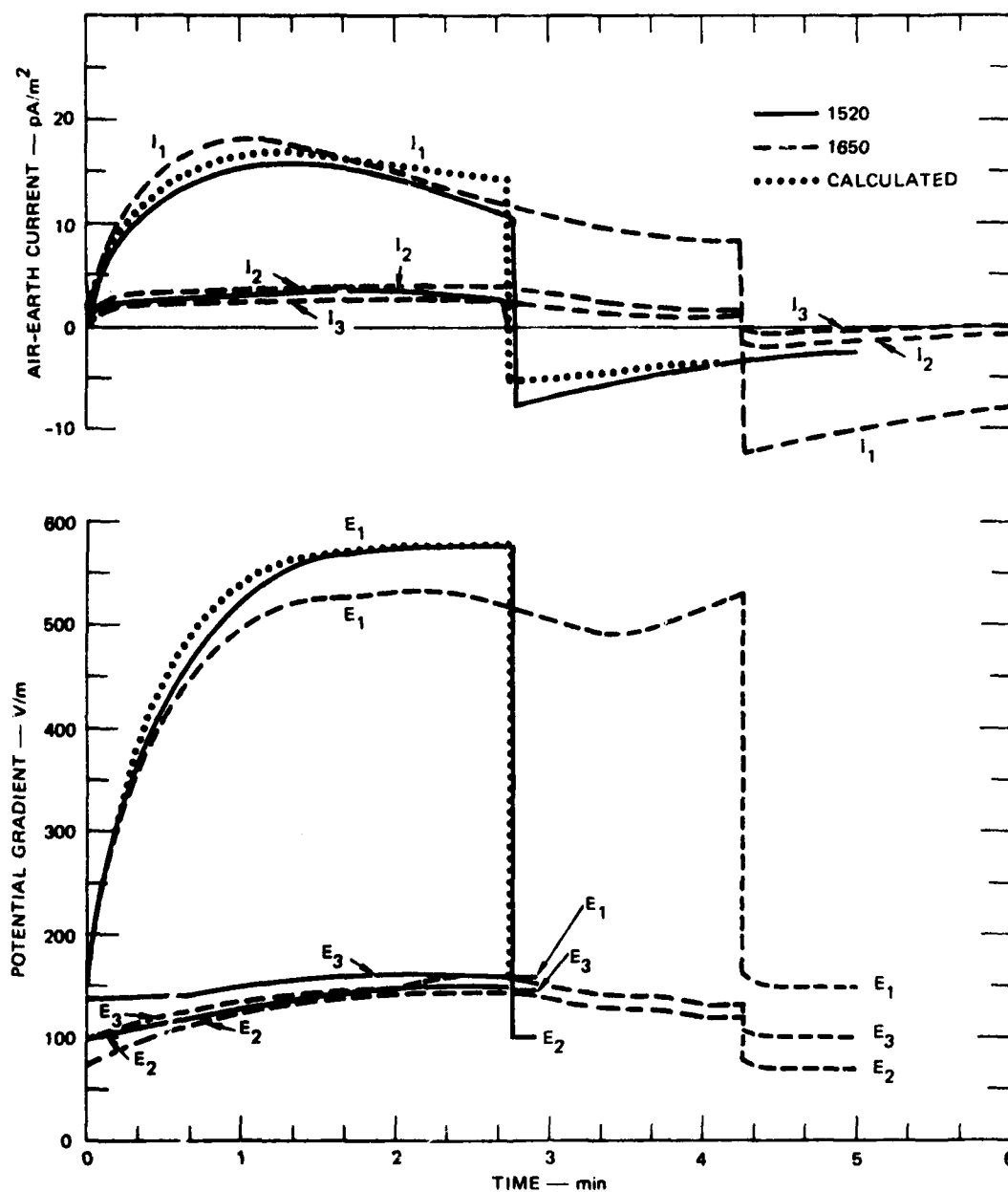
FIGURE 4   POTENTIAL GRADIENT AND CURRENT PERTURBATION CAUSED BY FLOATING
AND REGROUNDING OF CONDUCTING TETHER

19

approximately 25 s from the time taken for ΔE to attain one-half its ultimate value of about 444 V $\cdot$ m^{-1}.

The flight log for these tether-isolation experiments notes measurement of an equilibrium potential of 15 kV for the floating tether. This value is appreciably less than half the potential difference between the ground and the balloon height (832 m) that is obtained under the assumption that the potential gradient at the ground of about 100 V $\cdot$ m^{-1} persists to this height. Incorporation, into the tether-potential estimate, of the effects of the sometimes considerable lapse rate of the potential gradient in the lower atmosphere would probably resolve this apparent discrepancy.

The time constant for buildup of the tether potential should equal that observed in the potential-gradient measurements. This time constant can be estimated independently, given the capacitance to ground of the isolated tether, C,[*] its ultimate equilibrium voltage, V_o, and the current through the grounded tether before isolation, I_T. We write the capacitance in the form

$$C = \frac{Q}{V_T} = \frac{dQ/dt}{dV/dt} = \frac{I_T}{dV_T/dt} \quad . \tag{10}$$

Now, for

$$V_T = V_o\left(1 - e^{-t/\tau}\right) \quad , \tag{11}$$

we have

$$\frac{dV_T}{dt} = \frac{V_o}{\tau} e^{-t/\tau} \quad ,$$

---

[*] Not to be confused with the constant C in Eqs. (3) and (9).

20

whence, evaluating Eq. (10) at the instant of isolation of the tether,

$$\tau = \frac{CV_o}{I_T} \quad .$$ (12)

Determination of C presents something of a challenge; examination of the experimental layout suggests three potentially significant contributions to the total capacitance: (1) that from the approximately vertical tether segment, (2) that from the horizontal tether segment between a sheave at the rear of the winch trailer and the winch, located forward on the trailer, and (3) that of the winch framework. The capacitance of a vertical wire above ground is given approximately by[11]

$$C_V = \frac{2\pi\epsilon_o L}{\ln\left(\frac{L}{b}\right) - 1 - \frac{h}{L}\ln\left(\frac{4h}{L}\right)}$$ (13)

where h is the height of the bottom of the wire above the ground. The capacitance per unit length of a horizontal wire above ground is given by[12]

$$C_H = \frac{2\pi\epsilon_o}{\ln\left(\frac{2h}{b}\right)} \quad .$$ (14)

The framework capacitance can be modeled as that of parallel plates,

$$C_F = \frac{\epsilon_o}{h}$$ (15)

per unit area.

Equations (13) to (15) were evaluated for L = 2730 ft (832 m), h = 1 ft (0.3 m) and b = 1/16 inch. The value of h was estimated from

21

photographs of the winch trailer, as were a horizontal length of 30 ft (10 m) for the tether run along the trailer and an area of 40 ft^2 (2.7 m^2) for the winch framework. These values yield C_V 3.8 × 10^{-9} F, C_H 9.3 × 10^{-11} F, and C_F 4.3 × 10^{-9} F, for a total capacitance of 8.2 × 10^{-9} F.

Equation of Eq. (12) with these parameter values ($C = 8.2 × 10^{-9}$ F, V_o 15 kV, and $I_T = 8$ μA) yields a value for τ of 15 s. Given the roughness of the estimate, this value agrees reasonably well with that of 25 s determined directly from Figure 4.

The air-earth current behavior indicated in Figure 4 constitutes something of a puzzle upon initial examination. This current would be expected to be proportional to the potential gradient, which was measured along with the current at each location, but this expected proportionality is clearly violated, sometimes flagrantly. Resolution of this dilemma is straightforward, however, once displacement currents (i.e., current flow resulting in changes in the surface-charge density) are taken into account. The low-pass characteristic of the air-earth current data channel also modifies the recorded curve somewhat.

To demonstrate the consistency of the air-earth current and potential gradient measurements, the current was calculated for an assumed potential-gradient variation of the form given by Eq. (11), with a time constant $\tau = \alpha^{-1}$ of 25 s, and an equilibrium potential-gradient change of $E_o = 444$ V · m^{-1}, as determined from the 1520 UT data of Figure 4. This model curve is seen in the figure to fit the potential-gradient variation well. The air-earth current was assumed to be related to the potential gradient by

$$i_o(t) = \lambda E(t) + \epsilon_o \frac{dE}{dt} \quad , \qquad (16)$$

and a nominal value of 2×10^{-14} mho $\cdot$ m^{-1} was assumed for λ. The Fourier spectrum of i_o was then calculated, multiplied by the transfer function for an RC lowpass filter--$\omega_o/(\omega_o + i\omega)$, and inverse transformed to yield the measured current. A value of 200 s was taken for ω_o^{-1}.*

This calculation yields the result

$$
i(t) = \begin{cases} \left[\lambda\left(1 - e^{-\omega_o t}\right) + \dfrac{(4\pi\alpha\epsilon_o - \lambda)\omega_o}{\omega_o - \alpha}\left(e^{-\alpha t} - e^{-\omega_o t}\right) \right]E_o \,, & \\[4mm] \left[\lambda\left(1 - e^{-\omega_o t_o}\right) + \dfrac{(4\pi\alpha\epsilon_o - \lambda)\omega_o}{\omega_o - \alpha}\left(e^{-\alpha t_o} - e^{-\omega_o t_o}\right) \right. & 0 < t < t_o \\[4mm] \left. - 4\pi\epsilon_o\omega_o\left(1 - e^{-\omega t_o}\right) \right]E_o e^{-\omega_o(t - t_o)} \,, & \\[4mm] & t_o < t \end{cases}
$$

$$(17)$$

which is plotted in Figure 4 for $t_o = 164$ s. The agreement with the measured air-earth current is quite good, although it appears that use of a somewhat smaller value of λ, and perhaps some adjustment of ω_o, would improve it even further. Noteworthy is the agreement between the calculated and the observed magnitude of the current step at t_o. This step is purely a displacement-current phenomenon, the roll-off at high frequencies of the low-pass filter being only sufficient to convert the impulse in dE/dt at t_o into a step in i(t). The magnitude of the current step for the 1650 UT data is the same as for the 1650 UT data as well, even though the beginning and ending levels differ, since the potential-gradient changes in the two cases are essentially identical except for the difference in time of occurrence.

---

*Personal communication, T. Hall.

C. Lightning-Flash Incidence

1. General

The incidence of flashes to any tethered-balloon system cannot yet be calculated with any precision. There are major uncertainties. Nevertheless estimates can be made, although it is important to realize that predicted estimates may be considerably in error, and that--in the absence of a data base against which to compare the predictions--even the possible magnitudes of the errors are, as yet, quite unestablished.

If the tether is conducting, the balloon acts as a tall structure electrically connected to ground. Some guidance is available for the electrical behavior of such structures. If the tether is nonconducting the electrical situation is less well defined. However, we may say with confidence that the tip of a nonconducting tether will always be at a potential intermediate between that naturally present in the atmosphere adjacent to the tether tip, and ground potential (usually taken as zero). On the other hand, for a conducting tether the potential throughout the tether will be that of ground. It follows that the voltage discontinuity between the ambient atmosphere and the tether tip cannot be more and is almost certainly less for a nonconducting than it is for a conducting tether. Consequently, triggered lightning will develop more easily from the conducting tether; so also will upward leaders induced by conventional leaders from cloud to ground. Thus, lightning incidence with a nonconducting tether will certainly not be greater than that with a conducting tether and may be substantially less.

2. Flashes to Open Ground

Monthly and annual thunderstorm data can now be used with fair confidence in calculating the flash incidence to open ground. Several relationships that do not differ greatly over the most climatically

24

significant range of thunderstorm days are available.[5]   One of these is

$$\sigma_m^2 = aT_m + a^2T_m^4 \qquad (18)$$

where σ_m is the monthly flash density (flashes km^{-2}), T_m is the monthly number of thunderstorm days, and the constant a has the value of 3×10^{-2}. Table 2 gives information for T_m and σ_m for Patrick AFB, Florida.

Table 2

LIGHTNING INCIDENCE TO OPEN GROUND AT PATRICK AFB, FLORIDA

Month	Number of Thunderstorm Days T_m	Flash Incidence per km^2 per Month (σ_m)
January	0.5	0.1
February	1.8	0.3
March	3.7	0.6
April	3.3	0.5
May	6.7	1.4
June	14.0	5.9
July	13.8	5.8
August	15.8	7.6
September	10.8	3.5
October	3.8	0.6
November	0.7	0.2
December	0.7	0.2
Year	75.6	26.7

Thunderstorm occurrence has a diurnal variation.[5,13] This
variation can be incorporated so as to yield estimates of flash incidence
for any hour of the day during any month of the year. The form of the
diurnal variation depends on the "mix" of air-mass storms (occurring
dominantly in the local afternoon) and of frontal storms (comparatively
evenly distributed throughout the year). This "mix" varies from month
to month. Thus, in the Patrick AFB area in July, thunderstorms are more
than twenty times as frequent at 1600 LMT than they are at 0600 LMT;
however, in February the distribution is almost even throughout the day.[14]

In many instances--as at present--the primary concern is with
flashes to ground. The incidence of lightning to ground is of course
obtained when α_m is multiplied by p--the fraction of discharges to earth.
Although p is very variable from storm to storm, and even during different
phases of the same storm, it appears to increase systematically with
increasing latitude and may even also depend on T_m.[5,13] However, in the
Patrick area 0.2 seems a good average annual value for p.

3.   Flashes to Tall Structures

The incidence of flashes to tall structures electrically con-
nected to the ground is controlled by two factors. These are the
attractive radius and the triggering factor. The attractive radius, r_a,
and its associated attractive area A_a $(= \pi r_a^2)$ are primarily functions of
structure height h. The attractive radius is defined as the average
radius at which a downward leader from the cloud is just able to induce
an upward streamer from the structure that will unite with the downward
leader and thus divert the flash to the structure. The triggering factor
represents the propensity of flashes to be initiated at the tip of the
structure; it is negligible for h ≤ 100 m, but as h increases, triggered
flashes become increasingly common and for h ≥ 250 m the triggered
variety of discharge is by far the more important.

26

It is possible to calculate r_a. However, the calculations
that have been made can be criticized in many respects. Notably, a mode
of charge distribution on the downward leader must be assumed; also, the
postulation that breakdown from the downward leader to the structure
occurs when some average value of field over the gap is exceeded seems
very dubious. The data base that would allow us to estimate A_a from our
knowledge of p_{O_m} or p_{O_y} (annual value) is small, inconsistent, and in-
complete. Thus for $h \leq 150$ m, with triggered lightning therefore not
being of much significance, we would anticipate N_y, the number of flashes
per annum to a structure of known height, to be given by

$$N_y = p_{O_y} A_a(h) \quad .\tag{19}$$

The scanty available actual data suggest

$$N_y = K(h)h^c\tag{20}$$

where values of c ranging from one to two have been quoted, and the
factor K is both of uncertain size and of uncertainty in its dependence--
if any--on h. Consequently, any empirical evaluation of $A_a(h)$ by equating
Eqs. (19) and (20) is difficult.

Cianos and Pierce[5] have given a complicated expression for
r_a as a function of h. This is based both on the mathematical representa-
tions emerging from theoretical analysis, and on an empirical fit weighted
according to the degree of reliability of the various data sources.
Table 3 shows r_a as a function of h. Note that above about 150 m the
attractive radius does not change with a further height increase. This
is because calculations indicate that for $h \geq 150$ m the field distribution
between the tip of the structure and the downcoming leader is not much
influenced by the presence of the ground. Or, in other words, the im-
portant charges are those on the leader and those induced by the leader

27

Table 3

RELATION BETWEEN STRUCTURE HEIGHT (h)
AND ATTRACTIVE RADIUS (r_a)

h(m)	r_a (m)
25	~150
50	~250
100	~350
150	~400
>150	~400

at or near the structure tip; charges induced on the earth's surface (quasi-image charges) are of much less significance.

Pierce[15] has pointed out that reported instances of triggered lightning occur when the ambient general electric field E_a lies between 3 and 30 kV/m and the voltage discontinuity V_D, between the tip of the conductor causing the triggering and the unperturbed atmosphere, is 0.3 to 6 MV. It seems plausible that for the lower values of E_a and/or V_D there is a small but finite chance of lightning being triggered; this chance will obviously be greater the longer the values of E_a and V_D are maintained. As E_a and V_D increase so will the probability of triggered lightning, but the chance will again be dependent on the length of time for which any specific values of E_a and V_D exist. For two analyzed instances of a thundery environment, the percentage, P, of time for which a specified value of field E in kV/m is exceeded can be written approximately as

$$P = 2^{(9 - E)} \qquad E \geq 3 \text{ kV/m} \qquad (21a)$$

$$P = (0.3) \, 2.5^{(11 - E)} \qquad E \geq 5 \text{ kV/m} \qquad (21b)$$

28

Since the field below a thundercloud does not change drastically with height, we have $V_D \approx Eh$ for a structure of height h. It follows that we would expect the chance that the structure would trigger lightning to depend on appropriately mathematically manipulated aggregations of terms such as $c(P)P(E \cdot V_D/h)$, where $c(P)$ represents some probability of triggering over the various time periods (when specific values of E are exceeded) defined by P.

Obviously any attempt at the mathematical aggregation suggested above is presently--because of the immense uncertainties--quite unjustified. However, on the basis of Eqs. (21) and critical values of V_D of 1.5 and 2.0 MV respectively, two expressions for a triggering factor F_T have been suggested. These are:

$$F_T = \left\{ 1 + (1/12)(0.3)(2.5)^{(11 - 2000/h)} \right\} = \left\{ 1 + (10^{-2})(2 \cdot 5)^{(12 - 2000/h)} \right\}$$
(22a)

$$F_T = \left[1 + 2^{(9 - 1500/h)} \right] .$$
(22b)

The factor F_T is that by which the incidence of conventional lightning should be multiplied to take account of triggered lightning. The second term in the large bracket related to the first (unity) represents the proportion of flashes that are triggered as a function of height.

Table 4 summarizes in Column 1 the best presently available data on the incidence of triggered lightning as a function of height. The data base is so scanty that substantial future modifications could occur. Also shown in Table 4 are the information derived from Eq. (22) and some theoretical results due to Horvath.[16] None of the theoretical expressions agree well with the experimental data. Horvath's work much overestimates the incidence at lower values of h, and gives underestimates for high h. Equation (22b) fits well for $h \leq 150$ m but overestimates for

29

Table 4

PROPORTION OF TRIGGERED TO NATURAL LIGHTNING

Structure Height (m)	Actual Data	Expression (22a)	Expression (22b)	Korvath Theory
50	~0	~0	~0	0.1
100	~0	~0	~0	0.2
150	0.3	~0	0.5	0.4
200	1	0.1	2.8	0.7
300	4	1.3	16	1.4
400	10	6	38	3.0

large h. Equation (22a) underestimates throughout, but the agreement is becoming better for h ~ 400 m.

It is of some interest to evaluate an actual example. Over the years 1965 through 1973 the *Ground Wind Tower* (height 500 ft ~ 150 m) at Kennedy Space Center received at least one strike on 20 separate days.[17] Thus, the flash incidence per annum is ≥ 2.2. The incidence over open ground (Table 2) is ~27 per km^2 per annum; 20 percent of the flashes go to ground; and the attractive radius r_a (for h = 150 m) is about 400 m. Thus, the annual incidence of natural lightning to the tower should be $27 \times (0.2) \times \pi \times 400^2 \times 10^{-6} = 2.7$. Triggered lightning should contribute a further incidence of some $(0.4) \times 2.7 \approx 1.1$. Consequently the calculated flash incidence is 3.8 per annum; this compares reasonably with the value (≥ 2.2) actually observed.

4. **Tethered Balloons**

Tethered balloons, if the tether is conducting, can be regarded as very tall structures. Thus the corresponding analysis might possibly be extrapolated.

30

We note that the attractive radius r_a appears to stabilize at $r_a \approx 400$ m for $h \geq 150$ m. It seems reasonable that this value should also apply to the case of a vertical tethered balloon. However, the tether will often be inclined and thus the attractive area will be increased. This increase is not necessarily very large. Suppose that the length L of the tether is substantially greater than 150 m and that the angle (to ground) of the tether is θ. Then assuming the same attractive radius r_a, the added attractive area due to the inclined tether is $r_a L \cos \theta$. Typical values for L and θ might be 1000 m and 60°; thus, $r_a L \cos \theta$ is usually rather less than the original attractive area πr_a^2. Note that in our considerations of attractive areas we usually think in terms of vertically directed leaders. Inclined leaders undoubtedly occur, but there is some compensation between those inclined toward the structure (tending to augment the apparent attractive area) and those inclined away from the structure (tending to diminish the apparent attractive area).

Table 4 and Eq. (22) indicate that the occurrence of triggered lightning will continue to increase, and at an increasing rate with increases in structure height. However, the following considerations suggest that this will not indeed continue to be so, indefinitely:

(1) The analysis of triggered lightning incidents by Pierce[16] indicates that they occur when the voltage discontinuity V_D is approximately 1 or 2 MV and the ambient field E_a is on the order of 10 kV/m. Physical considerations would suggest that both conditions are required; the voltage discontinuity is needed to initiate a breakdown streamer, and this can then only subsequently propagate and develop into a full-scale lightning leader under certain ambient field conditions. The argument in Ref. 1 (p. 39) is quite wrong, since it considers only the V_D condition.

(2) Existing evidence supports the dual requirements for V_D and E_a. Thus, the fields associated with

many nonlightning weather situations--for example,
growing cumulus, rain, showers, and snow--are often
a few kilovolts per meter.[8],[16] Consequently, for
a very tall building (h $\sim$ 400 m), and certainly
for a tethered balloon (h $\sim$ 1000 m), V_D will often
approach 1 or 2 MV under weather circumstances
that are not naturally producing lightning. Yet
the great majority of instances of triggered
lightning (with the exception of such abnormal
events as the Apollo 12 and thermonuclear incidents)
have been reported at times when natural lightning
was also occurring. Some of the experiences
reported by Davis and Standring[6] for their tethered
balloons confirm the importance of the general
ambient E_a in triggering lightning. Thus, with
cumulonimbus and nimbostratus clouds overhead, no
triggered lightning occurred although it would have
been anticipated, from atmospheric electrical
climatology, that V_D would be on the order of 1 MV.
Indeed, the corona currents in the tether, then
being measured at a few milliamperes, are quite
consistent with $V_D \approx 1$ MV. Davis and Standring[6]
on many occasions observed charge transfer from
the tether of perhaps a coulomb occupying times
ranging from a millisecond to many seconds. No
lightning occurred, and the charge transfers were
identified with upward streamers from the tether
that failed to develop sufficiently to reach the
cloud charges; this identification seems very
plausible. The inference is inevitable; V_D at the
tether was enough to initiate the streamer, but
after it had advanced some distance the ambient
E_a was insufficient to support any further progress.

(3) An important paper by Bosart et al.,[18] has studied
the incidence of triggered and conventional
lightning to the towers on Monte San Salvatore in
Switzerland. They find that in very active air-
mass thunderstorms of considerable vertical develop-
ment, there are frequent flashes to the surrounding
countryside but relatively few to the towers; also,
for the actual discharges to the towers not many
are initiated by upward leaders from the towers.
On the other hand, for the weaker, frontal, storms,
in which the development is less pronounced, the
proportion of tower flashes relative to discharges

to adjacent areas is large while most of the tower
flashes are triggered. These results are quite
consistent with the significance of E_a. In frontal
thunderstorms the basic (frontal) instability is
large-scale and orderly, while the cloud base
and charges are at fairly low altitudes; consequently,
the ambient field tends to a uniformity between
the tower and the cloud, thus encouraging upward
leaders, once initiated, to bridge the gap from
tower to cloud. However, for air-mass storms the
basic (differential heating) instabilities are
small-scale and unorganized, while the altitudes of
the cloud charges and the vertical development of
the cloud are substantial; thus the ambient field
above the tower can be expected to be nonuniform
and many upward streamers from the tower will
perish when they move into a region of low ambient
field.

(4) The lightning-generating capacity of a thunderstorm
is not unlimited. In most thunderstorms only one
cell is active at any instant and an average
flashing rate is three per minute. Thus, even if
the whole lightning production of an overhead
storm were channeled, either as conventional or as
triggered lightning, to a tethered balloon the
upper limit is still only some three per minute.

Considering the above factors we now attempt to estimate the
lightning incidence to a balloon with a conducting tether of 1 km flown
throughout the year at Patrick AFB. The annual density of flashes to
ground is $p\,\sigma_y \approx 27 \times 0.2 \approx 5.4$ per km^2. If we take an attractive radius
r_a of 400 m, then $A_a \approx 0.5\ km^2$, giving a flash incidence of 2.7. The
additional triggering factor represents a great uncertainty. This is
particularly so because the results of Bosart et al.[18] suggest that for
the intense air-mass storms prevalent in Florida, initial breakdown
would occur within the cloud rather than be triggered at the balloon.
With this consideration in mind and extrapolating from the various di-
verse results of Table 4, it seems that 30 is not an unreasonable estimate
for the triggering factor, leading to an annual flash incidence of about 80.

We may make some quite independent estimates from storm-duration statistics. At Kennedy Space Center the mean duration of a thunderstorm is about 1.5 hours,[13] while there are on the average 1.7 thunderstorm events per thunderstorm day.[14] The average range[5] of audibility of thunder is about 15 km while the radius of an active cell[3] is perhaps 4 km. Suppose we assume that one cell is active per storm at any instant; that an average flashing rate by a cell is three per minute; and that every flash generated by an overhead cell strikes the 1-km balloon tether. Then the number of discharges to the balloon per annum is the product of:

76	(number of T/S days per annum)
1.7	(number of T/S events per T/S day)
1.5	(duration (hours) of T/S event)
3 × 60	(flashing rate per hour of T/S)
$(4/15)^2$	(chance of active cell being overhead).

This comes to about 250 per annum, and may be expected--mainly because of the assumption that every generated flash reaches the tether--to be an upper limit.

Another approach is to use Eq. (21) and to consider arbitrarily that triggering is 100 percent effective for $E_a \geq 10$ kV/m but does not occur for $E_a \leq 10$ kV/m. The corresponding percentages, P, for occurrence of $E_a \geq 10$ kV/m under thundery conditions, are given from Eq. (21) as 0.5 percent and 0.75 percent. We assume that the total annual time for which a thundery environment exists at the Kennedy Space Center is $76 \times 1.7 \times 1.5 \times 60 \approx 11,600$ minutes, and--using P = 0.5 percent--$E_a \geq 10$ kV/m for 58 minutes. This time, associated with a flash-generating capability of 3 per minute gives an annual discharge incidence to the tether of 174.

D.   Characteristics of Flashes to Tethered Balloons

Discharges to tall structures--and therefore presumably to tethered balloons--differ in certain respects from those to open ground. Some of these differences are now discussed.

It is well known that the vast majority (well over 90 percent) of flashes to open ground are negative--that is, they transport negative charge to earth. However, the proportion is much less for tall structures. Berger[20] has recently tabulated his observations from 1963 through 1971 at the towers on Monte San Salvatore; the effective height[15] of these structures is about 300 m. Berger finds that of all the discharges to the towers some 20 percent were positive as compared with less than 10 percent for discharges to open country. The proportion of positive flashes appears to vary significantly according to whether the flashes were initiated in the clouds or at the towers (triggered). For triggered flashes the positive proportion was 17 percent; however, for conventional flashes it was as high as 41 percent. Davis and Standring's results[6] for balloons with tether lengths of the order of 1 km support and extend the trend indicated by Berger's data. Thus, of all the flashes recorded by Davis and Standring,[6] 43 percent carried positive charge to earth.

The question of whether the distribution of peak currents for flashes to tall structures differs from that to open country is of some interest. The relevant data are represented in Table 5. We note that the results (for negative strokes) of the first three rows are reasonably consistent; the Cianos/Pierce[5] data are a composite mainly representative of discharges to low structures and open ground. Comparing rows three and four we note that positive currents occur more frequently than negative, both at the low and high (especially) ends of the distribution; the same effect is evident for the tethered balloon data (rows five and six). However, we have the rather disconcerting feature that the incidence of very low

Table 5

STATISTICAL DISTRIBUTION (PERCENTAGES)
OF PEAK LIGHTNING CURRENTS

Stroke	Current (kA)				
	<2	>2	>10	>40	>100
First return stroke[5] (negative)	0.8	99.2	80	23	4.0
Subsequent return stroke[5] (negative)	4.0	96.0	50	6	0.7
Monte San Salvatore[18] (negative)	0.2	99.8	75	13	1.0
Monte San Salvatore[18] (positive)	4.0	96.0	75	40	20.0
Tethered balloon[6] (negative)	54.0	46.0	22	1	?
Tethered balloon[6] (positive)	69.0	31.0	13	4	?

currents is apparently much more common for the tethered balloon than it
is either for Monte San Salvatore or for the composite data of Cianos/
Pierce.[5] The reason for this discrepancy is not entirely clear but may
well involve experimental sensitivity limitations for much of the data
summarized in Ref. 5; very small currents passed undetected. Berger's
work at Monte San Salvatore has increasingly concentrated on high-current
strokes, especially the positive "giants." This has led to a selection
of data that is statistically misleading. As discussed in Ref. 5, Berger's
earlier papers indicate a much higher proportion of low currents than do
his later studies.

Some of the increased incidence of positive high currents apparent
for tall structures can be plausible ascribed to closer proximity to the
lower positive thundercloud charge.[5]

36

Two conclusions related to flash characteristics have been advanced in Ref. 1 that do not seem well founded; they therefore merit comment. On p. 12 of Ref. 1 it is suggested that the peak currents experienced in a balloon tether over 150 m long will be rather less than those involved in flashes to open ground; the argument is based on the conclusion in Ref. 5 that the peak current is only attained within the lower 150 m of the ascending return-stroke channel. However, this conclusion is valid only for discharges involving objects not originally electrically connected to ground, such as free balloons or aircraft; it is not applicable to balloon tethers.

Reference 1 (pp. 55-56) also considers that the strike probabilities are greatest for tethers extending through the freezing zone of a thundercloud. This conclusion is based on aircraft data apparently suggesting maximum strike incidence at altitudes corresponding to the freezing level. There is presently some feeling that the aircraft data contain hidden biases in at least two respects. Firstly, the data have never been adjusted to account for the various times spent at the various altitudes while within a thundery environment. Secondly, much of the data is based on damage reports. An aircraft flying near or below the freezing level will experience predominately cloud-to-ground flashes[3] with their associated high-current return-stroke surges; however, within the upper parts of a thundercloud only intracloud discharges of comparatively low peak current will be encountered. Thus, reports of damage, sensitive as it is to peak currents, are biased against flashes above the freezing level. The work of Fitzgerald[21] is of extreme significance; using very well-instrumented aircraft, he was unable to detect any preferred level for lightning strikes during flights through active thunderstorms at altitudes from 0 to 10 km.

E.   "Conducting" and "Nonconducting" Tethers

The interaction of the balloon/tether system with the ambient elec-
trical environment differs significantly, for nonconducting tethers, from
that for conducting tethers. However, material resistivities approaching
that of air are difficult to attain, and nearly impossible to maintain,
so that it can be anticipated that the perturbation of the electrical
environment by a balloon flown with a poorly conducting tether may be no
better modeled by a perfect insulator than by a perfect conductor.

The transition from well-conducting to poorly-conducting-tether
behavior can be understood by consideration of the effects on the air-
earth current system of transfer of surface charge from the ground to the
balloon and tether. The effects of this transfer are characterized for
a well conducting tether by the collection area A(L), given by Eq. (2)
(Section III-A, above); this area is that from which complete diversion
of the unperturbed air-earth current would provide the tether-current
component not attributable to corona discharge. The transfer of surface
charge from the ground by which this diversion is accomplished reduces
the well conducting tether very nearly to ground potential since only a
very small potential gradient along the tether is necessary to sustain
the current in it.

The situation is markedly different for a poorly conducting tether.
A substantial potential gradient along the tether is necessary in this
case to drive current through it. Consequently, an estimate of the air-
earth current diverted from the air to a poorly conducting tether can be
obtained by comparison of its resistivity with that of the air, under the
assumption that the potential gradient along the tether is little changed
by the surface-charge redistribution through which the diversion occurs.
We again characterize the current diverted through the tether by the
surface area, A_R (sub R to distinguish it from that for the well conducting

38

tether), necessary to collect it under unperturbed conditions. We have, then,

$$I_T = \frac{E_o}{\rho} \quad \lambda E_o A_R(\rho) \quad (23)$$

with ρ the tether resistance per unit length, whence

$$A_R(\rho) = \frac{1}{\lambda \rho} \quad . \quad (24)$$

The transition from well conducting to poorly conducting tether can now be defined by the condition $A_R(\rho) = A(L)$. For $A_R > A$, the estimated surface-charge transfer from the ground, assuming little field distortion, exceeds the charge transfer necessary to bring the tether to ground potential. This condition--the tether at ground potential--is a state of maximum distortion. Thus, a substantial reduction of the tether potential gradient *must occur in the attainment* of equilibrium. This form of adjustment is just that which characterizes a well conducting tether. Conversely, for $A > A_R$, the estimated air-earth current diverted to the tether, assuming its reduction to ground potential, exceeds the current that can be driven through it by an unperturbed potential gradient. This condition--an unperturbed potential gradient--is a state of minimum distortion. Thus, the amount of surface-charge transfer must be small enough that the potential gradient along the tether is not severely reduced. The tether current is controlled in this case by the tether resistivity, a condition that characterizes a poorly conducting tether.

Insertion of Eqs. (2) and (24) into the condition $A_R(\rho) = A(L)$ yields the relation

$$\rho = \frac{\ln\left(\frac{2L}{b}\right) - 1}{\pi \lambda L^2} \quad (25)$$

between tether resistivity and balloon altitude for the boundary between well conducting and poorly conducting tether behavior. This curve has been plotted in Figure 5 for tether diameters of 1/4 inch, appropriate for the Baldy nylon tether, and 0.775 inch, appropriate for the larger Nolaro tether. The resistivity of the Nolaro tether has been measured to determine the effects of exposure; the results of these measurements are summarized in Figure 6. The 0.775 inch-Nolaro tether samples tended to divide into three distinct groups, which have been plotted separately. Comparison of the resistivity values in Figures 5 and 6 shows the Nolaro tether to vary from transitional to poorly conducting, depending on tether-surface contamination and balloon height. Comparable data are not available for the 1/4-inch nylon tether.

Under conditions for which the tether is well into the poorly con-ducting range, the balloon potential will remain near that of the un-perturbed field at the height of the balloon indefinitely, since equi-librium is established without the transfer of sufficient surface charge to appreciably perturb the field. Corona discharge from the balloon/tether system under these conditions is precluded, and measured tether currents should therefore be the order of $E_o \rho$, Eq. (23). The range of measured resistivities for the Nolaro tethers from 6×10^7 to 2×10^4 ohm $\cdot$ m^{-1}, thus implies a corresponding range of tether current from 5×10^{-4} μA to 2 μA for a nominal potential gradient of 100 V $\cdot$ m^{-1}. Observed tether currents typically lie in the range of 10^{-2} to 10^{-1} μA, well within these extremes, and depend only slightly on balloon altitude. Thus, their behavior is entirely consistent with this model.

The question of whether well conducting or poorly conducting tethers are to be practically preferred is important. We consider well conducting tethers to be preferable. The main argument in favor of poorly conducting tethers is that they are less likely to be struck by lightning; this may be so to a degree, but we do not believe this degree to be significant.
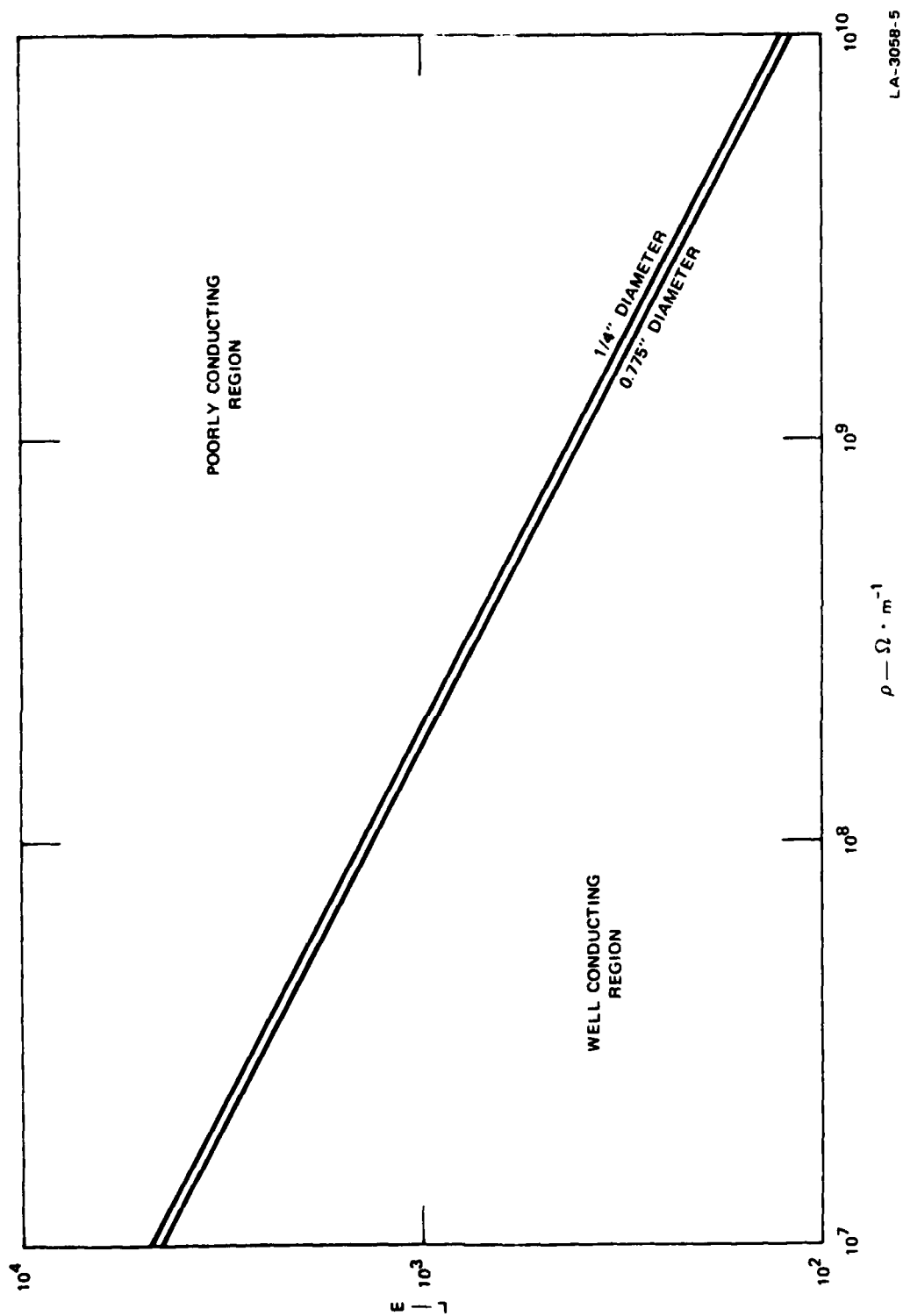
40

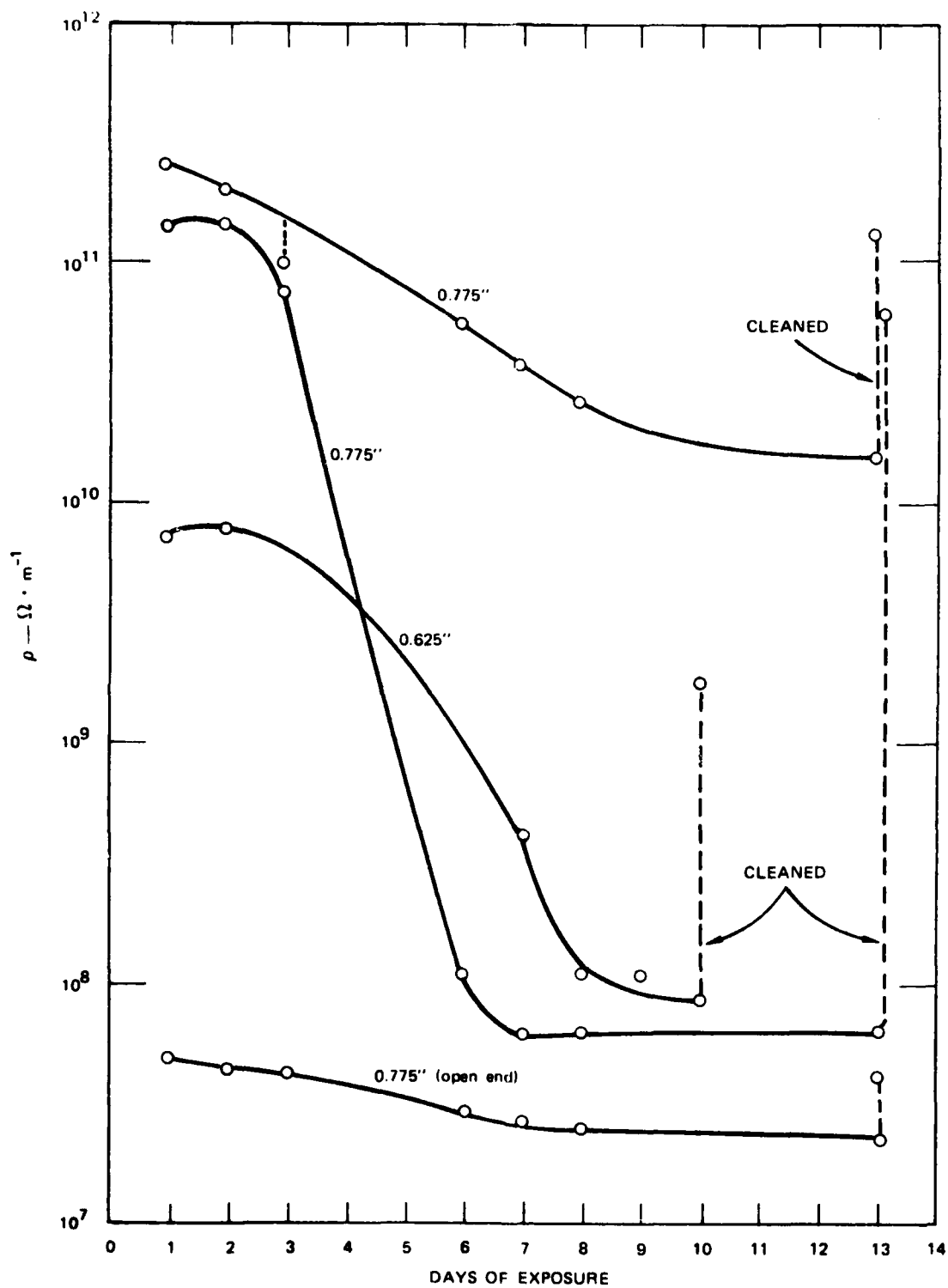FIGURE 5 REGIONS OF WELL CONDUCTING AND POORLY CONDUCTING TETHER BEHAVIOR

LA-3058-5

41

FIGURE 6   RESISTIVITY OF NOLARO TETHERS

LA-3058-6

A poorly conducting tether can never be completely "invisible" to the atmosphere; for it to be "invisible," the electrical properties of the tether would have to be everywhere identical with those of the adjacent atmosphere, and, since the electrical characteristics (conductivity for example) of the atmosphere change with height, this can never occur. Furthermore, it appears difficult, at best, to maintain a tether in the poorly conducting range indefinitely under all conditions. It may be anticipated that a poorly conducting tether that has been exposed for some time will have acquired a surface layer of contamination. In the rain of a thunderstorm environment this surface layer will become of low resistivity, so that the tether will be least likely to remain poorly conducting under the most critical conditions.

If a poorly conducting tether is struck by lightning, electrostatic considerations suggest that the current would be guided to ground down the dielectric discontinuity at the tether surface; it would not pass through the tether and on into the atmosphere. The actual lightning strike[22] of August 18, 1972, confirms this belief. Incidentally, the fact[23] that this flash apparently originated in an adjacent but not overhead thundercloud, strongly indicates that the "nonconducting" tether being used acted electrically as a well conducting tether in attracting and/or triggering lightning.

Damage considerations are important. If a poorly conducting tether is struck, the nonhomogeneity of the electrical properties ensures that the damage can be substantial.[22] On the other hand, if the well conducting tether is of sufficient conductivity and dimensions to handle the anticipated lightning current, the current will pass harmlessly to ground. The parallel with buildings is interesting. No one would construct a building of poorly conducting material without ensuring that it was adequately screened and shielded by a network of lightning

conductors well bonded to earth; he would not consider the insulating
nature of the building to prevent the occurrence of strikes.

We consider that the tether should be well conducting. This has
the very great advantage of facilitating power supplies to the balloon.
The balloon itself should be shielded so that lightning currents are
easily diverted along the tether to ground; Davis and Standring[6] have
shown how protective simple measures can be in this respect. We do not
believe, contrary to Ref. 1 (p. 15), that protection has necessarily
to be specially customized according to individual situations; good,
conventional lightning-protection practices will go a long way. Nor
do we agree (Ref. 1, p. 2) that the incidence of triggered lightning
can be significantly altered by the changing of structural shapes; this
is because the triggering depends more on the field magnitudes and con-
figurations some distance from the structure rather than those immediately
adjacent to the structure. Otherwise a minute point in corona would
suffice to trigger lightning!

IV SUMMARY

The main findings of the study may be summarized as follows:

(1) The balloon/tether system significantly perturbs the ambient electrical environment. Simple, idealized models of this system suffice to describe this perturbation qualitatively and to provide a rough quantitative guide to the interpretation of the data.

(2) Injection of space charge into the surrounding air by corona discharge plays an important role in the perturbation of the electrical environment by a balloon flown with a conducting tether.

(3) Tethers can be characterized as well conducting or poorly conducting in terms of their resistivity relative to that of the air. The classification of a given tether may change as the balloon altitude is altered.

(4) Lightning will strike a balloon, located in the Patrick AFB area, with a conducting tether of about 1 km length, on the order of 100 times per annum. Strike incidence with a nonconducting tether may be somewhat less, but not significantly less.

(5) Lightning to tethered balloons will include more positive strokes than do flashes to open ground. The distribution of currents for the positive strokes is more extreme than that for conventional negative lightning; both very high and very low current values are more likely.

(6) A balanced consideration of practical factors suggests that conducting tethers are to be preferred over nonconductors.

Appendix

PROLATE–SPHEROID CONDUCTING–TETHER MODEL

Appendix

PROLATE-SPHEROID CONDUCTING-TETHER MODEL

The perturbation of a uniform vertical electrical field above a conducting surface (the ground) by the projection vertically into the field of a long, thin grounded conductor (the tether) can be modeled as a conducting prolate spheroid in a uniform field, with the spheroid axis in the direction of the unperturbed field. The net charge on the spheroid is taken to be zero, and the image plane bisecting its axis represents the ground surface.

The induced surface charge on the spheroid produces a potential function for the total field of the form[7]

$$\psi = \frac{aE_o}{2} \xi \frac{\dfrac{\eta_o \eta}{2} \ln\left[\dfrac{(\eta + 1)(\eta_o - 1)}{(\eta_o + 1)(\eta - 1)}\right] + \eta - \eta_o}{\dfrac{\eta_o}{2} \ln\left(\dfrac{\eta_o + 1}{\eta_o - 1}\right) - 1} \qquad , \qquad (A-1)$$

where E_o is the unperturbed field strength, a is the interfocal distance, and (η, ξ) are the spheroidal coordinates. The rectangular coordinates (x,y,z) are related to the spheroidal coordinates (η, ξ, ϕ), with ϕ being the angular variable about the spheroid (and z) axis, by

$$x = \frac{a}{2}\left[\left(\eta^2 - 1\right)\left(1 - \xi^2\right)\right]^{1/2} \cos \phi$$

$$y = \frac{a}{2}\left[\left(\eta^2 - 1\right)\left(1 - \xi^2\right)\right]^{1/2} \sin \phi$$

$$z = \frac{a}{2} \eta\xi \qquad . \qquad (A-2)$$

The plane $z = 0$ ($\xi = 0$) is the bisector of the spheroid axis. The surface of the spheroid is defined by $\eta = \eta_o$.

At $z = 0$ (representing the ground), the perturbed field remains parallel to the spheroid (z) axis and has the magnitude

$$E_\xi(\xi = 0) = |E|$$

$$= E_o \left\{ 1 - \frac{\frac{1}{2} \ell n\left(\frac{\eta + 1}{\eta - 1}\right) - \frac{1}{\eta}}{\frac{1}{2} \ell n\left(\frac{\eta_o + 1}{\eta_o - 1}\right) - \frac{1}{\eta_o}} \right\} \quad . \tag{A-3a}$$

Equation (A-3a) can alternatively be written in terms of inverse hyperbolic functions

$$\frac{E_{\xi=0}}{E_o} = 1 - \frac{\coth^{-1}\eta - \frac{1}{\eta}}{\coth^{-1}\eta_o - \frac{1}{\eta_o}} \quad , \tag{A-3b}$$

which is the form given by Arnold et al.[9] The radial distance along the ground surface from the spheroid axis, r, is related to η on this surface by [cf. Eq. (A-2)]

$$r = \frac{a}{2}\left(\eta^2 - 1\right)^{1/2} \quad . \tag{A-4}$$

The collecting area of the tether is defined by

$$A = \frac{I_T}{i_o} \quad , \tag{A-5}$$

where I_T is the tether current and i_o is the unperturbed air-earth current. The tether current is the sum of the current increments diverted from each element of ground area; that is,

$$I_T = \int dA(i_o - i) \quad , \tag{A-6}$$

where i is the perturbed air-earth current to the area element dA. Combining Eqs. (A-5) and (A-6), we then have for the collecting area,

$$A = \int dA \left(1 - \frac{i}{i_o} \right)$$

$$= \int dA \left(1 - \frac{E_{\zeta=0}}{E_o} \right) \quad . \tag{A-7}$$

Now,

$$dA = 2\pi r dr \tag{A-8a}$$

or [cf. Eq. (A-4)] alternatively,

$$dA = 2\pi \left(\frac{a}{2}\right)^2 \eta d\eta \quad , \tag{A-8b}$$

whence, incorporating Eqs. (A-3a) and (A-8b) into Eq. (A-7),

$$A = \frac{2\pi \left(\frac{a}{2}\right)^2}{\frac{1}{2} \ln\left(\frac{\eta_o + 1}{\eta_o - 1}\right) - \frac{1}{\eta_o}} \int_{\eta_o}^{\infty} d\eta \eta \left[\frac{1}{2} \ln\left(\frac{\eta + 1}{\eta - 1}\right) - \frac{1}{\eta} \right]$$

$$+ 2\pi \left(\frac{a}{2}\right)^2 \int_{1}^{\eta_o} d\eta \eta \quad . \tag{A-9}$$

51

The second term in Eq. (A-9) accounts for the air-earth current that originally terminated on the ground area covered by the base of the tether and could be neglected to good approximation for realistic tether dimensions.

Evaluation of the first integral in Eq. (A-9) requires some care since a straightforward approach leads to the cancellation of infinities. It is therefore necessary to let the upper limit of integration in this term be finite and go to the limit only after the offensive terms have been cancelled out. We ultimately obtain

$$A = \pi \left(\frac{a}{2}\right)^2 \frac{1}{\dfrac{\eta_o}{2} \ln\left(\dfrac{\eta_o + 1}{\eta_o - 1}\right) - 1} \quad . \tag{A-10}$$

Expression of E/E_o, Eq. (A-3), and A, Eq. (A-10), in terms of the height, L, and base radius, b, of the tether is desirable. To this end, we note that

$$L = \frac{a}{2} \eta_o \tag{A-11}$$

and

$$b = \frac{a}{2} (\eta_o^2 - 1)^{1/2} \quad . \tag{A-12}$$

In terms of these parameters, Eq. (A-3) becomes

$$\frac{E_{z=0}}{E_o} = 1 - \frac{\dfrac{1}{2} \ln\left[\dfrac{\left(L^2 - b^2 + r^2\right)^{1/2} + \left(L^2 - b^2\right)^{1/2}}{\left(L^2 - b^2 + r^2\right)^{1/2} - \left(L^2 - b^2\right)^{1/2}}\right] - \left(\dfrac{L^2 - b^2}{L^2 - b^2 + r^2}\right)^{1/2}}{\dfrac{1}{2} \ln\left[\dfrac{L + \left(L^2 - b^2\right)^{1/2}}{L - \left(L^2 - b^2\right)^{1/2}}\right] - \dfrac{\left(L^2 - b^2\right)^{1/2}}{L}} \quad , \tag{A-13}$$

52

and Eq. (A-10) becomes

$$A = \frac{\pi\left(L^2 - b^2\right)}{\dfrac{L}{2\left(L^2 - b^2\right)^{1/2}} \ln\left[\dfrac{L + \left(L^2 - b^2\right)^{1/2}}{L - \left(L^2 - b^2\right)^{1/2}}\right] - 1} \qquad (A-14)$$

Numerical calculations can be performed to good accuracy with approximate forms of these equations, derived through application of the condition $b/L \ll 1$ for a realistic tether. From Eq. (A-13), we obtain for E/E_o

$$\frac{E_{z=o}}{E_o} \cong 1 - \frac{\dfrac{1}{2}\ln\left(\dfrac{X + 1}{X - 1}\right) - \dfrac{1}{X}}{\ln\left(\dfrac{2L}{b}\right) - 1} \qquad (A-15)$$

with, Eq. (A-4),

$$\eta \cong X \equiv \left[1 + \left(\frac{r}{L}\right)^2\right]^{1/2}$$

so long as $r \gg b$ is also satisfied. For A, we obtain from Eq. (A-14),

$$A(L) \cong \frac{\pi L^2}{\ln\left(\dfrac{2L}{b}\right) - 1} \qquad (A-16)$$

REFERENCES

1. P. E. Eggers, J. B. Brown, Jr., and R. G. Olilla, "Lightning Pro-
    tection Measures for Low-Altitude Tethered Balloon Systems," Tech-
    nical Report to Defense Advanced Research Projects Agency under
    Contract No. DAAH01-72-C-0982, Battelle-Columbus Laboratories,
    Columbus, Ohio (May 1973).

2. See, for example, R. D. Hake, Jr., E. T. Pierce, and W. Viezee,
    "Stratospheric Electricity," Final Report to Office of Naval Research,
    SRI Project 1724, Stanford Research Institute, Menlo Park, California
    (January 1973).

3. See, for example, N. Cianos and E. T. Pierce, "The Chances of In-Flight
    Lightning Strikes to Spartan Missiles," Appendix B in "Spartan In-
    Flight Lightning Analysis," Final Report, Vol. 1, McDonnell Douglas
    Astronautics Company--West, Huntington Beach, California (January 1973).

4. W. P. Winn, G. W. Schwede, and C. B. Moore, "Measurements of Intense
    Electric Fields in Thunderclouds," to be published.

5. N. Cianos and E. T. Pierce, "A Ground-Lightning Environment for
    Engineering Usage," Technical Report 1, prepared for McDonnell Douglas
    Astronautics Company under Contract L.S.-2817-A3, SRI Project 1834,
    Stanford Research Institute, Menlo Park, California (August 1972).

6. R. Davis and W. G. Standring, "Discharge Currents Associated with Kite
    Balloons," Proc. Roy. Soc., Vol. 191A, pp. 304-322 (1947).

7. P. H. Morse and H. Feshbach, Methods of Theoretical Physics (McGraw-Hill
    Book Company, Inc., New York, New York, 1953).

8. J. A. Chalmers, Atmospheric Electricity (Pergamon Press, New York and
    London, 1967).

9. H. R. Arnold, E. T. Pierce, and A. L. Whitson, "The Effect of a Living
    Tree upon the Fair Weather Potential Gradient," J. Atmos. Terr.
    Phys., Vol. 27, pp. 429-430 (1965).

10. J. E. Maund and J. A. Chalmers, "Point-Discharge Currents from Natural
    and Artificial Points," Quart. J. Roy. Meteorol. Soc., Vol. 86, pp. 63-
    90 (1960).

11. S. A. Schelkunoff and H. T. Friis, _Antennas, Theory and Practice_ (John Wiley and Sons, Inc., New York, New York, 1952).

12. B. I. Bleaney and B. Bleaney, _Electricity and Magnetism_ (Oxford University Press, London, 1957).

13. E. L. Maxwell, D. L. Stone, R. D. Crogham, L. Ball, and A. D. Watt, "Development of a VLF Atmospheric Noise Prediction Model," Final Report, Contract N00014-69-C-0150, Westinghouse Georesearch Laboratory, Boulder, Colorado (1970).

14. G. Daniels, ed., "Terrestrial Environment (Climatic) Criteria Guidelines for Use in Space Vehicle Development, 1971 Revision," NASA Technical Memorandum X-64589, Marshall Space Flight Center (1971).

15. E. T. Pierce, "Triggered Lightning and Its Application to Rockets and Aircraft," pp. 180-188, in _Proceedings of 1972 Lightning and Static Electricity Conference_, Air Force Systems Command, Wright-Patterson AFB, Ohio (1972).

16. T. Horvath, Contribution to International Conference on Lightning Conductors, Munich (1971); see R. H. Golde, _Lightning Protection_, p. 42 (Arnold, London, 1973).

17. Private communication, Glenn E. Daniels, Marshall Space Flight Center to E. T. Pierce, Stanford Research Institute.

18. L. F. Bosart, T. J. Chen, R. E. Orville, and H. B. Roesli, "A Study of the Synoptic Conditions Associated with Upward and Downward Lightning Flashes over Mt. San Salvatore, Lugano, Switzerland," to be published in _Tellus_.

19. C. J. Neumann, "The Thunderstorm Forecasting System at the Kennedy Space Center," _J. Appl. Meteorol._, Vol. 10, pp. 921-936 (1971).

20. K. Berger, "Methods and Results of Research Lightning on Mount San Salvatore 1963-1971," _Bull ASE_, Vol. 63, pp. 1403-1422 (1972).

21. D. R. Fitzgerald, "USAF Flight Lightning Research," pp. 123-124, in _Proceedings of the 1968 Lightning and Static Electricity Conference_, Air Force Avionics Laboratory (1968).

22. J. R. Stahmann, "Lightning Stroke to a Tethered Balloon Cable,"
     Investigative Report, Lightning and Transients Research Institute,
     Miami Beach, Florida (August 19, 1972).

23. Private communication, T. Hall (AFETR) to E. T. Pierce (SRI)
     (February 1974).

ADVANCED RESEARCH PROJECTS AGENCY

1400 WILSON BOULEVARD
ARLINGTON, VIRGINIA 22209

PART C

LIGHTNING PROTECTION
for a
RML TETHERED BALLOON SYSTEM
PHASE I
PERSONNEL PROTECTION

J. R. Stahmann

Contract F08606-73-C-0037   August, 1973

ARPA ORDER NO. __1876__

RANGE MEASUREMENTS LABORATORY
PATRICK AIR FORCE BASE, FLORIDA 32925

LIGHTNING PROTECTION
for a
RML TETHERED BALLOON SYSTEM

PHASE I
PERSONNEL PROTECTION

J. R. Stahmann

Lightning & Transients Research Institute
168 MacArthur Causeway
Miami Beach, Fla., 33139
Phone Area 305/ 672-5604

Contract No. F08606-73-C-0037

August, 1973

Prepared for

AIR FORCE EASTERN TEST RANGE (AFSC)
RANGE MEASUREMENTS LABORATORY
PATRICK AIR FORCE BASE, FLORIDA

ABSTRACT

Operating personnel at tethered balloon sites stand a greater than normal chance of being struck by lightning. The cable winch operator is particularly vulnerable because he is at the junction of the tether and the ground.

To determine lightning protection techniques for such personnel, the Lightning & Transients Research Institute simulated lightning strokes on a vertical steel ladder with and without Faraday shield cages. As a result of these experiments and an analysis of previous studies, Faraday cages are concluded to offer much better protection than grounding does. (Grounding is useful in remotely dissipating lightning strike energy.)

Site trailers and trucks act as natural Faraday enclosures and only slight modifications would be necessary to use these vehicles for protection. Entry cables should be bonded to walls of structures they enter. A lightning warning system should be installed to warn personnel when to stay inside, and appropriate procedures implemented.

To protect the winch operator, it will be necessary to also add a screen enclosure and staircase door to the operator's cage, ground the winch, and require insulated gloves for the winch operator.

The ideal lightning warning system should be able to respond to low initial warning levels and to high storm levels; yet it should give a low percentage of false alarms. A corona point on a pole, connected to ground through a microammeter, is a simple inexpensive detection device. The electric field mill is more sensitive and reliable but may be difficult to obtain.

Preliminary experiments to determine proper wire size for Faraday cages and for tether cables indicate that a 1/4-inch diameter steel cable should withstand current peaks up to 100 kiloamperes.

Proof testing of lightning protection devices is recommended.

Toxey A. Hall, RML

CONTENTS

I. Introduction

This report covers Phase I, personnel protection, of a program covering the lightning hazards to a tethered balloon system. The basic requirements for personnel protection have necessarily been worked out and well understood by those working with natural and simulated lightning strokes at close range. That they have survived exposure to nearby natural strokes and many simulated strokes to various enclosures testifies as to the efficacy of their protective measures.
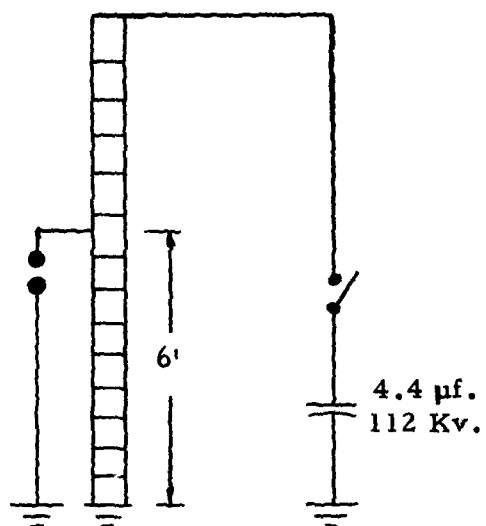
The lightning stroke about a year ago to a Nolaro cable tethering a balloon[1] spotlights the need for better personnel protection. In this instance, had the lightning stroke occurred just a few minutes later, the winch operator would have been exposed to direct stroke contact. Personnel protection and shielding has been discussed in many other reports covering balloon systems[2] and launch sites for rockets[3][4]. While the salient points of other reports are reviewed and extended here, the main effort in this report is to put the various measures in proper perspective and to simplify and condense the basic techniques, giving only their primary justification.
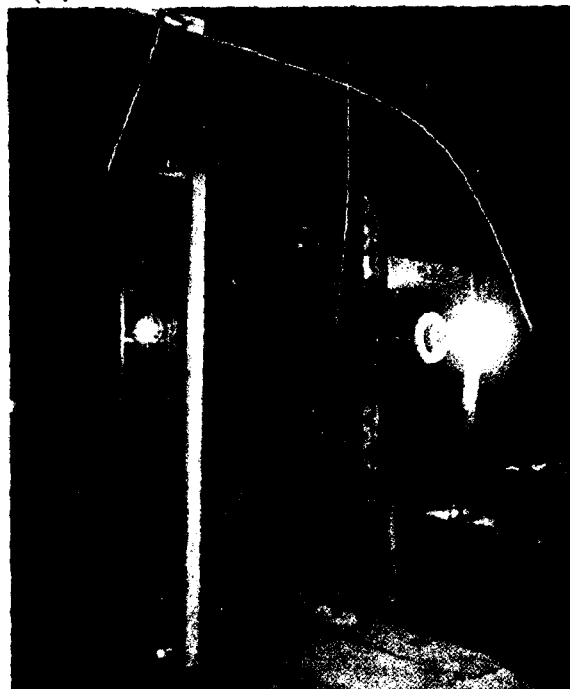
II. The "Faraday" Cage

The most important shielding technique for personnel utilizes the "Faraday" cage principle. While the Faraday cage usually refers to eliminating electric fields inside a closed conducting surface, the extension of this method to shielding under dynamic electric and magnetic conditions can be effected with an understanding of the principles involved and careful application. A closed surface with excellent surface conductivity offers good lightning protection. Next best is an all metal enclosure of good conductivity, such as an aircraft, which has a few openings, plastic sections or other discontinuities. The magnetic shielding is obtained from induced surface currents which usually have a small depth of penetration. There remains some field penetration through openings and other discontinuities and internal displacement current and surface Ri drop. Currents can also be conducted into an aircraft via penetrating conductors such as antenna lead ins. However, with proper lightning arresters on the antennas and protection of the plastic sections, an aircraft can be a good shield cage, despite its openings. This is also true of automobiles, trucks and trailers if the lightning is not conducted inside by external conductors insulated from and penetrating the vehicles.

An example of a minimal Faraday shield cage for direct lightning strokes is illustrated in Figure 1. As shown in Figure 1 (a) and (b), a simulated lightning stroke is passed through a vertical ladder.

(a)

(b)

6'

4.4 µf.
112 Kv.

Voltage across unprotected ladder.
measured by spark gap shown on ladder
at left.

(c)

(d)

10,000

Voltage

1000

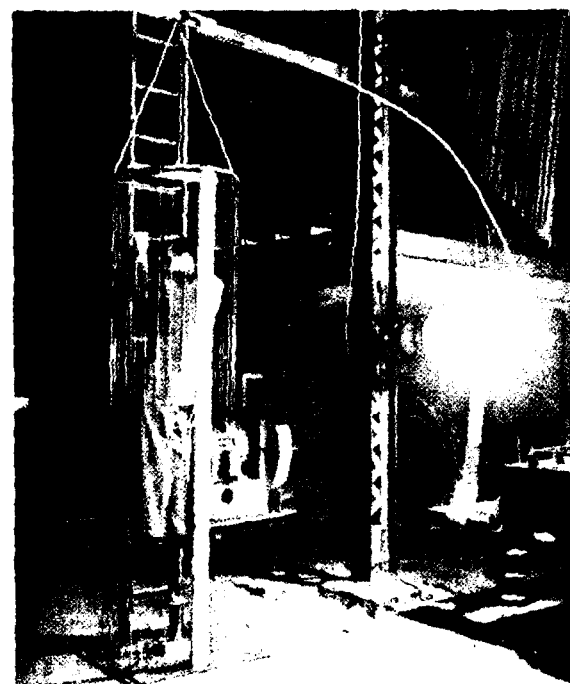$\frac{di}{dt}$ = 10,000 AMP/µSEC

100

10

0   4   8   16   32

Number of conductors
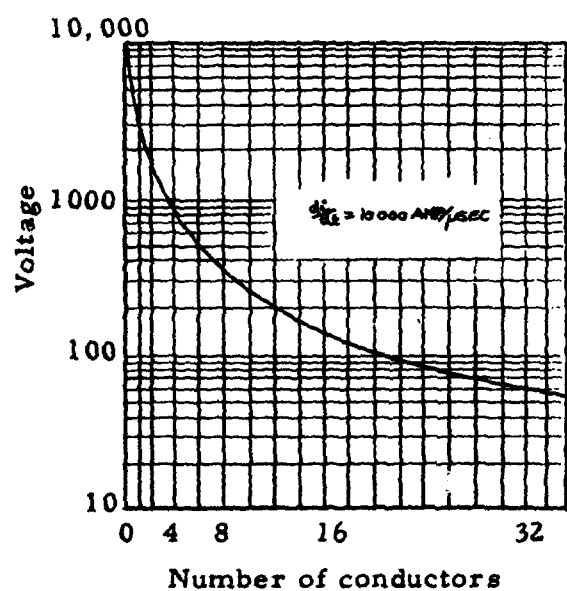
Voltage as function of number of
shield wires.

$(di/dt)_{max}$ = 12,500 amps/µsec

Figure 1.   Illustration of reduction of hazard on an airship tunnel ladder
subject to lightning, using a shielding cylinder of wires.

The ladder is shunted by a six foot conductor with series gap to represent a six foot man in contact with the ladder. Flashover of the gap, Figure 1(b), demonstrates the current which could flow through the man at a voltage in excess of 20 kilovolts under the conditions shown. The basic equation for the voltage in the man-wire loop is $Ri + (L-M)di/dt$. If an additional conductor is placed on the opposite side of the man from the ladder, the mutual coupling to the man, M, is increased so that $(L-M)$ is reduced, and the voltage in the man-wire loop is reduced by about one-half. If more conductors are added symmetrically about the man, this voltage can be reduced to acceptable levels, Figure 1(c), so that a man can safely enter such a Faraday shield cage and be safe from direct lightning strokes, Figure 1(d). The effectiveness of such a shield cage was demonstrated by applying a 100 kiloampere peak current having a rate of rise of 12,500 amperes per microsecond. Leather shoes provided sufficient insulation against any residual short duration transient voltage. It is important, in implementing such a shield system, which can only approximate a closed surface, to arrange the conductors to maximize the mutual coupling to the man or equipment to be protected. In effect a counter EMF is induced so that the net loop voltage is minimized. From the point of view of an observer on the inside of the cage, the net magnetic field is minimized by proper arrangement of the conductors.

An aircraft flying in a thunderstorm may easily assume the potential of its position in space, for example 50 megavolts, without the passengers being aware of it. The aircraft may also be struck by lightning without the passengers receiving electrical shock. Inside the enclosure, personnel and instruments alike detect only minor electrical disturbances. A direct stroke to the enclosure is usually preferred over a nearby stroke since it usually results in less induced voltage due to magnetic induction. Thus, for lightning protection of personnel, the basic requirement is to provide Faraday cage enclosures for personnel and make sure they are inside when a nearby stroke is possible. Such "cages" can be trailers or trucks normally on site that have been examined for lightning hardening and slightly modified if necessary as discussed in Section IV.

III. Grounding

Probably the most generally misunderstood protective measure is grounding and its effectiveness. The Faraday cage of Section II does not require grounding any more than an airplane in a lightning storm. Grounding the enclosure, Figure 2, affects only its external potential. It has little effect on the relative potentials inside the enclosure of exclusive interest to those inside. In certain instances, of interest
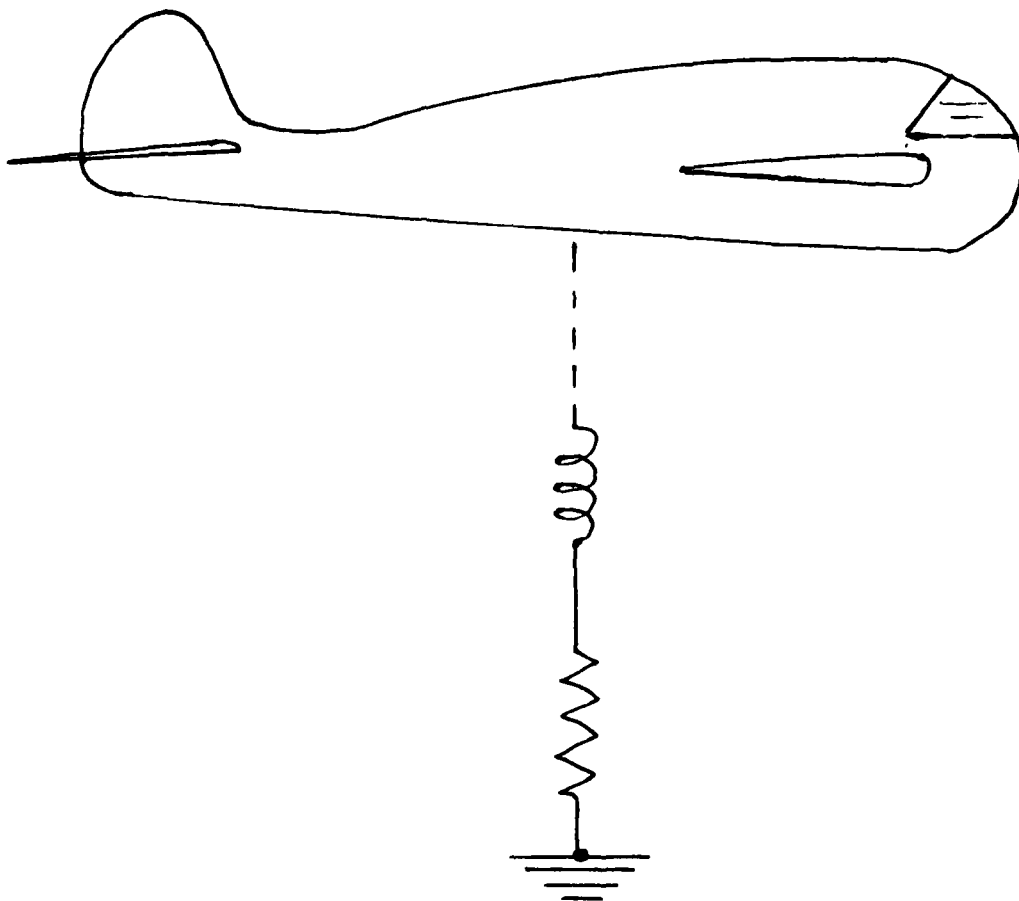
Figure 2. The external potential of a good conducting metal enclosure, such as an aircraft, has little effect on the relative potentials inside. Grounding has little effect and is not necessary to protect those inside the enclosure.

mainly in protecting sensitive equipment, improper external grounding can increase internal induced voltages.

Study of the characteristics of the earth shows a wide variability of ground resistivity, from the 0.25 ohm-meter of sea water to 10^4 ohm-meter for industrial areas in cities. From a lightning point of view a ground of 100 ohms, 10 ohms or even a one ohm ground is not effective to significantly reduce the voltage of a 100 kiloampere stroke. A short (10 foot) large one inch diameter copper ground cable is not effective, because it has an inductance of the order of a few microhenries which results in a L di/dt voltage component of 100 kilovolts or more for a high rate of rise of current lightning stroke. Thus, grounding, per se, as, for example, grounding of the tether cable winch, cannot be used for personnel protection near the stroke terminal point. However, proper grounding can be used to dissipate the energy of the lightning stroke at a remote point. For example, grounding at a remote flying sheave could be used to keep most of the current away from the winch area. The use of a remote separate conductor, both for power transmission and lightning protection, has been suggested as a result of our earlier balloon work.[5] A conducting ground plane may be used as a foundation for a large site enclosure or to interconnect site enclosures to help protect interconnecting cabling. However, because of the variability and generally high resistivity of the earth, only complete diversion of the lightning stroke to a remote ground could possibly be effective for personnel protection. At the present state-of-the-art no such technique has been tested and shown reliable. On the other hand, we know that natural lightning may fork, form parallel paths or violate "cone of protection" rules due to the varying angle of approach. Therefore, providing Faraday enclosures is presently the only safe method of proven lightning protective reliability for personnel.

IV.   Practical Protective Enclosures

Faraday cages of the type discussed are approximated by trailers and trucks available at balloon launch sites. These are usually constructed with metal walls and roof. The floor usually is also metallic in structure and often does not require modification. Bonding should be added if the metal parts are not electrically interconnected.

The most common violation of the electrical integrity of a trailer enclosure housing various equipments is feeding a cable into the trailer through an opening without bonding it to the trailer, Figure 3. This essentially brings the potentials of the outside world into a formerly safe enclosure. Under lightning conditions a grounded cable of this type

Trailer voltage = 200 Kv. due to / lightning

Remote
Grounded
Cable

ΔV = 200 Kv. − 0 = 200 Kv.

V=0

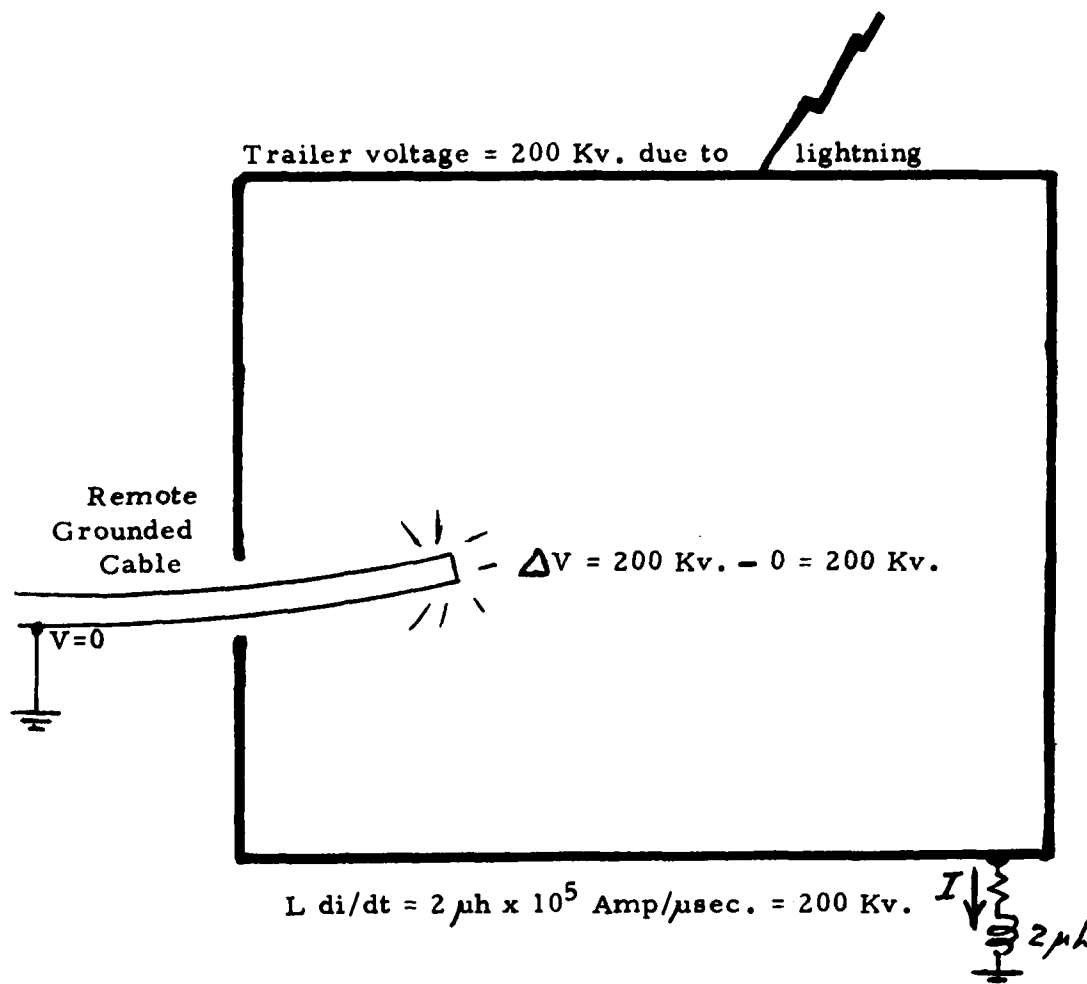L di/dt = 2 μh x 10^5 Amp/μsec. = 200 Kv. I 2μh

Figure 3.   A common mistake is to run a cable into an enclosure
without properly bonding it to the wall. This permits
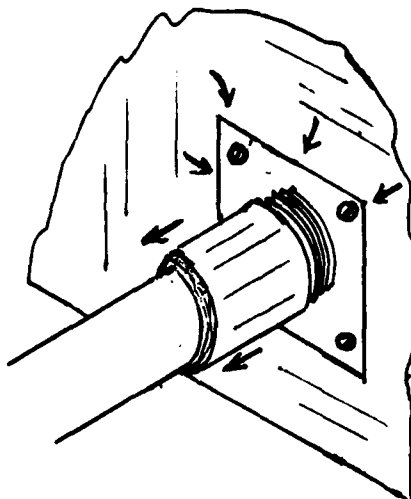large voltage differences to enter the enclosure.

Figure 4.   The lightning current should be forced to flow
externally through a peripherally bonded connector.

-6-

may be as dangerous as a live wire. Currents may flow in it which produce high fields in the trailer or burn up the cable. All such cables should be brought into the trailer or other enclosure through feed through connections. The cables should be well shielded or in conduit. Pigtail connections to the trailer at the point of entry are not a satisfactory substitute for complete peripheral bonding to the trailer terminal panel, Figure 4.

V. <u>Protection of the Cable Winch Operator</u>

Specific measures for protection of the winch operator are:

(1) Modify the winch operator's cage, Figure 5, to make it a better electrically shielded enclosure by adding a partial screen around the controls, bonded to the control housing and the rest of the cage and by adding a similarly screened door on the staircase side.

(2) The integrity of the cage should be maintained, as discussed previously, by making sure that any cables required to enter the cage are shielded with the shield peripherally bonded to a feed through panel mounted in the outside wall so that lightning currents flow on the external surface. An incorrect method, illustrated in Figure 6, shows an insulated communication cable entering around a corner of the wall of the cage.

(3) Insulated gloves could be worn by the operator at his option to avoid possible small shocks due to minor imperfections in the cage.

(4) Procedures must <u>require</u> that the operator remain in the enclosure during thunderstorm warning periods, possibly signaled by a warning device to be discussed in the next section.

(5) It would be advisable to proof test the final cage design with simulated lightning.

(6) Grounding of the winch is optional for the reasons previously discussed.

VI. <u>Protection of All Personnel</u>

Partially shielded enclosures, such as trailers and trucks, should be modified with improved bonding, added screening, feed through

Figure 5. The winch operator's protective cage could be easily converted to a Faraday lightning protective enclosure.
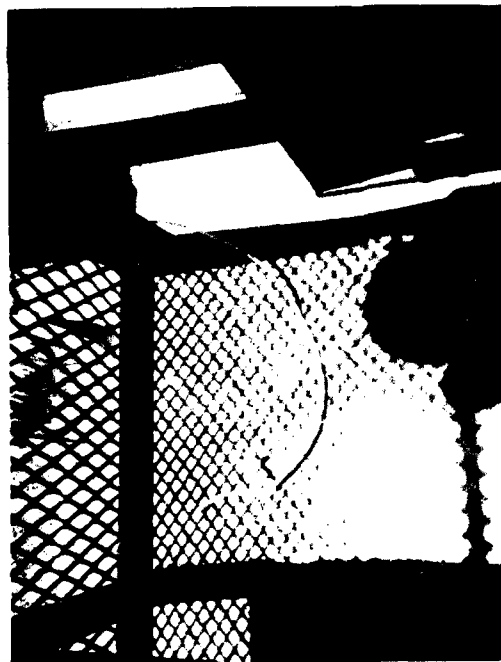
Figure 6. In an actual installation it is often easy to
circumvent the integrity of a protective enclosure.
In this example, a communications cable brings
a ground into the enclosure.

connectors in enclosure walls for cables and whatever other steps
are necessary to provide well shielded enclosures for all personnel.
Typical enclosures, with these modifications, could also be proof
tested with simulated lightning to verify adequacy.

Procedures should require that all personnel be in the enclosures
provided during periods of moderate-to-high lightning stroke inter-
ception probability. Three warning levels have been suggested:

(a) Condition green - Safe

(b) Condition yellow - Low stroke probability
During this period, stay in a shielded enclosure unless required
to be exposed. (Similar to fasten your seat belt when in your sea

(c) Condition red - Moderate to high probability
During this period all personnel, especially the winch operator,
should remain in a shielded enclosure.

VII. Warning Systems

Lightning warning systems have measured the various thunder-
storm parameters in an attempt to predict the occurrence of a stroke
in terms of an estimate of its probability of occurrence. The atmos-
pheric electric field near the ground is often measured; lightning sferics
can also be measured, located and counted; and radar, with the basic
meteorological subsystems, can monitor storm buildup. Much of the
data gathered has to be classified "after the fact" information. Pin-
point thunderstorm prediction is extremely difficult, especially for
Florida type individual buildups not associated with a broad frontal
system or other more easily recognizable weather patterns.

An ideal lightning warning system would identify periods of lightning
hazard to personnel in a specified area and only these periods. It
would provide enough advance warning to allow personnel to reach a
safe enclosure. It should be more reliable than ordinary weather
observation methods and remain reliable in heavy rain and high wind.
It should not be susceptible to high electric transients and other storm
conditions present. Its dynamic range should be broad enough to re-
spond to the low initial warning levels and the high storm levels. It
should also give a low percentage of false alarms.

For electric-field measurement, the corona point on a pole, Figure 7, is a simple, easy to install and inexpensive detection device for field use. A brush point, made of coax shield braid, is usually placed on a convenient pole or other high point and connected to ground through a microammeter with, if possible, a recorder. Of course, several such installations give a better prediction than only one measurement point, but one installation can warn of the approach of a highly charged cloud and distinguish a charged cloud from one of the same appearance that is not significantly charged. Interpretation of the absolute readings depend on the pole height and location, but typical warning levels might be 10 to 100 microamperes. More accurate devices for electric field measurement include the field mill, radioactive probe (β rays) and electrometers. The electric field mill is the most sensitive and reliable instrument, but may be difficult to obtain. Two or more field mills, located for storm tracking, can be effective for detecting storms approaching from a distance such as frontal disturbances. KSC has used eight electric field measurement locations.

Information from sferics locators and counters has limited value. Many storms change in intensity quickly so that their activity at a distance does not forecast what they will be overhead. Thunderstorm cells are continually building and dissipating so that the storm overhead can be a new buildup triggered by the nearby storm activity. Radar gives good and useful information on the storm buildup, but good radars are expensive and usually not available in the field.

A new, relatively inexpensive system for measuring lightning hazard level is called Thorguard by its manufacturer. It utilizes an electric field mill to measure field strength, but also responds to the dynamics of a thunderstorm field, including polarity changes. If the data fits a typical, preconceived thunderstorm profile, a colored warning light indicates the stroke probability to the area where the instrument is located. An alarm is used in conjunction with the highest warning levels. This instrument is new, but it has been installed at FPL in Miami so that about a year's experience with good results has been obtained.

VIII. Wire Mesh Enclosures

Of special interest, both for wire mesh enclosures for personnel and for tether cables, is the lightning current carrying capacity of wires. Since lightning has a high current pulse of short duration, a
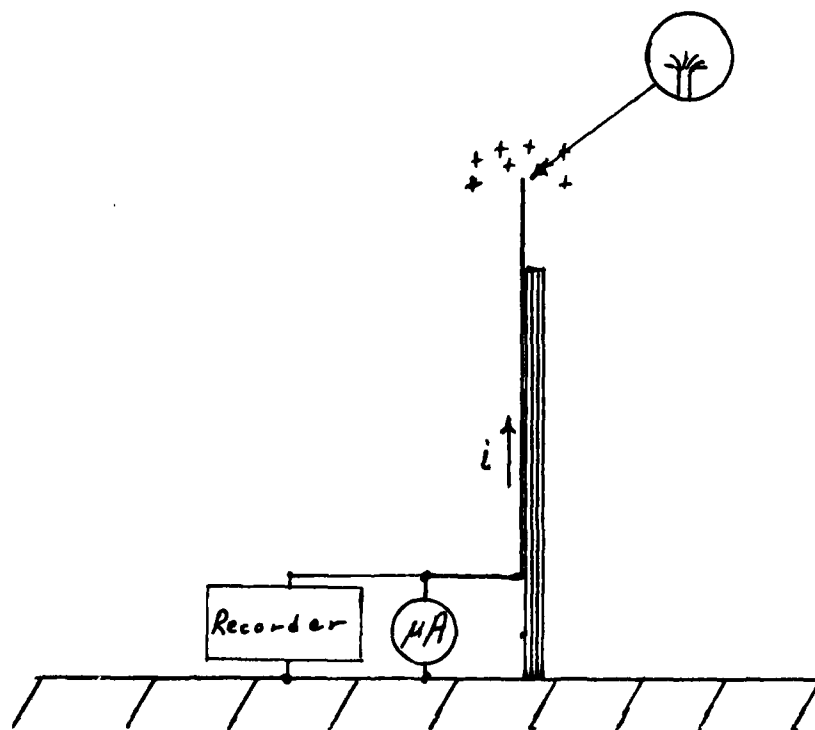
Figure 7. The corona point is the simplest device for electric field measurement. It is inexpensive and easy to install.

small wire can usually withstand a surprisingly high peak current. The time to half-value for the high current component of a stroke is usually less than 50 microseconds. A continuing current of the order of 100 amperes for less than a second may also be present.

A short study of a length of 1/16" diameter galvanized steel tie wire was conducted to obtain "ball park" data. A 10-50 current wave was applied from a 110 μf bank to give an average lightning current. A four foot length of wire was checked in the setup shown in Figure 8(a). The current waveform first applied is shown in Figure 8(b). Under these conditions the wire flashed brightly at a peak current of 24 kiloamps. It was red hot at 25 kiloamps and burned off at the ends when 27 kiloamps was applied. It was estimated that the wire would tolerate a peak current of about 15 kiloamps, an average stroke current, without serious damage. The breaking strength of the wire, about 200 pounds, did not decrease as a result of the passage of this current level; however, the wire was not checked under tension for distortion due to the heating.

To check the effect of a current of longer duration, a longer waveform, Figure 8(c), was applied to the wire from a 281 μf bank. The wire now became red hot at 19 kiloamps and broke at 20 kiloamps. After passing a peak current of 15 kiloamps, the breaking strength remained at about 190 pounds. As an estimate, the lightning current capacity of the wire was probably reduced proportionate to the breaking current or about $(20/27) \times 15 = 11$ kiloamps. These results illustrate that a steel cable of about 1/4" diameter or greater should withstand current peaks of up to 100 kiloamps (99th percentile probability of occurrence). Results of previous tests[6] on stainless steel cable showed compatible results.

IX.   Conclusions and Recommendations

(1) For personnel protection from lightning on a balloon launch site, enclosures should be provided. These enclosures may be trucks and trailers which have been examined from a lightning point of view and modified, if necessary, to improve conductivity.

(2) All cables, entering shielded enclosures, should be connected externally to a feed through panel so the cable currents flow externally.
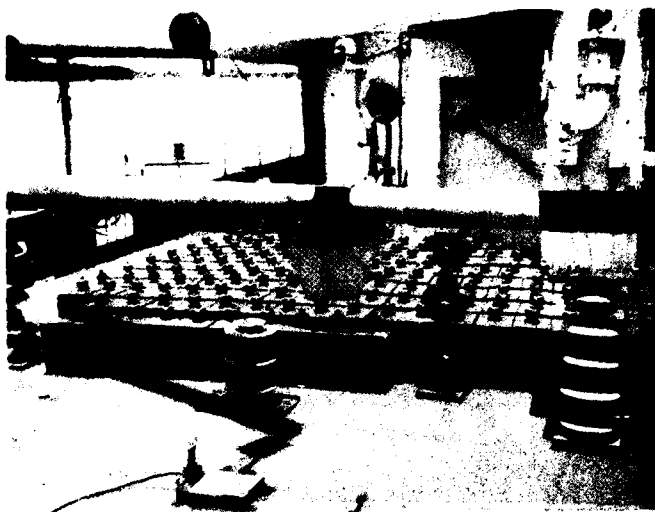
Figure 8(a). Set up for measuring the lightning carrying capability of 1/16" diameter steel wire.

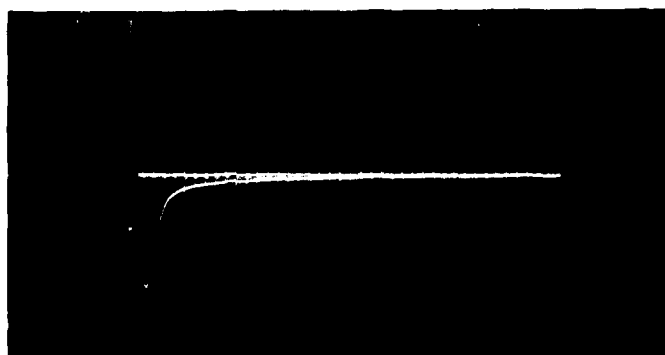Figure 8(b). Applied 10 x 20 waveform from a 110 uf. bank. Calibration 7 Ka. and 100 μsec. / large division.

Figure 8(c). Longer waveform applied from a 281 uf. bank. Calibration 7 Ka. and 100 μsec./ large division.

(3) While good grounding can reduce stroke voltages and remote grounding can reduce stroke currents, this technique cannot be relied upon for protection of personnel. Grounding is basically useful as a first stage in certain equipment and site protective problems. Remote grounding with a grounded flying sheave or a separate conducting cable is desirable, if feasible.

(4) The winch operator's cage should be modified to provide a good shielded enclosure for the winch operator. Again, any necessary cable entering the enclosure must be bonded externally to the enclosure as described in this report.

(5) A lightning warning system should be selected and installed. The performance of the warning device should be checked on site against storm conditions and experience. A warning device at the balloon would also be advisable.

(6) Procedures should require that all personnel be protected in an enclosure provided when the probability of stroke occurrence is moderate to high. The winch operator should stay in his enclosure during all stroke warning periods. Others should stay in enclosures during periods of low stroke probability when possible as a precautionary measure.

(7) A conducting cross section at least equivalent to a 1/4" - 3/8" steel cable is necessary to conduct a 100 kiloampere peak current stroke. Most available enclosures have at least this cross section.

(8) Typical enclosures should be proof tested with simulated lightning on site, if possible. A portable simulator can be moved to a site at minimal cost for such tests.

References

(1)   Stahmann, J. R., "Investigative Report, Lightning Stroke
        To a Tethered Balloon Cable", Lightning and Transients
        Research Institute, Miami Beach, Florida, prepared for
        Air Force Eastern Test Range, Patrick Air Force Base,
        Florida, August 19, 1972.

(2)   Stahmann, J. R. and Robb, J. D., "Lightning Protection
        for Tethered Balloon with Power Cable", Final Report,
        Lightning and Transients Research Institute, Miami
        Beach, Florida, Contract F8606-69-C-0030, prepared
        for Air Force Eastern Test Range, Patrick Air Force
        Base, Florida, April, 1969.

(3)   Newman, M. M., et. al., "Prevention and Control of
        Lightning at KSC, Final Summary Report", Contract
        NAS 10-5134, Lightning and Transients Research
        Institute Report 478, April, 1968.

(4)   Stahmann, J. R., "Lightning Protection for Navy 2D2
        Site, Pinecastle, Florida", Lightning and Transients
        Research Institute, Miami Beach, Florida, prepared
        for Department of The Navy, NTDC, Orlando, Florida,
        May, 1969.

(5)   Stahmann, J. R., "Improvement of Protection against
        Atmospheric Electrical Effects on a Tethered Balloon-
        Antenna System, Lightning and Transients Research
        Institute, Miami Beach, Florida, Contract DAAB07-
        70-C-A118, prepared for the United States Army
        Electronics Command, Fort Monmouth, New Jersey,
        November, 1969.

(6)   Stahmann, J. R., "Lightning Survivability of Tethered
        Balloon Cables", Lightning and Transients Research
        Institute, Miami Beach, Florida, Final Report Contract
        F19628-67-C-0377, prepared for Air Force Cambridge
        Research Laboratories, Bedford, Massachusetts,
        February, 1969.

ADVANCED RESEARCH PROJECTS AGENCY

1400 WILSON BOULEVARD
ARLINGTON, VIRGINIA 22209

PART D

LIGHTNING PROTECTION
FOR A
RML TETHERED BALLOON SYSTEM

PHASES II AND III

WINCH, CABLE AND BALLOON PROTECTION

J. R. STAHMANN

CONTRACT F08606-74-C-0031   MAY, 1974

ARPA ORDER NO. 1876

RANGE MEASUREMENTS LABORATORY
PATRICK AIR FORCE BASE, FLORIDA 32925

LIGHTNING PROTECTION
for a
RML TETHERED BALLOON SYSTEM

PHASES II AND III
WINCH, CABLE AND BALLOON PROTECTION

J. R. Stahmann

Lightning & Transients Research Institute
168 MacArthur Causeway
Miami Beach, Fla. 33139
Phone Area 305 672-5604

Contract No. F08606-74-C-0031

May, 1974

Prepared for

AIR FORCE EASTERN TEST RANGE (AFSC)
RANGE MEASUREMENTS LABORATORY
PATRICK AIR FORCE BASE, FLORIDA

FOREWORD

Phases II and III of a study of the lightning susceptibility and protection of a RML tethered balloon system are presented in this report. These phases included the winch, tether cables, balloon and on-board electronics. Personnel lightning protection was covered in the report on Phase I.

This work was performed under Contract F08606-74-C-0031 with Mr. Toxey Hall participating in the research as the RML project engineer.

ABSTRACT

Since nonconducting tethers can be struck by lightning, both conducting and nonconducting tether cable specimens were tested to determine those with the highest probability of surviving average to severe lightning discharges. Stainless steel and Fiber B samples showed least damage of the cables tested. Exhaustive tests showed that the nonconducting cables could be further improved. Power conductors, if placed inside a Nolaro cable, would destroy the cable; but externally placed conductors would protect it. Gaseous fuel could be safely transported to the balloon in a plastic tube placed inside a Nolaro cable, but the cable itself would still be subject to damage.

Lightning diverters at nose and tail, with interconnecting cables attached to the diverters and the top of conducting confluence cables, could be used to protect the balloon and some of its equipment. The confluence cables could form a Faraday cage for protecting electronic equipment inside it and for conducting the lightning current to the tether cable.

On-board electronics should be protected against voltage transients with surge arresters or limiters, operating at high, medium and low levels, if necessary. Electroexplosive devices should be short circuited until activated.

-iii-

TABLE OF CONTENTS

I. Introduction

This report covers Phases II and III, winch and tether cable lightning protection and other balloon and cable protective measures, of a program studying the lightning protection for a RML tethered balloon system. The primary emphasis of this part of the study was on the experimental evaluation and test of the lightning susceptibility of various tether cable specimens supplied by RML. It should be pointed out that, because of the dielectric discontinuity at the surface of a nonconducting tether, the tether cannot be considered electrically "invisible" to its environment. The cable conductivity due to moisture absorption and surface contamination affects the quasi-static electric field intensities and lightning triggering, but the lightning streamers and high currents are not conducted by the cable but in an ionized air channel near the cable surface. The guiding prestrike streamers form suddenly along the cable-air boundary during the relatively rapid field changes of the prestrike phase. Thus measures for sealing out moisture by cable impregnation or special coatings, designed to reduce cable conductivity, cannot prevent stroke guidance and cable involvement in a lightning stroke. As a practical matter, it is also virtually impossible to prevent surface contamination and conduction of the microampere currents which flow in thunderstorm fields of the order of 20 kilovolts per meter or even in earth fields. Cable protective schemes for nonconducting tethers then have, as a basic purpose, to keep the high lightning currents out of the cable and in an ionized air path alongside the cable, similar to the purpose of the segmented lightning diverter strips used on radomes. However, prestrike streamers, guided by the cable, ocassionally enter the cable and provide a path for the later high current into the cable, damaging the cable section. About 4% of a Nolaro cable, struck by natural lightning, was damaged.[3] The damage reduced the tensile strength of the cable from about 26,000 pounds to only 8,000 pounds at a time when the flight load was of the order of 5,000 pounds. As will be discussed, moisture absorption, particularly if nonlinear, does appear to increase the probability of streamer puncturing and the resultant cable damage.

II. Personnel Protection

Personnel protection was the subject of our report on Phase I of this program.[1] During the natural lightning stroke to a Nolaro cable[3] the winch operator was only fortuitously not seriously injured. Briefly the salient steps required for personnel protection were:

(1) Select and install a lightning warning system.

(2) Require that all personnel be inside a protected enclosure during lightning warning periods.

(3) Require the winch operator be in a carefully constructed electro-magnetic "Faraday Cage" and take necessary special precautions during warning periods.

(4) Check the shielding integrity of all enclosures and ground support systems. Proof testing with a portable lightning simulator is recommended.

(5) The protective measures required must be tailored to each site as illustrated in references 2, 3 and 4.

III. Winch Protection

The objective of winch protection is to prevent damage to the winch electrical and hydraulic systems and to the cable stored on the winch. The shielding techniques required for personnel protection can also be used to prevent damage to the winch control system. The hydraulic cables often use steel reenforcing and must be treated as conducting cables.

During the reported natural lightning stroke to the winch[3] the operator saw a ball of plasma engulf the reel. Heavy currents flowed through the winch and across the tires to ground. Where, as in this case, the flying sheave was on the winch vehicle, it is difficult to prevent large currents from flowing in the winch. A separate ground cable to a driven ground stake limits the motion of the vehicle and is generally not very effective because the inductance of the ground cable still allows the vehicle tires to flashover, with a large proportion of the current still flowing in the winch. Because of its limited effectiveness, a ground cable should not be required where mobility is important. For example, requiring the operator to leave the winch to connect a ground cable could be more dangerous than leaving it off.

If operations permit, better winch protection is afforded by a stationary, permanently grounded flying sheave. Depending on the nature of the ground, the winch tires may still flashover, but the inductance of the long path to the winch will considerably reduce the winch current. Because of the variability of earth grounding in different locations and the variability of methods of achieving "grounds", grounding cannot be relied upon for protection and should be considered only as a method of current amplitude reduction.

Other techniques for diverting the stroke energy away from the winch have also been considered, such as the use of a separate diverter balloon[2] or a separate winch for a power cable used as a diverter. This winch would be well grounded and remotely controlled.

IV. Cable Survivability

Various cable specimens, provided by RML for joint evaluation, were tested for their susceptibility to lightning damage. Such damage might result in releasing the balloon. The samples submitted for test are listed below:

1. Nolaro   0.775 inch diameter.
   0.625 inch diameter.
   0.490 inch diameter.

2. Fiber B   0.460 inch diameter.

3. Plow Steel (7/19), 3/8" diameter.

4. Stainless Steel, 3/8" diameter.

5. Well logging cable (3/19), 3/8" diameter.
   with AWG #24 copper wire center strand.

6. Nolaro, 0.625 diameter, with three external wires, AWG #14, coiled around the outside for power transmission.

7. Nolaro, 0.775 diameter, with internal plastic tubing for transporting combustible gas.

8. Nolaro, 0.775 diameter, jacket for striation pressure test.

9. Nolaro, 0.775 diameter, with internal AWG 14 wire.

10. Long lengths of 0.625 Nolaro and 0.460 Fiber B for separate evaluation.

11. Steel cable, 1/4" diameter,

12. Stainless steel cable, 1/4" diameter.

As has been discussed briefly in the introduction, on nonconducting tethers the lightning current follows the paths of the prestrike streamer ionization. Unless the streamer punctures the jacket of a Nolaro or Fiber B cable, the large lightning current flows near the surface of the cable in an ionized air path. In this respect, the result is similar to the action of the new segmented strip diverters, where most of the current flows over the strip, not in it. This means that very high peak currents can be guided by a Nolaro or Fiber B cable without damaging the cable, unless puncture occurs. The heat of the discharge generally just polishes the jacket surface without seriously damaging it. As has also been

mentioned, only about 4% of a Nolaro cable, struck by natural lightning, was damaged. As will be seen from our test results, most nonconducting samples withstood several discharges without damage. Of course, the strength of a chain is limited to that of its weakest link and even a short section of damage is not acceptable.

Conducting tethers, on the other hand, must conduct all the lightning current. Their conducting ability depends on their size, materials and construction. Conducting cables can generally tolerate high peak currents better than the burning and melting at the stroke attach point(s) as a result of high coulomb transfer. It is often desirable, for this reason, to provide a relatively large contact point or air terminal for stroke attach in a position to divert the stroke away from the cable. Both high current conduction and discharge attach conditions were simulated in our tests.

The collateral problem of transporting electricity or gas to the balloon for operating the on-board equipment was also considered. Lightning effects on wires externally placed on a nonconducting tether was studied and internal wire placement effects were demonstrated. A specimen with a plastic tube inside a nonconducting tether was tested with propane flowing in the tube. A Nolaro cable jacket was exploded with air pressure to show that the striation marks thus produced on the jacket are similar to those caused by natural lightning and therefore due to internal pressure buildup and not to lightning channel direct effects scoring the surface. Other parameters, such as the shape of the cable and the effects of artificial punctures in the jacket, were added to the program to measure their significance.

Four of the current waveforms, representative of the basic waveforms used to simulate lightning for cable test purposes, are shown in Figures 1 through 4. Long arcs were produced over five to six feet of cable surface by a Marx type generator at a voltage of about two million volts. The resulting peak current, as shown in Figure 1, is about 17 kiloamperes. The damped oscillatory wave has a first half cycle duration of about three microseconds. While this peak current is the lowest of the test currents used, it should be pointed out that its magnitude is representative of that of the average lightning stroke. The higher currents were applied directly to conducting cables for lengths of four to six feet and over about six inches of a nonconducting cable, usually triggered by the high voltage generator. In the latter case the high voltage discharge current was combined with the high current making it a multiple component discharge. The conducted 200 kiloampere peak current shown in Figure 2 has a first half cycle duration of about 100 microseconds. A typical multiple discharge, Figure 3, has a peak current of about 150 kiloamperes and a first half cycle duration of about 120 microseconds. The wire used for power transmission has a

-4-

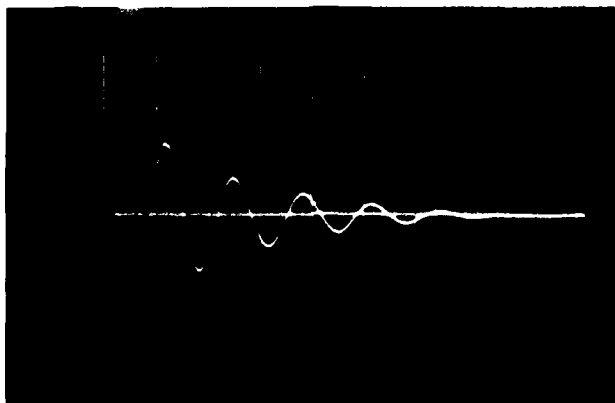Figure 1. Typical current waveform of high voltage generator, 17 Ka. peak and 5 μsec. per large division.
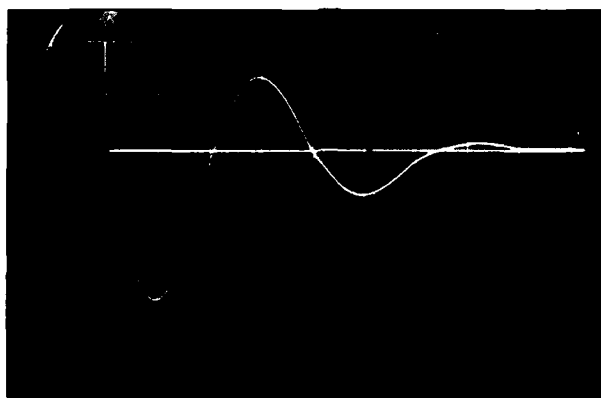

Figure 2. Typical high current waveform, 200 Ka. peak and 50 μsec. per large division.

Figure 3. Typical multiple high voltage and high current waveforms, 150 Ka. peak and 50 μsec. per large division.

Figure 4. Waveform of current with three conductor exploding wires, 150 Ka. peak and 50 μsec. per large division.

relatively high resistance and chops the high current wave, as in the case of the explosive destruction of the three external wires on the Nolaro, the current of which is shown in Figure 4. A peak current of 200 kilo-amperes was reached, but the duration was reduced to about 35 micro-seconds. A fifth waveform not shown is used for high coulomb transfers. It is essentially a rectangular current of constant amplitude and variable duration. Its amplitude is usually about 160 amperes at a driving voltage of about 600 volts. The coulomb transfer is controlled by the time of application.

The test data is summarized in Table I. Each data group is numbered in sequence and will be referred to as I-1, I-2, etc. A typical discharge over a length of nonconducting cable, I-17, is shown in Figure 5. A typical multiple discharge with the high current applied at the bottom of the cable, I-10, is shown in Figure 6. A typical high voltage discharge applied to a curved cable, I-15, is shown in Figure 7. This stroke damaged a three inch section of cable at the bottom. The dark length near the bottom of the cable, which is seen in Figure 7, confirms cable penetration. A typical three inch damaged section of saturated 0.625 Nolaro, which occurred between the 57" and 60" points measured from the bottom and just above the curve in the cable, I-12, is shown in Figure 8. The damage was similar to that shown closeup in Figure 9 which shows a damged 4.5 inch section of saturated 0.490 Nolaro . This cable was damaged on the sixth high voltage discharge, I-8. Pressure striations produced by a high voltage to a 0.775 Nolaro cable, I-7, are shown in Figure 10. Similar marks were found on the cable struck by natural lightning. Such striations were also produced by rupturing the outer jacket of 0.775 Nolaro with an air pressure source of 155 pounds/ in^2, I-45.

The nonconducting cables were tested dry, wet and saturated. The wet cables were thoroughly wetted on the outside surface. The saturated cables were soaked at least overnight to thoroughly vet the inside of the cable. The nonlinear wetness, confirmed by resistance measurements, resulting from partial drying or wetting was of particular interest in our tests of nonconducting cables. These conditions appeared to favor Nolaro jacket puncturing and should be representative of natural conditions.

As summarized in Table I, both the Nolaro and Fiber B cables withstood a "standard" test of three high voltage discharges and one high current discharge, dry, wet and saturated, except for one instance where a saturated 0.775 Nolaro cable was punctured on the second discharge, I-3. For further testing the parameters of nonuniform resistance, such as might occur during a rainstorm or after it, and cable curving were introduced. Both of these appeared to increase the likelihood of nonconducting cable damage due to streamer puncturing. Many discharges were applied, as

TABLE I.

DATA SUMMARY -1

Sample	Condition	Discharge(s) Applied	Results
1. Nolaro 0.775, #1	Dry	3 high voltage	No visible damage.
2. " "	Wet	" "	" " "
3. " "	Saturated	2 high voltage	Five punctures on 2nd discharge.
4. " "	"	1 Multiple (high voltage and 140 Ka. Hi I.	Surface polished.
5. Nolaro 0.775, #2	Dry	1 high current, 150 Ka.	" "
6. Nolaro 0.775, #4	Saturated	15 high voltage (11-15 prepunctured)	Three punctures on 13th discharge.
7. Nolaro 0.775, #4 after 3 days.	Saturated (7&8 Curved cable)	8 high voltage	Three punctures during 1 to 6. 2 inch damaged length on 8th.
8. Nolaro 0.490, #1	Saturated	6 high voltage	4.5" damaged length on sixth (R=100k over 4.5")
9. Nolaro 0.490, #2	Dry	1 high voltage and one multiple Hi V & II(150Ka)	No visible damage.
10. " "	Saturated	3 high voltage and one multiple Hi V&I (140 Ka)	No visible damage.

TABLE I.

DATA SUMMARY-2

Sample	Condition	Discharge(s) Applied	Results
11. Nolaro 0.625, #1 Curved	Saturated 2.3 meg., 110"	10 high voltage	No visible damage.
12. "	Saturated 4.7 meg., 110"	14 high voltage (6-14 prepunctured)	Striations at bend on 13. 3 inch damaged length on 14.
13. Nolaro 0.625, #2 Center of 45' pc.	Dry	5 high voltage and 1 high current (200Ka.)	Sent to RML for test.
14. Nolaro 0.625, #3 Center of 45' pc.	Dry	1 high current (200Ka.)	Sent to RML for test.
15. Nolaro 0.625, #4 Curved	Weathered, (moist at ends)	2 high voltage	3 inch damaged length on second discharge.
16. Nolaro 0.625, #5 Curved	Dry	15 high voltage	No visible damage.
17. Fiber B 0.460, #1	Dry	3 high voltage	No visible damage.
18. Fiber B 0.460, #1	Wet	3 high voltage	No visible damage.
19. Fiber B 0.460, #2	Saturated	3 high voltage	No visible damage.
20. Fiber B 0.460, #2	Dry	1 high voltage and one multiple (150 Ka.)	Surface polished.

TABLE I.

DATA SUMMARY - 3

Sample	Condition	Discharge(s) Applied	Results
21. Fiber B 0.460, #2	Saturated	1 high voltage and one multiple (130 Ka.)	Surface polished.
22. Fiber B 0.460, #3 Center of 35' pc.	Dry	5 high voltage and 1 high current (200 Ka.)	Sent to RML for test.
23. Fiber B 0.460, #4 Center of 35' pc.	Dry	1 high current (200 Ka.)	Sent to RML for test.
24. Plow steel, 3/8" Ave 13,930# #1		1 high current (200Ka.)	Tensile strength 14,600#
25. " " #2		3 high coulomb (150 C)	Burning and melting, tensile strength reduced to 4,600#
26. " " #3		1 high coulomb (300 C)	Burning and melting, tensile strength reduced to 3,200#
27. Stainless steel, 3/8" Ave. 14,200# #1		1 high current (100 Ka.) & 1 " " (200 Ka.)	Tensile strength reduced to 13,000#
28. " " #2		1 high coulomb (300 C)	Burning and melting, tensile strength reduced to 8,000#
29. Well logging, 3/8" (One strand tested) Ave. 4,200# #1		1 high current, 50 Ka.	Tensile strength reduced to 3,600#
30. " " #2		1 high current, 75 Ka.	Tensile strength reduced to 3,400#

TABLE I.

DATA SUMMARY -4

Sample	Condition	Discharge(s) Applied	Results
31 Well logging, 3/8" (One strand tested) Ave. 4,200# #3		1 high current, 125 Ka.	Tensile strength reduced to 2,400#
32. " " #4		1 high current, 160 Ka.	Tensile strength reduced to 3,200#
33. " " #5		High voltage to check insulation failure of AWG 24 center conductor.	Electrical breakdown at ends- 14 to 18 kilovolts.
34. Stainless steel, 1/4"	Under a 1,500 lb. tension.	1 high coulomb, 312 C	5 out of 7 strands broke.
35. "	"	1 high coulomb, 156 C	5 out of 7 strands broke.
36. "	"	1 high coulomb, 100 C	" " "
37. Steel cable, 1/4"	"	1 high coulomb, 80 C	4 out of 7 strands broke.
38 Sample 1. Nolaro 0.625 with 3 #14 ext. wires.	Dry	1 high current, 200 Ka.	All wires blew up, cable not damaged.
39 Sample 2. Nolaro 0.625 with one ext. wire, #14	Dry	1 high current, 50 Ka. 2nd " " 90 Ka.	Wire and cable undamaged. Broke wire in three places.
40 Sample 3. Nolaro 0.625 with one ext. wire, #14	Dry	1st high current, 70 Ka. 2nd " " " 75 Ka. 3rd " " " 75 Ka.	Wire heated. Insulation broken. Broke at both ends. Cable OK.

TABLE I.

DATA SUMMARY -5

Sample	Condition	Discharge(s) Applied	Results
#1 Sample 4. Nolaro 0.625 with one ext. wire, #14	Dry	1 high current, 125 Ka.	Wire blew up. Cable not damaged.
#2 Sample 5. Nolaro 0.625 with two ext.#16 wires.	Dry	1st high current, 50Ka. 2nd " " 70Ka. 3rd " " 100Ka.	No damage. No damage. Wire broke thru insulation, 2 places.
#3 Sample 6. Nolaro 0.775 with plastic tubing int.	Dry Propane flowing.	1 high current, 175 Ka. forced to penetrate cable	Fastax movie. Cable blew up but tubing not damaged. No ignition of propane gas.
#4. Plastic tubing alone.	Dry Propane flowing.	10 high voltage	No puncture or ignition. (Pressure tested at 150 #/in^2)
#5. Nolaro 0.775 outer jacket alone.	Dry	Pressure test at 155 #/in.^{2}	Jacket ruptured with striation marks as in lightning damage.
#6 Samples 7 & 8. Nolaro 0.775 with one int.#14 wire.	Dry	1ea. high current, 175Ka.	Cable blew up. Fastax movie taken.

Figure 5. Typical 17 Ka. high voltage discharge applied over 5 feet of dry 0.460 Fiber B cable.

Figure 6. Typical high voltage-high current multiple discharge. The high voltage was applied at the top with the high current added at the bottom.
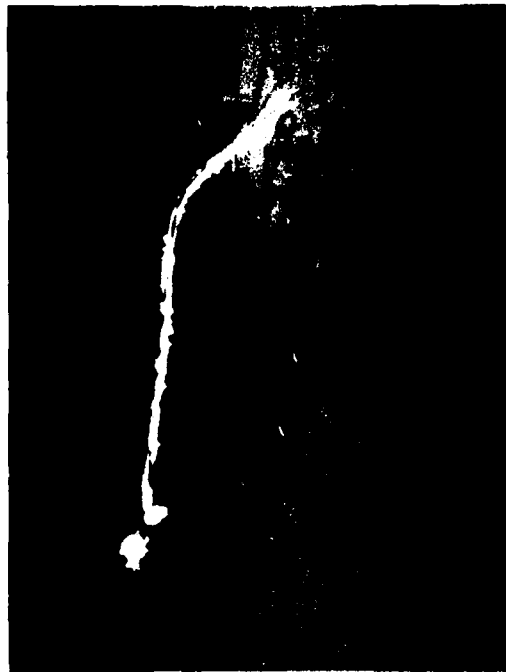
Figure 7. Typical high voltage discharge to a curved cable, 0.625 Nolaro, shows penetration near bottom which damaged a length of cable three inches long.

Figure 8. A high voltage discharge penetrated saturated 0.625 Nolaro near the bend at the top and damaged a three inch length of cable.

-14-

Figure 9. A 4.5 inch length of 0.490 Nolaro was damaged
on the sixth high voltage discharge to the cable.
Damage was similar to that shown in Figure 8.

Figure 10. The 23rd high voltage discharge to a 0.775 Nolaro
cable resulted in a two inch damaged section.
The striations in the jacket were similar to those
produced by natural lightning.

summarized in Table I, to test some of the Nolaro cables to failure.

A specimen of saturated 0.775 Nolaro was punctured on the 13th high voltage discharge when 15 discharges were applied, I-6. When the cable was dried out at the ends and curved slightly, a two inch section of cable jacket was ruptured on the 8th high voltage discharge, I-7. A saturated specimen of 0.490 Nolaro was similarly damaged over a 4.5 inch section on the 6th high voltage discharge, I-8. A curved section of saturated 0.625 Nolaro had its jacket ruptured over a three inch length near the cable curve by the 24th high voltage discharge, I-12. Artificial punctures had been added after the 15th discharge. Striations were noted on the 23rd discharge. A similar specimen was left in the weather about three days and showed lowest resistance at the ends. This specimen was damaged over a three inch length on the 2nd high voltage discharge, I-15. Fiber B cable appeared to be less susceptible to lightning damage than Nolaro, but it was not tested to destruction. Except for polishing the cable surface, the simulated lightning strokes had little effect on the Nolaro type cables unless streamer puncture occurred and guided the high currents into the cable.

Conducting steel cables were tested by application of high current and high coulomb discharges. Stainless steel, 3/8 inch diameter, lost less than 10% of its tensile strength due to a conducted 100 kiloampere peak current followed by a 200 kiloampere discharge, I-27. A high coulomb discharge, representing a lightning channel attach to the cable, of 300 coulombs reduced the tensile strength of stainless steel cable, 3/8 inch diameter, from 14,200 pounds average to 8,000 pounds or by about 45%, I-28. A 100 coulomb discharge to a 1/4 inch stainless steel cable, loaded with a 1500 pound tension, resulted in breaking five out of its seven strands, I-36, as did higher coulomb transfers, I-34 and I-35. On the other hand, the tensile strength of 3/8 inch plow steel, not under tension, increased a little, I-24, after conducting a 200 kiloampere peak current, probably due to tempering resulting from the heating due to the high current. Application of high coulomb transfers caused large reductions in the tensile strength of 3/8 inch plow steel, up to about 75% for a 300 coulomb discharge, I-26, and about 65% for a 150 coulomb discharge, I-25. The damage due to high coulomb application to the loaded 1/4 inch steel cable was also severe. When a 80 coulomb discharge was applied, I-37, four out of seven strands broke. It should be pointed out that these tests are representative of severe lightning conditions. The high coulomb transfers are representative of about 2% of strokes to ground. Further, a long duration natural stroke attach point would be expected to move along the cable somewhat tending to distribute its energy and cause less local damage. These tests represent "worst case" conditions for evaluation of the relative lightning susceptibility of the cables. While both 3/8 inch cables would withstand the average 20 kiloampere, 20 coulomb lightning stroke, the stainless steel cables conducted the high peak currents with

-16-

the least loss of tensile strength.

One strand of 3/19 well logging cable with an insulated copper conductor in the center conducted a 75 kiloampere peak current with a loss of about 20% in tensile strength, I-30. The high coulomb test was not applied since it would destroy the single strand. High voltage was applied to the center conducter to measure the electrical breakdown of the insulation. Breakdown occurred at 14 to 18 kilovolts, I-33. It is possible then for the cable voltage drop to periodically puncture the insulation of the center power conductor. For example, assuming impulse breakdown at 20 kilo-volts and a 100 to 200 kiloampere lightning peak current with a cable resistance of one ohm per 1,000 feet, we might expect breakdown to the cable every 100 to 200 feet due to a voltage drop of 200 to 100 volts per foot.

Power transport wires were also placed externally on the surface of nonconducting Nolaro cables. High current discharges generally destroyed the conductors, but did not damage the cable. Thus this technique could be used where the power conductors are expendable, until they can be replaced. As shown in Figure 11, three # 14 external wires were destroyed by a 125 kiloampere peak current, I-41. One external #14 wire withstood a 50 kiloampere discharge, I-39. Thus we could expect these conductors to withstand an average lightning stroke. The limit for a single # 14 wire was about 70 kiloamperes, I-40. Two #16 wires on a 0.625 Nolaro specimen were not damaged by a 70 kilo-ampere discharge, I-42, but, as shown in Figure 12, the wire broke through the insulation when a 100 kiloampere peak current discharge was applied.

While the electrical transport wires can be placed on the outside surface of Nolaro cable, they cannot be placed inside without seriously damaging the cable. To illustrate this point a # 14 wire was placed inside a sample of 0.775 Nolaro, I-46. Upon application of a 175 kilo-ampere peak current discharge, the cable was completely destroyed. A Fastax movie of the explosion was taken for tutorial purposes.

Gaseous fuel flowing in a plastic tube proved a good method of power transport from a lightning point of view. A 1/4 inch plastic tube was placed in the center of a specimen of 0.775 Nolaro and propane was passed through the tubing during the simulated lightning tests. In the first test, a worst case condition was set up by forcing or guiding the 175 kiloampere high peak current into the cable with a .007 inch steel wire, I-43. Under these conditions, the cable was severely damaged, as shown in Figure 13, but the plastic tube was not penetrated and ignition did not occur. A Fastax motion picture was also made of this test. Finally, ten high voltage discharges were applied to the plastic

Figure 11. A 200 Ka. discharge to three #14 wires,externally
wrapped around a 0.625 Nolaro cable, vaporized
the wire without damaging the cable. A wire inside
the cable would have destroyed the cable.

Figure 12. Two #16 wires withstood a 70 Ka. discharge.
A 100 Ka. discharge caused the wire to break
through its insulation.

Figure 13. Damage caused by a 200 Ka. discharge forced
to penetrate a 0.775 Nolaro cable with an internal
plastic tube in which propane was flowing. The
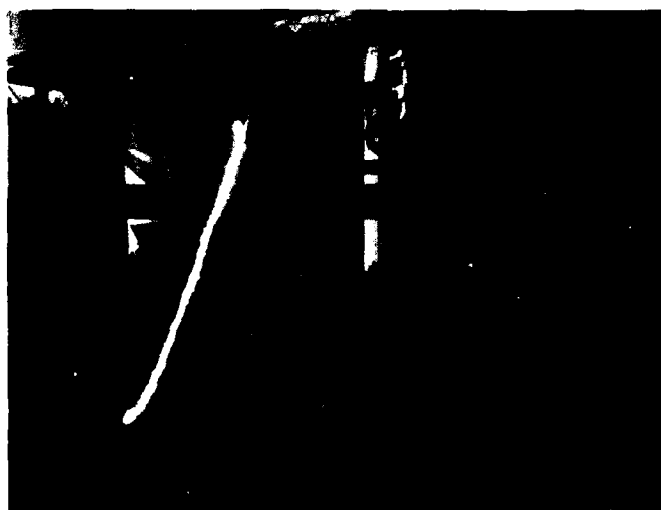tube was not damaged or penetrated and the propane
was not ignited.

Figure 14. The plastic tube alone withstood the ten high voltage
discharges applied without damage.

tubing alone with propane flowing, I-44, as shown in Figure 14. No ignition or punctures occurred. The tubing was tested for punctures with 150 lb/in^2 air pressure.

The lightning susceptibility of Nolaro type nonconducting cables can probably be reduced by the use of coatings, such as aluminum paint, which could reduce the probability of cable puncture. Prevention of moisture absorption also would reduce puncturing. Other measures, such as increasing the thickness of the Nolaro jacket, may also prove effective. Such cable improvements were not tested in this program.

As has been discussed, externally placed electric power conductors, if used, could also prevent cable damage by providing a path for the lightning current. At a safe height the wire could leave the cable and go to a separate well grounded remote controlled winch located at a safe distance from the main winch.

As indicated by the results of the conducting tether tests, reduction of their susceptibility to lightning damage is largely a matter of selection of cable size and material. Diversion measures, which can be used near the balloon, would prevent direct lightning attachment to the cable and the resultant damage.

V.   Balloon Protective Measures

Lightning protection of balloons or other vehicles usually requires measures that insure safe attach points and paths on the surface of the vehicle for the lightning currents. In the case of a balloon a safe path from the top of the balloon to the tether cable must be provided. Air terminals or lightning rods should be provided for attach points, at least at the nose and tail, along with an interconnecting cable or foil strip. To minimize electromagnetic interference the air terminals should be graded resistance diverters instead of metal rods. These diverters also act as quiet dischargers for static-electrification.

A typical RML balloon is shown in Figure 15. The confluence lines should be made conducting, at least for the lightning currents. If necessary resistive diverter strips, using the techniques developed for the button diverter strips, might be used. Of course, a metal cable or a nonconducting line with an external conductor is preferable where it can be used. The confluence lines then form a Faraday cage around the equipment inside it, protecting the equipment from the lightning currents and greatly reducing induced voltages. The upper ends of the confluence lines should be electrically connected together and to the nose and tail diverters by underside conductors. Conducting cables or foil strips

-20-

FIGURE 15

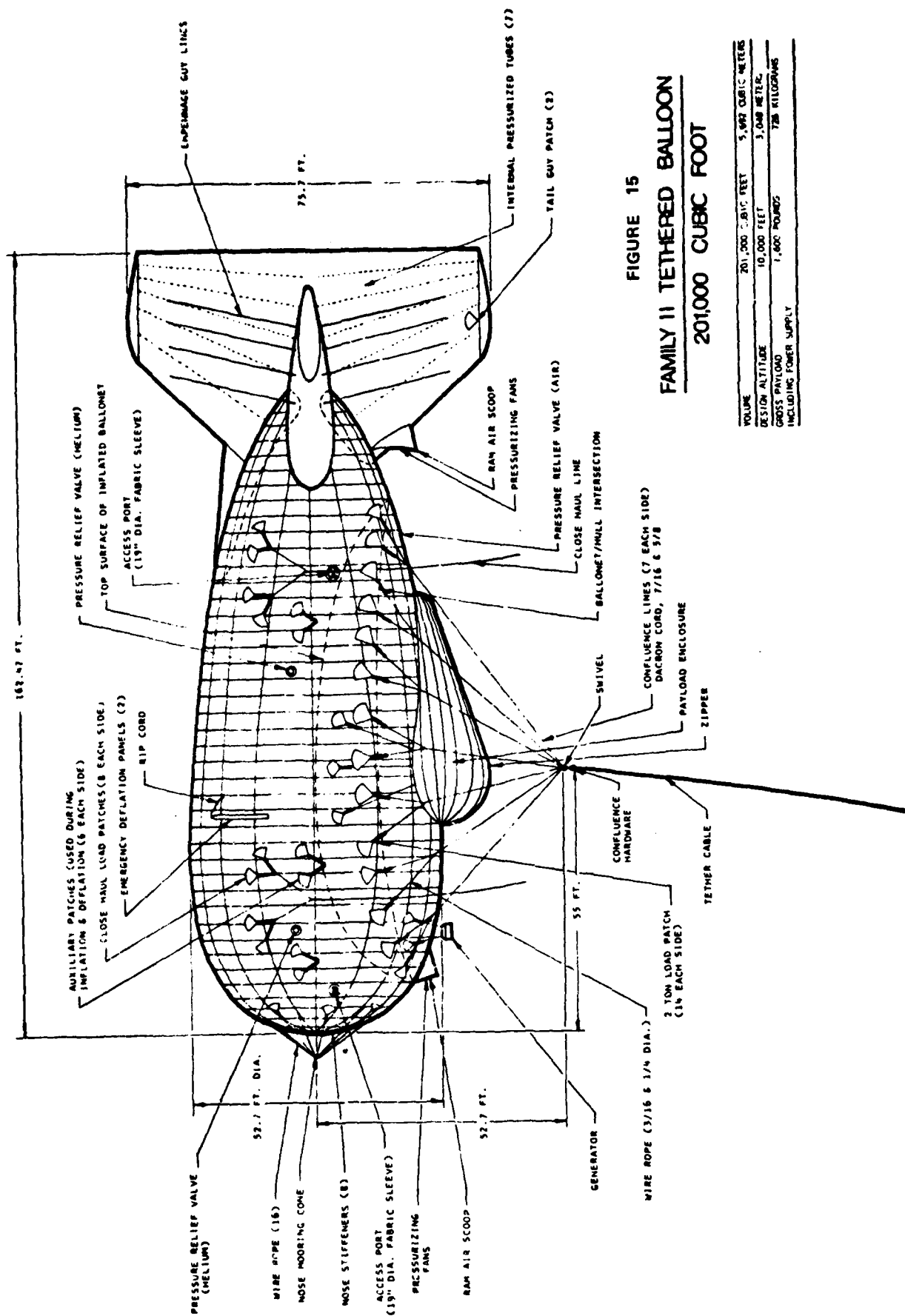**FAMILY II TETHERED BALLOON**
201,000 CUBIC FOOT

VOLUME	201,000 CUBIC FEET	5,947 CUBIC METERS
DESIGN ALTITUDE	10,000 FEET	3,048 METER.
GROSS PAYLOAD	1,600 POUNDS	726 KILOGRAMS
INCLUDING POWER SUPPLY		

should be used on both sides of the balloon to connect the ι p strip to the confluence lines. If one set is used, it should be placed in the middle.

When lightning strikes the balloon at one of the attach points provided, the conductors and confluence cage carry the lightning currents to the tether cable. If the tether cable is metal, the balloon diverter system will prevent direct lightning attach to the upper end of the tether. If the tether is nonconducting with a power cable which is conducting, the result is the same. A nonconducting tether will generally have enough conductivity to cause high field intensity and corona discharge at the diverters, but not enough to support quick formation of long streamers. For this reason the probability of lightning attach to the tether will be greater for a nonconducting tether than for a conducting tether,

The diverter system described is also effective for removing static-electrification from the balloon. Generally the electrically "quiet" graded resistance diverters are used. Conductive fabric coatings may, of course, also be used, but they are not essential.

On the ground personnel should be made aware of the possibility of receiving electrical shocks from ungrounded power or tether cables due to atmospheric field gradients and to balloon static-electrification. As with similar high voltage safety problems, procedure should require grounding the cables prior to touching them.

VI. Protection of On-Board Electronics

As discussed in the previous section, on-board electronics, located inside the electromagnetic Faraday cage formed by the confluence lines, receives primary protection from lightning currents of a stroke attaching to the balloon diverter system by distributing the current so as to reduce electromagnetic induction inside the cage. In addition, the equipment cabling and the electronic packages should be well shielded, particularly if they must be located outside the confluence cage. Shielding techniques have been discussed in previous reports[1,2,4] and in the literature.

Where necessary three stage surge protection should be provided:

(1) Provide a surge arrester capable of transferring high currents and energy. Occasionally a component, such as a quarter wave stub, can serve as a short circuit for the lightning current. Surge arresters would be necessary on tether cable power conductors, if used.

(2) At the input to shielded electronic equipment provide a secondary surge protector to reduce the peak voltage at the equipment input to the order of 100 volts.

(3) For susceptible circuits provide back-to-back zener diodes or the
     equivalent to further reduce the remaining surge voltage.

An example of a three stage protective system for a tethered balloon
antenna system, which successfully passed the test of operating during
a nearby natural lightning stroke as well as simulated lightning tests,
was reported in an earlier Army report.[5]

On-board EED's should be shielded and shorted by a nearby relay
or other means to minimize loop induction. Exploding bridge wires are
least vulnerable to low energy surges. Both relay and firing circuit are
actuated by the firing switch. An example of this type of circuit was
given in an earlier report to RML[2].

Specific equipment problems were not part of this program. Of
course, optimum protection must be tailored to the configuration and
needs of the equipment being protected.

VII. Conclusions and Recommendations

Personnel in the ground handling crews should be warned when the
possibility of a lightning stroke exists. They can be protected during
a stroke by requiring that they remain inside an electromagnetic Fara-
day cage type enclosure during the warning period. Cables to these
enclosures should be properly shielded. Particular attention should be
given the winch equipment with special precautions to be taken by the
winch operator. Proof testing of the final installations with a portable
lightning simulator is recommended. Grounding, per se, cannot be
considered effective protection, but can be used to reduce current
amplitudes, particularly if a sufficiently remote ground can be used.

Balloons with nonconducting tethers can be struck by lightning. In
practice, quasi-static field distortion still occurs at the balloon due to
the microampere currents that flow in the tether. If struck by lightning,
Nolaro type nonconducting cables can be seriously damaged by lightning,
possibly resulting in release of the balloon.

While Fiber B samples were not damaged in the limited testing
reported, Nolaro type cables generally required many simulated discharges
before damage occurred. Damage was not cumulative in many cases,
but occurred explosively during a single discharge. If such a non-
conducting tether is selected for use, it should be exhaustively tested
and, if possible, improved by using a thicker jacket or other measures.
It should be clearly improved over the conventional Nolaro tether cable
which was damaged by natural lightning.

External electrical wires for power transport on nonconducting cables can be used to both transfer power and to protect the cable from lightning penetration. Most strokes would not damage these wires or the cable. If the wires were damaged, they could be replaced.

Transporting gaseous combustible fuel with a plastic tube in the center of a Nolaro type tether cable does not introduce any new lightning problems such as fuel ignition. While the plastic tube was not damaged by any of the tests, the possibility of cable damage and separation still exists. If the cable itself can be made lightning proof, the gas transfer method would not be susceptible even to large lightning current damage.

Of the conducting cables tested, stainless steel appeared somewhat less susceptible to lightning damage than plow steel or well logging cable. All metal cables were less susceptible to damage from high peak currents than from the burning and heating of the long duration, low current or high coulomb transfers at a direct lightning attach point. Diverters should be used on the balloon to prevent lightning attach to the upper end of the metal tether cables and well as to protect the balloon and its equipment. The insulation on the copper conductors of the well logging cable could be punctured due to the resistive voltage developed in the tether during a lightning stroke.

Graded resistance diverters or other air terminals should be used on the nose and tail of the balloon to serve as lightning attach points. A configuration of interconnecting conductors should be used between the diverters and a conducting ring at the top of the confluence cables. The confluence cables should be conducting and form an electromagnetic shield cage for enclosed equipment and a connecting path for the lightning current to the tether cable.

The confluence cage serves as initial protection for on-board electronics located inside the cage. For further protection the circuitry can be provided with three stages or levels of protection, as required for high, intermediate and low voltages and energies. Electroexplosive devices should be protected by shorting with a small loop until they are activated.

References

(1)   Stahmann, J.R., "Lightning Protection for a RML Tethered
        Balloon System, Phase I, Personnel Protection", Lightning
        and Transients Research Institute, Miami Beach, Florida,
        Contract F08606-73-C-0037, ARPA 1876, RML, PAFB, FL,
        August, 1973.

(2)   Stahmann, J.R. and Robb, J.D., "Lightning Protection for
        Tethered Balloon with Power Cable", Final Report, Lightning
        and Transients Research Institute, Miami Beach, Florida,
        Contract F8606-69-C-0030, prepared for Air Force Eastern
        Test Range, RML, PAFB, FL, April, 1969.

(3)   Stahmann, J.R., "Investigative Report, Lightning Stroke to a
        Tethered Balloon Cable", Lightning and Transients Research
        Institute, Miami Beach, Florida, prepared for Air Force
        Eastern Test Range, RML, PAFB, FL, August 19, 1972.

(4)   Stahmann, J.R., "Lightning Protection for Navy 2D2 Site,
        Pinecastle, Florida", Lightning and Transients Research
        Institute, Miami Beach, Florida, prepared for Department
        of the Navy, NTDC, Orlando, Florida, May, 1969.

(5)   Stahmann, J.R., "Improvement of Protection against Atmos-
        pheric Electrical Effects on a Tethered Balloon-Antenna System",
        Lightning and Transients Research Institute, Miami Beach,
        Florida, Contract DAAB07-70-C-A118, prepared for the United
        States Army Electronics Command, Fort Monmouth, New Jersey,
        November, 1969.

(6)   Stahmann, J.R., "Lightning Survivability of Tethered Balloon
        Cables", Lightning and Transients Research Institute, Miami
        Beach, Florida, Final Report, Contract F19628-67-C-0377,
        prepared for Air Force Cambridge Research Laboratories,
        Bedford, Mass., February, 1969.